THE HONG KONG
POLYTECHNIC UNIVERSITY
香港理工大學
Pao Yue-kong Library
包玉剛圖書館

Copyright Undertaking

This thesis is protected by copyright, with all rights reserved.

By reading and using the thesis, the reader understands and agrees to the following terms:

1. The reader will abide by the rules and legal ordinances governing copyright regarding the use of the thesis.
2. The reader will use the thesis for the purpose of research or private study only and not for distribution or further reproduction or any other purpose.
3. The reader agrees to indemnify and hold the University harmless from and against any loss, damage, cost, liability or expenses arising from copyright infringement or unauthorized usage.

IMPORTANT

If you have reasons to believe that any materials in this thesis are deemed not suitable to be distributed in this form, or a copyright owner having difficulty with the material being included in our database, please contact lbsys@polyu.edu.hk providing details. The Library will look into your claim and consider taking remedial action upon receipt of the written requests.

Pao Yue-kong Library, The Hong Kong Polytechnic University, Hung Hom, Kowloon, Hong Kong

http://www.lib.polyu.edu.hk

SUPPLY-BASED COOLING DISTRIBUTION MANAGEMENT OF AIR-CONDITIONING SYSTEMS FOR DEMAND LIMITING AND BUILDING-GRID INTERACTION

DAI Mingkun

PhD

The Hong Kong Polytechnic University

2025

The Hong Kong Polytechnic University

Department of Building Environment and Energy Engineering

SUPPLY-BASED COOLING DISTRIBUTION MANAGEMENT OF AIR-CONDITIONING SYSTEMS FOR DEMAND LIMITING AND BUILDING-GRID INTERACTION

DAI Mingkun

A thesis submitted in partial fulfillment of the requirements for the degree of Doctor of Philosophy

Aug 2024

CERTIFICATE OF ORIGINALITY

I hereby declare that this thesis is my own work and that, to the best of my knowledge and belief, it reproduces no materials previously published or written, nor material that has been accepted for the award of any other degree or diploma, except where due acknowledgement has been made in the text.

__________________(Signed)

DAI Mingkun (Name of student)

ABSTRACT

Abstract of thesis entitled:		Supply-based cooling distribution management of air-conditioning systems for demand limiting and building-grid interaction
Submitted by	:	DAI Mingkun
For the degree of	:	Doctor of Philosophy

at The Hong Kong Polytechnic University in August, 2024

Energy and environmental issues are critical concerns that have attracted great attention in recent decades. The building energy consumption plays a significant role in the broader context of these issues, given the increasing demand for commercial spaces and the need for sustainable development alongside urbanization and industrialization. Air-conditioning systems account for a substantial portion of a building's energy usage, making their efficient control vital for overall energy performance. Proper control strategies have the potential to unlock significant energy savings and provide energy flexibility services to power grids.

Conventional process control utilized in building central air-conditioning systems can be viewed as demand-based feedback control. In this situation, the control of cooling distribution in the air-conditioning system depends on the individual cooling demands of each air-conditioned space. However, demand-based control fails to effectively manage the cooling distribution when cooling supply is limited. The limitations of conventional demand-based control become evident in the following scenarios: First, air-conditioning systems in commercial buildings are usually switched on in advance to precool the indoor spaces to create an acceptable working environment by office

hours. However, the central cooling systems often cannot provide enough cooling supply capacity due to high demand during the morning start period, especially in hot seasons. In this situation, imbalanced cooling distribution often results in significant differences of cooling-down speed among different building zones, requiring an extension of precooling time and leading to considerable energy waste. Moreover, air-conditioning systems have great potential to provide energy flexibility services to the power grids of high-renewable penetration. Direct load control, by switching off some operating chillers, is the simplest and most effective means for air-conditioning systems in buildings to respond to urgent power reduction requests from power grids. However, the implementation this approach in today's buildings, which widely adopt demand-based feedback controls, could lead to serious issues, including disordered cooling distribution and additionally energy consumption. Therefore, this PhD study aims to theoretically and practically develop smart cooling distribution management strategies of air-conditioning systems, focusing on demand limiting and building grid-interaction.

To begin with, the concept of supply-based control is proposed as an effective approach for cooling distribution when the cooling supply is limited. To implement this approach in today's buildings, a reconfigurable supply-based feedback control is proposed. This system integrates supply-based feedback control for demand limiting control under limited cooling supply and demand-based feedback control during normal operation with sufficient cooling supply. In particular, this strategy can be conveniently deployed in today's conventional digital controllers. The proposed strategy incorporates a control loop reconfiguration scheme and a setpoint reset scheme, facilitating effective demand limiting control and enabling smooth transitions between the two control modes. The control loop reconfiguration scheme reconnects the controlled variable and resets the control parameters when switching from one mode to another while determining the proper timing for this transition. The commonly used PID control function is adopted. The setpoint reset scheme establishes the setpoint of the feedback loop in demand limiting mode. The proposed control strategy is implemented in a commonly used digital controller to conduct hardware-in-the-loop control tests on an air-conditioning system involving six air handling units (AHUs). Test results show that the reconfigurable control achieves commendable control performance. Proper chilled water distribution enables even thermal comfort control among building zones during demand response and rebound periods. Temperature deviation among building zones is maintained below 0.2 K most of the time. Power demand reductions of 11.6% and 27% are achieved during demand response and rebound periods, respectively, when using the proposed reconfigurable control compared to conventional controls.

Advanced control strategies for specific enhancement are proposed in the following sections. Specifically, to address the problems and challenges during the morning start period, an iterative learning control strategy for building air-conditioning systems under limited cooling supply is introduced. This simple control strategy can determine the AHU water valve openings during the morning start period to achieve uniform cooling among building zones by updating the valve opening control values of individual AHUs using iterative learning control. A reinforcement learning approach is developed for setting the control parameters by adopting a classical reinforcement learning method, namely Q-learning. The proposed control strategy is model-free and does not require extra sensors or additional experimental work for thermodynamic characteristic parameter identification. Validation tests are conducted, and results show that the proposed control strategy could reduce the daily precooling time by up to 12.1% during typical days in Hong Kong by achieving uniform cooling. Daily energy consumption could be reduced between 5.1% and 17.8% by shortening the morning start period, corresponding to a weekly electrical energy savings of between 1,376 kWh and 2,916kWh in the test building.

To address the problems and challenges of building grid-interaction, an event-driven control strategy is proposed to effectively unlock building energy flexibility for fast demand response using air-conditioning systems. The proposed control strategy determines the optimal AHU water valve openings based on real-time indoor environment data from different air-conditioned zones for even distribution of the limited cooling supply after shutting down part of the operating chillers during the demand response period. A cooling distribution control scheme is proposed and used in the control strategy for even cooling distribution. An event-driven scheme is introduced into the cooling distribution control for the first time to minimize adjustments of the valve openings. This event-driven scheme could avoid frequent adjustments of the AHU valves, reducing unnecessary wear and tear during the control process. Validation tests demonstrate that the limited cooling supply can be distributed properly and that the same indoor air temperature profiles can be achieved eventually among the indoor spaces. The power demand of the chiller plant is reduced by 170 kW (5%) with the proposed event-driven control while maintaining the same comfort levels as existing time-driven control. The average accumulated valve travel distance is also reduced by 54.6%, significantly decreasing the wear and tear of the AHU valves.

To improve control generality and scalability, a distributed cooperative control strategy for air-conditioning systems based on the multi-agent system is proposed to facilitate fast demand response. The control architecture is deployed on field control stations of corresponding terminals (i.e., valves and dampers) based on environmental variable measurements of individual air-conditioned spaces. The multi-agent system comprises agents that serve as local controllers for their respective terminals, working collaboratively to achieve even cooling distribution. Each agent performs on-site control using information collected from its own terminal and its neighbors through a distributed architecture. Validation tests demonstrate that the proposed control approach can efficiently manage uneven temperature increases in different zones of the building. During the demand response event, a significant reduction of 2,562 kWh of electricity is achieved, accounting for 19.7% of the electricity consumption compared to the conventional control.

Finally, to further facilitate the integration of the reconfigurable feedback control in existing building automation systems, strategies implementing reconfigurable feedback control are proposed for supply-based cooling management throughout the entire daily cycle of the building daily, including demand limiting, morning start and soft stop. The implementation involves a detailed control strategy along with corresponding hardware placement. Hardware-in-the-loop control tests are conducted to validate the deployment plan. Test results indicate that the reconfigurable supply-based feedback control method can be conveniently deployed in today's practical building automation systems. Significant energy savings are obtained during the morning start period (i.e., 9.1 %) and soft stop period (i.e., 13.3 %). Besides, power limiting can be further reduced by an additional 30.8 % during the demand limiting period.

In conclusion, the development and implementation of the control strategies and real application plans in this PhD study can theoretically and practically provide guidance for demand limiting and building-grid interaction utilizing air-conditioning systems.

PUBLICATIONS ARISING FROM THIS THESIS

Journal Papers

2023 **Mingkun Dai**, Hangxin Li, Shengwei Wang. (2023). A reinforcement learning-enabled iterative learning control strategy of air-conditioning systems for building energy saving by shortening the morning start period. *Applied Energy, 334*, 120650.

2023 **Mingkun Dai**, Hangxin Li, Shengwei Wang. (2023). Event-driven demand response control of air-conditioning to enable grid-responsive buildings. *Automation in Construction, 150*, 104815.

2023 **Mingkun Dai**, Hangxin Li, Shengwei Wang. (2023). Multi-agent based distributed cooperative control of air-conditioning systems for building fast demand response. *Journal of Building Engineering*, *77*, 107463.

2024 **Mingkun Dai**, Hangxin Li, Xiuming Li, Shengwei Wang. (2024). Reconfigurable supply-based feedback control for enhanced energy flexibility of air-conditioning systems facilitating grid-interactive buildings. *Advances in Applied Energy, 14*, 100176.

2024 **Mingkun Dai**, Hangxin Li, Shengwei Wang. (2024). Development and implementation of supply-based feedback controls for energy-efficient and grid-interactive cooling management over entire building daily cycle. *Energy, 313*, 133858.

Conference Papers

2023 **Mingkun Dai**, Hangxin Li, Shengwei Wang. (2023). An adaptive reconfigurable control of air-conditioning systems for building grid-interaction. *11th International Conference on Sustainable Development in Building and Environment*, August 14 to 18, 2023, Espool, Finland.

2023 **Mingkun Dai**, Hangxin Li, Shengwei Wang. (2023). A smart feedback control strategy for building fast demand response using air-conditioning systems. *18th International IBPSA Conference,* September 4 to 6, 2023, Shanghai, China.

2024 **Mingkun Dai**, Hangxin Li, Shengwei Wang. (2024). Model-based control optimization of air-conditioning for proactive building demand response. *Herrick Conferences 2024,* July 15 to 18, 2024, West Lafayette, USA.

Patents

2022 Shengwei Wang, **Mingkun Dai**. A distribution control method based on iterative learning mechanism under limited cooling supply conditions. *China patent:* 202210752907.8.

2023 Shengwei Wang, **Mingkun Dai,** Hangxin Li. A reconfigurable feedback control method of air-conditioning system for demand response. *China patent:* 202311416561.5.

ACKNOWLEDGEMENTS

First and foremost, I would like to express my deepest appreciation to my supervisor, Professor Shengwei Wang, for his readily available supervision, valuable guidance, and continuous support during my PhD study. I have gained a great deal of knowledge and insight into academic research from him, and his research attitude has profoundly influenced me. Also, I would like to thank Professor Fu Xiao for her willingness to engage in discussions and provide valuable suggestions throughout my PhD journey.

I would also like to thank all my colleagues in the research team, especially Dr. Kui Shan and Dr. Hangxin Li, who are always willing to help and share their thoughts; Dr. Rui Tang, Dr. Bing Su, Dr. Chaoqun Zhuang, Dr. Huilong Wang, and Dr. Shaobo Sun for their significant assistance in honing my modeling skills; Dr. Jianing Luo, Dr. Wenxuan Zhao and Dr. Xinyue Li who are always willing to share their experiences. I will fondly remember and cherish the time spent with my research team colleagues and friends in Hong Kong.

Furthermore, I would like to express my gratitude to the Hong Kong PhD Fellowship Scheme (HKPFS) for its financial support.

Finally, I would like to extend my sincerest gratitude to my family members for their unconditional trust, encouragement and support throughout my life.

TABLE OF CONTENTS

LIST OF FIGURES

LIST OF TABLES

NOMENCLATURE

A	action of Q-learning agent
a	coefficient related to bypass pipe water flowrate
AHU	air handling unit
AI	artificial intelligence
AVTD	accumulated valve travel distance
b	control parameter
BAS	building automation system
cdi	cooling diversity indicator
E	edge set
G	graph
HVAC	heating, ventilation and air-conditioning
ILC	iterative learning control
IoT	internet of things
K	proportional gain
k	control parameter
L	graph laplacian matrix
ML	machine learning
N	set of neighbors
P	event interval
PID	proportional-integral-derivative
R	reward
RL	reinforcement learning
S, *s*	state of Q-learning agent
T	temperature
t	return time from night setback
Δt	time deviation
TII	temperature imbalance indicator
TDI	temperature diversity indicator
u	valve opening
Δu	valve opening correction
V	vector set

VAV	variable air volume

Subscripts

ave	average
by	bypass pipe
i	control interval
max	maximum
min	minimum
n	number of building zones
sup	supply air
sp	setpoint
zone	indoor air

Greek symbols

α, γ	learning parameter of Q-learning agent
ε	parameter of ε-greedy policy

CHAPTER 1 INTRODUCTION

This chapter provides an outline of the thesis, which is divided into three sections. Section 1.1 introduces the background and motivation behind the study. In Section 1.2, the aim and objectives of the thesis are presented. Section 1.3 outlines the organization of the thesis and provides a brief description of each chapter.

1.1 Background and motivation

In recent decades, the global community has witnessed growing awareness and concern regarding energy and environmental issues. These concerns have become critical due to their profound impact on various dimensions of human existence, including health, the economy, and the overall sustainability of our planet. The world's incessant appetite for energy, driven by population growth, industrialization, and technological advancements, has resulted in an unprecedented escalation in energy consumption. Global energy consumption has been undergoing rapid growth, especially in the past decade. Worldwide energy consumption grew by 2.3 % in 2018, nearly twice the average rate of growth since 2010 (Global Energy and CO_2 Status Report 2018, 2018). Traditional energy sources, predominantly fossil fuels, have played a dominant role in meeting this growing demand. Coal-fired power generation increased in response to the surging energy demand and reached an all-time high in 2021 (Renewables 2019. Analysis and Forecast to 2024, 2019). The combustion of fossil fuels has been closely linked to greenhouse gas emissions, air pollution, and climate change.

The building sector has become one of the largest energy consumers today, accounting for more than 30 % of total energy use worldwide and over 90 % of electricity consumption in Hong Kong (Hong Kong Energy End-Use Data, 2023). Improving the energy efficiency of buildings has become an urgent challenge. Energy-efficient buildings are designed and constructed to optimize energy performance while minimizing the use of resources. By significantly reducing energy consumption, these buildings contribute to greenhouse gas emissions reduction, conserve resources, and promote sustainable practices. On the supply side, renewable energy has emerged as a crucial solution to address the pressing energy and environmental challenges. Renewable energy sources offer a sustainable and clean alternative, harnessing the power of natural resources such as sunlight, wind, water, and geothermal heat. This form of energy generation not only reduces greenhouse gas emissions and air pollution but also helps mitigate climate change and promote a more sustainable future. It is projected that the renewable power capacity worldwide will increase by half from 2019 to 2024 (Renewables 2019. Analysis and Forecast to 2024, 2019). However, the integration of large amounts of intermittent renewable energy generation, such as photovoltaic and wind power, can cause power imbalance between supply and demand, and thus lead to voltage and frequency oscillations in the power system (Karimi et al., 2016). The concept of the smart grid is proposed as an electric grid capable of delivering electricity in a controlled and smart way, which is a promising solution to these problems (Siano, 2014). With a designed smart grid, the overall performance of power reliability, energy efficiency, economics, and sustainability could be achieved through coordination between power supply and demand. Buildings therefore have great potential in contributing to the power balance by reducing or shifting their electricity demands during peak periods in response to various power balance needs of the power system, which is known as demand response. Demand response control of buildings can not only bring economic benefits to building owners but also benefit the supply side of electricity grids by alleviating the capacity challenges. Grid-interactive buildings are designed to actively interact with the electrical grid, enabling bi-directional energy flows and providing flexibility to support grid stability and resilience. These buildings have the capability to adjust their energy usage patterns, such as shifting loads or curtailing demand during peak periods, in response to grid demands or price signals. Overall, energy-efficient and grid- interactive buildings have become increasingly important in recent years due to the growing demand for energy and the need to reduce greenhouse gas emissions.

The heating, ventilation, and air-conditioning (HVAC) system, as one of the major energy consumers in buildings, has great potential to enable energy-efficient buildings and grid- interactive buildings. It is therefore necessary to monitor, control, and manage the major energy-consumer (e.g. HVAC system) in buildings. Conventional control methods often rely on fixed setpoints and schedules, which can result in unnecessary energy wastage and discomfort for occupants. For energy-efficient buildings, control strategies for HVAC systems focus on minimizing energy consumption while maintaining occupant comfort. This involves dynamically adjusting temperature setpoints, ventilation rates, and airflow distribution based on actual needs. By utilizing occupancy sensors, occupancy patterns can be analyzed to determine optimal operation schedules and adjust cooling or heating levels in unoccupied zones. Additionally, weather forecasts and indoor/outdoor temperature differentials can be considered to optimize cooling and reduce reliance on energy-intensive mechanical cooling. In the context of grid-interactive buildings, HVAC systems can actively contribute to grid stability and support the integration of renewable energy sources. These buildings can respond to grid signals, such as peak demand periods or variable electricity pricing, by adjusting their cooling loads or shifting energy usage to non-peak hours. This demand response capability helps alleviate strain on the grid during high demand periods and enables the utilization of excess renewable energy generation by temporarily increasing cooling loads or charging thermal energy storage systems. Moreover, control strategies for grid-interactive buildings can facilitate the provision of grid services, such as frequency regulation or load balancing. By participating in grid operations, air-conditioning systems can dynamically adjust their power consumption to help maintain grid stability and support the reliable integration of intermittent renewable energy sources.

Modern building automation systems rely on digital controllers at the field level, e.g., direct digital control (DDC) and programmable logic controller (PLC), for the centralized control and monitoring of HVAC systems in buildings (S. Wang, 2009). Their implementation in a process control system for HVAC systems involves the integration of a sensor, which continuously monitors the controlled variable, such as temperature, humidity, pressure, and flow, and an actuator. According to the actual state of the controlled variable, the controller modulates process input via the actuator to maintain the controlled variable at the desired set-point. Such feedback control is, in fact, by means of modulating the use of the supplied resource based on the demand of the process. Demand-based feedback control is widely adopted in digital controllers for process controls of HVAC systems and many other industrial applications today (S. Wang & Tang, 2017). The PID (Proportional-Integral-Derivative) control algorithm of various forms has been commonly used as the feedback control mechanism (Astrom, 1995). However, the conventional demand-based control is not suitable for the fast demand response of building-grid interaction of (Bae et al., 2021; Tang, Wang, & Yan, 2018; S. Wang & Tang, 2017; Xue et al., 2015). This is because such demand-based feedback control loops work well only under the provision of sufficient resources, such as the cooling supply provided by chillers that is enough to fully meet the needs of terminal units. If the cooling supply is insufficient, the existing control systems would suffer from serious operational problems including serious imbalances in chilled water distribution among terminal units, over-speeding of pumps and fans. In order to enable energy-efficient and grid-interactive buildings, smart cooling distribution management strategies of air-conditioning systems that focus on demand limiting and building-grid interaction are urgently needed.

1.2 Aim and objectives

This PhD study, therefore, aims to theoretically and practically develop smart cooling distribution management strategies for air-conditioning systems for demand limiting and building-grid interaction to enable energy-efficient and grid- interactive buildings. The aim and objectives of this thesis are outlined below, providing detailed insights into the focus and goals of the PhD study.

i. Identifiy the problems arising from disordered cooling distribution in conventional demand-based feedback control. Introduce the concept of supply-based feedback control to deal with the problems.

ii. Develop a comprehensive and robust reconfigurable control strategy for the implementation of the concept of supply-based control in conventional building automation systems. The reconfigurable control strategy should integrate supply-based feedback controls, for demand response and demand limiting events, and demand-based feedback controls for normal situations with sufficient cooling supply.

iii. Develop a smart control strategy for air-conditioning systems at the morning start period to effectively shorten the precooling time and reduce the energy consumption. The control strategy is expected to be model-free and not require extra sensors or additional experimental work for thermodynamic characteristic parameter identification.

iv. Develop a smart control strategy for air-conditioning systems to properly distribute the limited cooling supply when facing urgent requests from smart grids. The control strategy should be convenient for on-site implementation and avoid unnecessary wear and tear of the terminal units during the control process.

v. Develop a multi-agent based control system to allow cost-effective and efficient control strategies to be applied in large commercial buildings for demand limiting. The control strategy should allow good scalability and reconfigurability

vi. Implement the reconfigurable control strategy in situations with limited cooling supply throughout the building daily cycle, including the morning start period, demand limiting period and soft stop period. It should incorporate the detailed control strategy architecture along with corresponding hardware placement.

1.3 Organization of this thesis

This PhD thesis consists of nine chapters, which are organized as follows.

Chapter 1 introduces the background and the motivation of this PhD study by presenting the needs of developing smart cooling distribution management strategies for air-conditioning systems for demand limiting and building-grid interaction. Then the aim and objectives, along with the organization of this thesis, are presented.

Chapter 2 presents a comprehensive literature review on conventional feedback control principle, applicability, and applications, HVAC controls for enhancing energy efficiency, and facilitating building-grid interaction, which aims to provide a thorough understanding of the existing research and reveal the problems and limitations of conventional control in demand limiting and building-grid interaction. Research gaps identified in the existing literature are provided to propose novel approaches and methodologies.

Chapter 3 introduces the concept of supply-based control and presents the framework of the proposed control strategies. It aims to provide a solid foundation for understanding the principles, components, and objectives of the control strategies that will be discussed in detail in the following chapters.

Chapter 4 presents a reconfigurable supply-based feedback control for air-conditioning systems, which integrates supply-based feedback control, for demand limiting control under limited cooling supply, and demand-based feedback control under normal operation with sufficient cooling supply. The proposed control strategy is deployed in a commonly-used digital controller to conduct hardware-in-the-loop control tests on an air-conditioning system. Test results and analysis are presented in this chapter.

Chapter 5 presents an iterative learning control strategy for building air-conditioning systems under limited cooling supply in the morning start period. This simple control strategy can determine the AHU water valve openings at morning start period to achieve uniform cooling among building zones effectively. The basic control mechanism, the operation, and the parameter setting method, as well as the test and validation of the control strategy, are presented in this chapter.

Chapter 6 presents an event-driven control strategy for air-conditioning systems for fast demand response towards smart grids. The proposed control strategy can determine the optimal AHU water valve openings based on real-time indoor environment data of different air-conditioned zones for even distribution of the limited cooling supply after shutting down part of the operating chillers during the demand response period. The basic control mechanism and operation procedure, the test arrangement, and the test performance of the control strategy are presented in this chapter.

Chapter 7 presents a distributed cooperative control strategy for air-conditioning systems based on the multi-agent system to perform building fast demand response. The control architecture is deployed on field control stations of corresponding terminals (i.e., valves and dampers) based on the environmental variable measurements of individual air-conditioned spaces. The multi-agent system comprises agents that act as local controllers for their respective terminals, working in collaboration to achieve an even cooling distribution. The fundamental control mechanism and operational procedures, the test arrangement, and the performance evaluation of the control strategy are presented in this chapter.

Chapter 8 presents the implementation of reconfigurable feedback control for supply-based cooling management in the limited cooling supply situations throughout the entire building daily cycle, including the morning start period, demand limiting period and soft stop period. The implementation incorporates the detailed control strategy architecture along with corresponding hardware placement. Hardware-in-the-loop control tests are conducted for validation.

Chapter 9 summarizes the main contributions of this PhD study and outlines the future directions for research based on the findings and contributions of this study.

CHAPTER 2 LITERATURE REVIEW

The efficient control of HVAC systems is of paramount importance in today's world, where energy conservation and sustainability have become critical concerns. HVAC systems typically account for a significant portion of a building's energy consumption, making it essential to optimize their operation to reduce energy usage and minimize environmental impact. Additionally, with the increasing integration of renewable energy sources into the power grid, HVAC control must also be responsive and adaptable to fluctuating energy availability and demand. This chapter presents a comprehensive literature review on conventional feedback control principles, applicability, and applications, HVAC controls for enhancing energy efficiency and facilitating building-grid interaction, which aims to provide a thorough understanding of the existing research and reveal the problems and limitations of conventional control in demand limiting and building-grid interaction. Section 2.1 focuses specifically on feedback control principles, applicabilitys and applications. In Section 2.2 and Section 2.3, HVAC controls for enhancing energy efficiency and facilitating building-grid interaction are reviewed, respectively. Section 2.4 focuses on the problems and limitations of conventional control in demand limiting and building-grid interaction. Finally, in Section 2.5, a summary of research gaps identified in the existing literature is provided to propose novel approaches and methodologies in subsequent chapters.

2.1 Feedback control principle, applicability and applications

Feedback control is a fundamental principle used in various fields to regulate and maintain desired system behavior. It operates based on a closed-loop control system, where the output or performance of the system is continuously measured, compared to a desired setpoint or reference value, and used to adjust the system's inputs or actions. The feedback control loop consists of four main components: a sensor or measurement device, a controller, an actuator, and a process or system being controlled. The sensor measures the system's output, which is then compared to the desired setpoint by the controller. The controller calculates the necessary corrective action and sends control signals to the actuator, which adjusts the system's inputs to bring the output closer to the desired setpoint. The feedback control aims to minimize the difference or error between the actual output and the desired state by continuously adjusting the system's inputs. This iterative process ensures that the system remains stable, accurate, and responsive to changes in operating conditions or disturbances (Doyle et al., 2013). The applicability of feedback control is widespread across various engineering, scientific, and technological domains. It is commonly used in control systems for mechanical, electrical, chemical, and other control processes. It is also applied in automation, robotics, information systems, biological systems, environmental monitoring, and social and economic systems. It is particularly useful in situations where precise regulation, stability, and adaptation to changing conditions are required. It provides a robust and reliable approach to maintain desired system behavior and performance in the presence of uncertainties, disturbances, and dynamic changes.

Feedback control plays a crucial role in HVAC systems by ensuring precise regulation, energy efficiency, and indoor comfort. By continuously monitoring and adjusting system parameters based on feedback from sensors, HVAC systems can maintain desired setpoints, optimize energy consumption, and provide occupants with a comfortable and healthy indoor environment. As long as the cooling supply can meet the demand, the control system can effectively regulate the system operation to maintain desired setpoints. Such feedback controls are, actually, “demand-based feedback control” (S. Wang & Tang, 2017). The building automation system (BAS) is a conventional and effective tool for efficient management of the building HVAC systems and the control functions can be divided into local control functions and supervisory control functions (S. Wang & Ma, 2008). By using building automation systems, the control strategies developed can be applied in real buildings. For local control functions, one of the most commonly-used control strategies is the demand-based feedback control, where the PID control is commonly used (Tang, Wang, Shan, et al., 2018). With the local PID control, a building zone can maintain the indoor temperature setpoint by controlling the terminal units such as the air handling units (AHUs) to modulate the cooling intake from the central cooling systems when the cooling supply is sufficient. The demand-based feedback control with the PID controllers is a mature technology, it can track the control set-point with acceptable accuracy, adaptiveness and simplicity, so it is widely used in a building’s local control functions and the research in PID control has never ceased (Geng & Geary, 1993; Tang, Wang, Shan, et al., 2018).

2.2 HVAC controls for enhancing energy efficiency

Energy and environmental issues are critical concerns that have gained significant attention in the past decades. As the world's population continues to grow and industrialization expands, the demand for energy has skyrocketed, leading to a range of environmental challenges. The production, distribution, and consumption of energy have profound implications for the environment, including climate change, air and water pollution, etc. The building energy consumption plays a significant role in the broader context of energy and environmental issues, given the increasing demand for commercial spaces and the need for sustainable practices with the growth of urbanization and industrialization. Energy-efficient buildings are designed and constructed to optimize energy performance while minimizing the use of resources. By significantly reducing energy consumption, these buildings contribute to greenhouse gas emissions reduction, conserve resources, and promote sustainable practices. Air-conditioning systems account for a significant portion of a building's energy usage, making their efficient control vital for overall energy performance.

Conventional control methods often rely on fixed setpoints and schedules, which can result in unnecessary energy wastage and discomfort for occupants. For the supervisory control, also known as optimal control, it aims at choosing the best local control setpoints to minimize or maximize an objective function, such minimizing energy consumption, operating cost etc. (S. Wang & Ma, 2008). For energy-efficient buildings, optimal control strategies of the air-conditioning systems focus on minimizing energy consumption while maintaining occupant comfort. This involves dynamically adjusting temperature setpoints, ventilation rates, and airflow distribution based on actual needs. By utilizing occupancy sensors, occupancy patterns can be analyzed to determine optimal operation schedules and adjust cooling or heating levels in unoccupied zones. Additionally, weather forecasts and indoor/outdoor temperature differentials can be considered to optimize cooling and reduce reliance on energy-intensive mechanical cooling. Many studies have been conducted in the domain of optimal control for HVAC systems (Álvarez et al., 2013; Liang et al., 2015; Lu et al., 2022; S. Wang & Ma, 2008).

With the rapid development of big data, computing resources, and advanced algorithms, machine learning has been explored to improve the building control performance (Hong et al., 2020). Reinforcement Learning (RL), as a branch of machine learning specifically for control problems, is becoming a promising method to revolutionize building controls (Z. Wang & Hong, 2020). Zhang et al. (Zhang et al., 2019) proposed a control strategy based on deep reinforcement learning for a radiant heating system and the results showed that, compared with the rule-based control, the proposed control strategy could achieve 16.7% heating demand reduction with more than 95% probability. Zou et al. (Zou et al., 2020) also implemented the deep reinforcement learning algorithms for optimal control over the AHUs, they revealed that the deep reinforcement learning agents could achieve 27%–30% energy saving comparing to the actual energy consumption. As a popular application of AI (Artificial Intelligence), machine learning has been studied widely for enhancing the building control performance, but it is worth mentioning that the implementation of AI-assisted control strategy in real application is still an ongoing research endeavour (Halhoul Merabet et al., 2021), mainly due to the data-demanding and time-consuming problems of the machine learning methods. In addition, the security of on-site application of such AI-assisted control strategy (e.g. RL controller) also needs to be addressed (Z. Wang & Hong, 2020). It can be concluded that integrating advanced AI algorithms into building automation systems is promising to formulate smart control strategies for building HVAC systems to enhance the energy efficiency. Moreover, the advanced control strategies should be convenient and reliable enough for real applications.

2.3 HVAC controls for facilitating building-grid interaction

On the supply side, renewable energy has emerged as a crucial solution to address the pressing energy and environmental challenges. Renewable energy sources offer a sustainable and clean alternative, harnessing the power of natural resources such as sunlight, wind, water, and geothermal heat. This form of energy generation not only reduces greenhouse gas emissions and air pollution but also helps mitigate climate change and promote a more sustainable future. Grid- interactive buildings are designed to actively interact with the electrical grid, enabling bi-directional energy flows and providing flexibility to support grid stability and resilience. These buildings have the capability to adjust their energy usage patterns, such as shifting loads or curtailing demand during peak periods, in response to grid demands or price signals. Overall, grid-interactive buildings have become increasingly important in recent years due to the growing demand for energy and the need to reduce greenhouse gas emissions.

In the context of grid-interactive buildings, air-conditioning systems can actively contribute to grid stability and support the integration of renewable energy sources. These buildings can respond to grid signals, such as peak demand periods or variable electricity pricing, by adjusting their cooling loads or shifting energy usage to non-peak hours (J. E. Braun, 1990). This demand response capability helps alleviate strain on the grid during high demand periods and enables the utilization of excess renewable energy generation by temporarily increasing cooling loads or charging thermal energy storage systems. Moreover, control strategies for grid-interactive buildings can facilitate the provision of grid services, such as frequency regulation (Vrettos et al., 2018a, 2018b). By participating in grid operations, air-conditioning systems can dynamically adjust their power consumption to help maintain grid stability and support the reliable integration of intermittent renewable energy sources.

2.4 Problems and limitations of conventional control in demand limiting and building-grid interaction

For commercial buildings, their air-conditioning systems are usually switched on before office hours in the morning, known as precooling. It is an effective and essential means to creating an acceptable indoor environment at the beginning of the office hours (Tang, Wang, Shan, et al., 2018). However, extended precooling time can cause serious energy waste, so the length of precooling time is important for enhancing the energy efficiency, especially for large commercial buildings. Therefore, an effective control strategy for building air-conditioning systems to shorten the morning start period is very important.

For precooling control, previous studies mainly focused on predicting the time required to cool down a building from the night setback condition by applying the optimal start algorithms. Seem et al. (Seem et al., 2016) made a comparison of 57 models for estimating the return time from a night setback condition and they recommended the room air temperature and the exponentially weighted moving averages (EWMA) of the normalized heating or cooling demand should be considered as predictor variables for the optimal start algorithms. Gunay et al. (Gunay et al., 2019) developed a morning start algorithm using a data-driven method. They proposed a clustering-based method by using a dataset from a large office building and their results show that the potential saving by tuning daily start times was estimated to be 7% for cooling. It is obvious that the building precooling at morning start period is beneficial but the extended precooling time should be avoided.

The cooling demand of commercial buildings is usually very high at morning start period, the indoor temperatures of individual building zones are much higher than their corresponding setpoints, but the cooling supply from central cooling plant is usually limited and each air-conditioned zone competes for the limited cooling supply. In this situation, all the terminal units such as water valves and air dampers would be fully open under the traditional PID feedback control, the cooling-down speed between individual zones is often significantly varied due to the differences between hydraulic resistances and pressure losses associated with different terminal units. This imbalanced cooling distribution would result in extended precooling time to allow all the building zones to reach their temperature setpoints at the start of office hours. This problem is well-illustrated through on-site data collected from a super-high-rise commercial building in Hong Kong by Tang et al. (Tang, Wang, Shan, et al., 2018), and they proposed an optimal control strategy for morning start period to optimize the limited cooling supply distribution among the building zones. However, there are some limitations to the implementation of the presented method in (Tang, Wang, Shan, et al., 2018). First, the existing method requires a physical water flowmeter to be installed for each AHU, but flowmeters are rarely installed in individual AHUs due to the high cost for practicalapplications. In addition, this existing method requires additional experimental work for the thermodynamic characteristic parameter identification of individual building zones, requesting serious effort, especially for large commercial buildings.

Building fast demand response is of particularly high value to satisfy urgent power balance needs in grids. But resetting the indoor air temperature setpoints cannot fulfill the requirements of fast demand response (i.e., respond within minutes). This is because the conventional control strategies of air-conditioning systems are cooling demand-based controls and inevitable delays would be resulted from the demand-based control process (S. Wang & Tang, 2017). Actually, chillers are the major energy consumers in central air-conditioning systems especially for large commercial buildings (Shan, Wang, Gao, et al., 2016). Shutting down part of the operating chillers is an effective demand limiting method when the power grids need an immediate power reduction on the demand side. However, simply shutting down some operating chillers would result in disordered chilled water flow distribution and uneven indoor thermal comfort degradation (Shan, Wang, Yan, et al., 2016; Xue et al., 2015). To address this problem, Tang et al. (Tang et al., 2016) proposed a power limiting control strategy based on an adaptive utility function by updating the chilled water flow setpoints of individual zones online. The test results show that the proposed control strategy could solve the problem of disordered water distribution and achieve evenly-spread thermal comfort compromises among different building zones under fast demand response. Wang and Tang (S. Wang & Tang, 2017) also pointed out that excessive speeding of chilled water pumps would occur, under conventional demand-based controls, in such cases with limited cooling supply, leading to extra power consumption and thus reducing the demand reduction effect of demand/power limiting control. So, they proposed the concept of supply-based feedback control and developed a cooling distributor based on adaptive utility function.

However, there are still some problems with these control strategies for real implementation. First, the implementation of these adaptive utility function-based control strategies requires measurement of chilled water flow rate through each air handling unit (AHU). In this situation, physical water flowmeters need to be installed for individual AHUs. However, such water flowmeters are rarely installed in practice due to the high investment cost. Second, these control strategies require additional work for the parameter identification of the thermodynamic characteristics of building zones, making them inconvenient for practical implementation, especially for large commercial buildings. Ran et al. (Ran et al., 2020) developed a virtual flowmeter to estimate the water flow rates through individual AHUs. However, the modeling of the virtual flow meter needs extra measurements on the air side and the accuracy of the model cannot be guaranteed in real implementation. Third, these control strategies adopt a periodic mechanism to trigger the control actions at equidistant sampling intervals (known as time-driven control), even though the optimization tasks and control actions may not be necessary at some intervals (Åarzén, 1999; Heemels et al., 2008). There are considerable studies using the event-driven control method in the HVAC field. Wang et al. (J. Wang et al., 2016) proposed an event-driven optimal control strategy for the complex HVAC systems. The results show that the event-driven optimization could significantly reduce the computational load (60-84%) without sacrificingenergy performance, when compared with conventional time-driven optimization. Wang et al. (J. Wang et al., 2021) further proposed a data-mining-powered event-driven optimal control strategy for improving operation efficiency of HVAC systems. The results show that the energy saving could be improved by 0.9%-4.6% compared with the conventional time-driven control strategy. Besides, the event-driven optimal control strategy was easy for implementation and could be easily understood by the designers, engineers and building operators. Li et al. (W. Li et al., 2021) proposed an event-driven multi-agent based distributed optimal control strategy for HVAC systems. The results show that the proposed control strategy could provide satisfactory system performance while reducing the energy consumption of IoT (Internet of Things) sensors. The previous studies have proven the effectiveness of the event-driven control method in reducing unnecessary control actions in the energy-efficient control of HVAC systems. However, rare application of fast demand response control has been observed. Existing studies of fast demand response control

(Ran et al., 2020; Tang et al., 2016; Tang, Wang, & Shan, 2018; S. Wang & Tang, 2017; Xue et al., 2015) all adopt the conventional time-driven control. This could lead to high optimization frequency and computational burden especially for large complex systems, as well as increased wear and tear of system components (e.g., water valves of AHUs).

Besides, existing HVAC-based fast demand response strategies (Ran et al., 2020; Tang et al., 2016; S. Wang & Tang, 2017; Xue et al., 2015) all adopted centralized control approaches that depend on a central controller to gather and analyze data from the entire air-conditioning system. This would placet the entire burden on one central station and result in high computational complexity. Such control methods also lack generality. It would be inconvenient to reconfigure/redesign the control system for large commercial buildings if their air-conditioning systems are retrofitted. Distributed control methods present an effective solution to these problems. The distributed control methods refer to techniques and algorithms used to achieve decentralized decision-making and coordination among multiple subsystems/components based on local information and local interactions. In this way, distributed control methods do not need to rely on the central controller to makes all the decisions for the whole system like the traditional centralized control methods. They can leverage the capabilities and intelligence of individual subsystems/components to achieve more efficient control. The Internet of Things (IoT) has experienced a significant expansion in the past few years, which has made the implementation of distributed control methods more practical and allows the field data to be stored, processed and analyzed at the edge side with the use of edge intelligence methods (B. Li et al., 2022; Su & Wang, 2020). Distributed control can be effectively achieved through the agent-based method, which involves using agents to represent various components and subsystems.

These agents are capable of communicating, negotiating and making decisions autonomously, without the need for operator intervention (Windham & Treado, 2016). Previous studies on agent-based distributed control of HVAC systems mainly focus on improving building energy efficiency and indoor thermal comfort (Su & Wang, 2020). However, the agent-based control of building air-conditioning systems for fast demand response has not been extensively studied in the existing literature.

2.5 Summary of research gaps

This chapter presented a comprehensive review on feedback control principles, applicability and applications, HVAC controls for enhancing energy efficiency and facilitating building-grid interaction; and problems and limitations of conventional control in demand limiting and building-grid interaction. Conventional automatic control strategies utilized in building central air-conditioning systems adopt demand-based feedback control. However, the demand-based control fails to properly manage the cooling distribution when cooling supply is limited. How to apply the concept of supply-based control from theoretical and practical perspectives remains unre solved. From the above review, the detailed existing gaps can be summarized as follows:

- Air-conditioning systems in commercial buildings are usually switched on in advance to precool the indoor spaces to create an acceptable working environment upon office hours. However, the central cooling systems often fail to provide enough cooling supply capacity due to the high cooling demand at the morning start period, especially in hot seasons. The imbalanced cooling distribution in the air-conditioning systems often results in large difference of cooling-down speed among different building zones, leading to extended precooling time, leading to significant energy waste. A comprehensive and efficient approach to resolving this issue remains elusive.

- Air-conditioning systems have great potential to provide energy flexibility services to power grids of high-renewable penetration. Direct load control by switching off some operating chillers is the simplest and effective means for air-conditioning systems in buildings to respond to urgent power reduction requests from power grids. However, the implementation of this approach in today's buildings, which widely adopt demand-based feedback controls, results in serious problems, including disordered cooling distribution and likely extra energy consumption. The pursuit of effective and succinct solutions to this problem continues.
- Modern building automation systems rely on digital controllers at the field level for the centralized control and monitoring of HVAC systems in buildings. Based on the existing architecture of building automation system, the implementation issues of integrating supply-based control and demand-based control remain challenges.
- The implementation of detailed control strategy architecture, along with corresponding hardware placement for supply-based cooling management in limited cooling supply situations (i.e., morning start period, demand limiting period and soft stop period) is needed to become a new norm for future buildings to facilitate the high renewable penetration of the power system towards carbon neutrality.

CHAPTER 3 CONCEPT OF SUPPLY-BASED CONTROL AND FRAMEWORK OF THE PROPOSED CONTROL STRATEGIES

This chapter introduces the concept of supply-based control and presents the framework of the proposed control strategies. Section 3.1 provides an introduction to the conventional demand-based control approach commonly used in the existing building automation system, and then presents the concept of supply-based control as an alternative approach to address the problems arising from insufficient cooling supply. Section 3.2 indicates the needs and contributions of supply-based control in the entire building daily cycle. In Section 3.3, the framework of the proposed control strategies that are based on the concept of supply-based control in this PhD study is presented.

3.1 Concept of supply-based control

Conventional process control for building and industrial processes typically adopts closed-loop feedback controls. The basic principle of closed-loop feedback controls is the utilization of feedback information from the controlled variable to regulate and stabilize the system. By continuously measuring the output or performance of the system, the control system can dynamically adapt and respond to changes or disturbances, ensuring that the desired setpoint is achieved and maintained (S. Wang, 2009). The basic components of a closed-loop feedback control system include a sensor to measure the system output, a controller to process the feedback information and generate control signals, and an actuator to adjust the system inputs based on the control signals. These components work together in a closed-loop fashion, where the output is fed back to the controller to continuously adjust and optimize the control actions. When applied to air-conditioning systems in commercial buildings, such feedback control works to meet the demand (i.e., specific requirements for cooling) of the air-conditioned spaces. The measurements of the controlled variables are compared to the desired setpoints, and the control system determines the appropriate control actions based on this comparison. As long as the cooling supply can meet the demand, the control system can effectively regulate the system operation to maintain desired setpoints. Such feedback controls are, in fact, "demand-based feedback control" as shown in Figure 3.1.

The basic idea of demand-based feedback control involves adjusting the cooling supply based on the demand signals received from individual zones or spaces within a building. These demand signals, i.e., indoor air temperature setpoints and supply air temperature setpoints, are used to determine the cooling requirements of each zone. The control system (i.e., regulators in Figure 3.1) then adjusts the cooling distribution accordingly to meet these demands by adjusting the VAV dampers and AHU valve openings. However, demand-based control has inherent limitations; when the cooling supply is insufficient, the existing control systems would suffer from serious operational problems including, including significant imbalances in chilled water distribution among terminal units, over-speeding of pumps and fans.

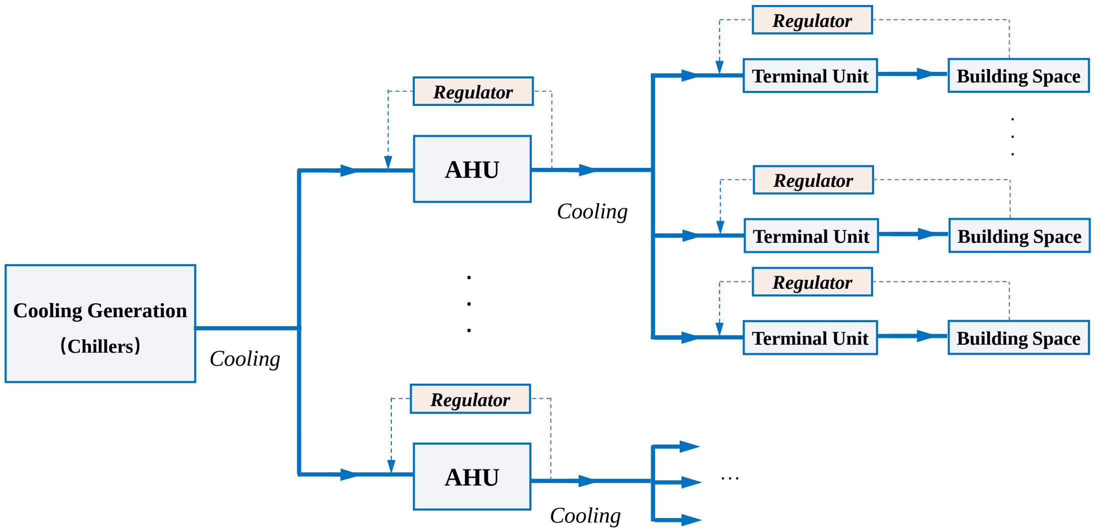

Figure 3.1 Schematic of demand-based feedback control

To deal with these problems resulting from improper cooling distribution, the concept of supply-based feedback control is proposed as an effective approach when the cooling supply from the air-conditioning system is limited as shown in Figure 3.2 (S. Wang & Tang, 2017). In contrast to conventional demand-based control, the feedback in this approach (i.e., the distributor as shown in Figure 3.2) relies on end-user inputs, specifically the indoor temperature of the space, rather than utilizing immediate outlet measurement, i.e., the supply air temperature of air handling unit (AHU), to determine the control outputs. In summary, while demand-based feedback control has been widely used in HVAC systems and industrial applications, it faces limitations in scenarios with insufficient cooling supply. Supply-based control, on the other hand, offers a more dynamic and flexible approach by considering the available supply capacity and optimizing the distribution of cooling resources. By incorporating real-time data analysis and advanced control algorithms, supply-based control aims to achieve improved energy and environmental performance. The control strategies proposed in this PhD study are based on the concept of supply-based control.

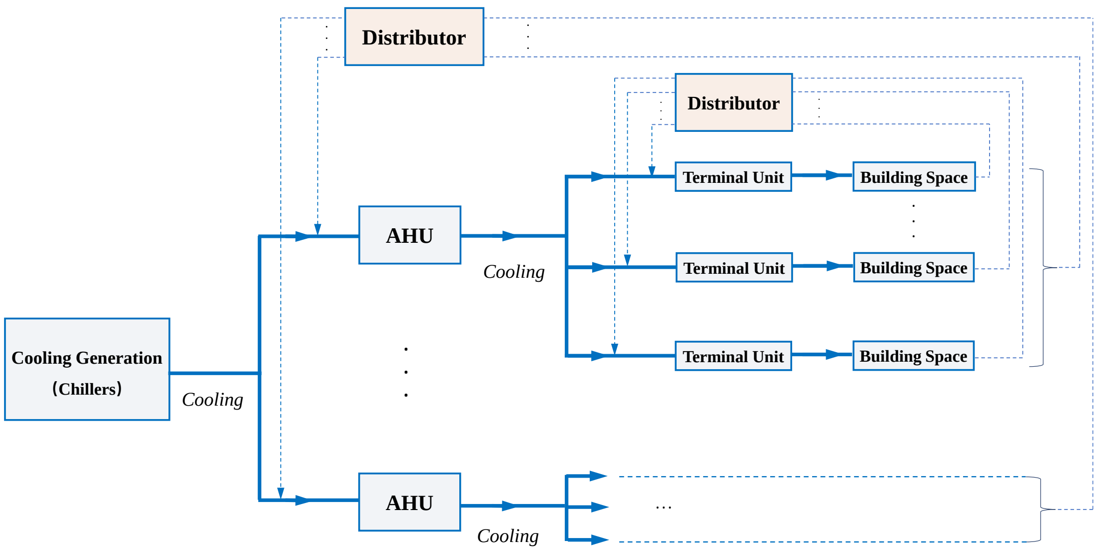

Figure 3.2 Schematic of supply-based feedback control

3.2 Needs and contributions of supply-based control in entire building daily cycle

In the entire building daily cycle, conventional controls fall short in the following scenarios where the available cooling supply is inadequate to meet the cooling demand.

- ***Morning start***: To establish a comfortable working environment during office hours, the central air-conditioning systems in buildings are usually switched on in advance to precool the indoor spaces (Tang, Wang, Shan, et al., 2018). During the morning start period, the buildings often experience a surge in cooling demand, which exceeds the cooling capacities of the central cooling plants. In this situation, different air-conditioned spaces compete for the limited cooling supply under conventional feedback controls, resulting in an uneven cooling distribution due to different hydraulic resistances and pressure losses. Consequently, the duration of precooling (i.e., determined by the time for the latest air-conditioned zone to reach its desired indoor temperature setpoint) would be extended, thereby compromising building energy efficiency.

- ***Demand limiting***: The air-conditioning systems may need to limit their energy consumption below a predetermined threshold through switching off some operating chillers (Xue et al., 2015). This approach is simple and effective, allowing buildings to provide fast demand response during peak demand periods when there is a grid request for immediate reduction in energy consumption, typically during peak demand periods. However, in this situation, indoor temperature rise is unavoidable due to the limited cooling supply. Imbalanced temperature rises among different spaces would occur due to the uneven allocation of the limited cooling supply under the conventional feedback controls. In addition, excessive speed of chilled water pumps in this situation would undermine effectiveness of demand response.
- ***Soft stop***: Switching off some operating chillers prior to the end of office hours is an effective approach to enhance energy efficiency in commercial buildings (Shan et al., 2019). The buffering effect resulting from building thermal inertia helps to maintain a relatively comfortable indoor environment for occupants while the cooling supply decreases during the soft stop period (J. Braun et al., 2001; Shan et al., 2019). However, this approach also introduces a competition of the limited cooling supply among the air-conditioned zones. Similar problems, including uneven temperature rises, imbalanced thermal comfort sacrifices among building zones, and additional pump energy consumption, would arise under conventional feedback controls, and undermine the overall energy efficiency of buildings.

By adopting supply-based controls in this PhD study, energy-efficient and grid-interactive cooling management can be achieved in the entire building daily cycle, including the morning start period, soft stop period and demand limiting period.

3.3 Framework of the proposed control strategies

Figure 3.3 shows the framework of the proposed control strategies in this PhD study. The development of the control strategies is based on the supply-based control, as illustrated in Section 3.1. However, applying this concept in practice inevitably faces several challenges. The first challenge is to develop a basic supply-based feedback control in existing building automation systems. Addressing this point, in this PhD study, a basic reconfigurable supply-based feedback control (**Chapter 4**) is creatively proposed for real application. The second challenge lies in developing advanced control strategies for the special enhancement of the supply-based control. Three advanced control strategies, including the iterative learning control strategy (**Chapter 5**), the event-driven driven control strategy (**Chapter 6**) and the multi-agent based control strategy (**Chapter 7**), are proposed to address the issue of limited cooling distribution in various scenarios (e.g., morning start period and demand limiting period). These strategies are theoretically analyzed and designed to provide solutions for efficient implementation. Finally, in order to deploy the control strategies in practice for the entire building daily cycle, the implementation (**Chapter 8**) of the reconfigurable feedback control is developed for supply-based cooling management in limited cooling supply situations, including the morning start period, demand limiting period and soft stop period.

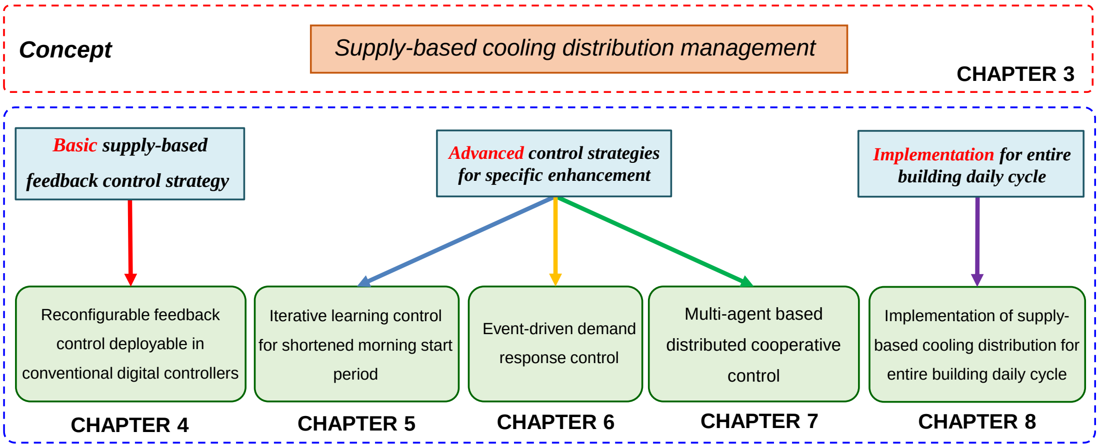

Figure 3.3 Framework of the proposed control strategies

CHAPTER 4 RECONFIGURABLE FEEDBACK CONTROL DEPLOYABLE IN CONVENTIONAL DIGITAL CONTROLLERS

In order to develop a basic supply-based feedback control in existing building automation systems, this chapter proposes a reconfigurable supply-based feedback control for air-conditioning systems, which integrates supply-based feedback control, for demand limiting control under limited cooling supply, and demand-based feedback control under normal operation with sufficient cooling supply. Section 4.1 introduces the concept of reconfigurable supply-based feedback control strategy. The proposed control strategy is deployed in a typical commercial digital controller and tested by conducting hardware-in-the-loop control tests as illustrated in Section 4.2. Section 4.3 analyzes the test results of control performance, environmental and energy performance. Conclusive remarks of this chapter are presented in Section 4.4.

4.1 Concept of reconfigurable supply-based feedback control strategy

4.1.1 Principle of feedback loop reconfiguration

Figure 4.1 depicts the block diagram of the reconfigurable feedback control. The basic mechanism of the proposed reconfigurable control is to adjust or reconfigure the feedback control loop online to match different needs or objectives of the controls under demand limiting with limited resource/supply and under normal conditions with sufficient supply. The strategy can be deployed in the commonly-used digital controllers of building automation systems, facilitating the possibility and convenience of its wide implementation. The control loop reconfiguration scheme reconnects the controlled variable when switching the control mode from one to another. In the implementation case of this study, Process 1 refers to the AHU, while Process 2 refers to the building zone. As the dynamics of the controlled processes managed by the same digital controller in two different control modes are different, the parameters of the feedback controller are reset to enable smooth transition between the two different control modes. The setpoint reset scheme determines the setpoint of the feedback controller. In the system under consideration, the controlled variables are the AHU valve openings. In normal operating mode (demand-based feedback control), the operational objective is maintaining a specific supply air temperature. When the fast demand response is conducted, specific chillers are shut down immediately. The control objective is to achieve proper cooling distribution. The detailed working mechanism of the control loop reconfiguration scheme and the setpoint reset scheme is elaborated in the following section (i.e., Chapter 4.1.2).

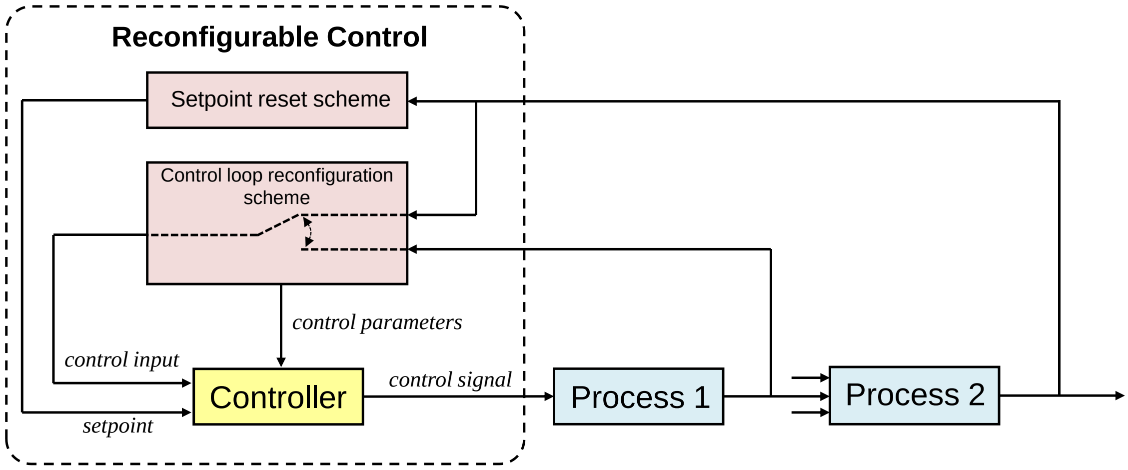

Figure 4.1 Block diagram of the feedback loop reconfiguration

4.1.2 Reconfigurable feedback control strategy

4.1.2.1 Basic feedback control law

Eq. (4.1) shows the basic control law of a basic PID controller (Astrom, 1995), where, *u(t)* is the control signal and *e(t)* is the error signal at time *t*. The PID controller continuously calculates this control signal based on the error signal and the proportional gain *K*, the integral time T_i and the derivative time T_d, to control the controlled process output at the desired setpoint. *y* is the controlled variable and y_{sp} is the setpoint for the controlled variable. The PID control law consists of three terms as shown in Eq. (4.1). The proportional term provides a direct relationship between the error and the control output. The integral term integrates the error over time, which helps to eliminate steady-state errors. The derivative term anticipates future errors by measuring the change rate of the error.

$$u(t) = K\left(e(t) + \frac{1}{T_i}\int_0^t e(\tau)d(\tau) + T_d\frac{de(t)}{dt}\right) \tag{4.1}$$

$$e(t) = y_{sp}(t) - y(t) \tag{4.2}$$

In the normal operating mode (i.e., demand-based control), the AHU valve position is adjusted to maintain a specific supply air temperature. In this situation, the controlled variable is the supply air temperature. A combination of proportional and integral control (i.e., PI control) is often used in practical applications.

4.1.2.2 Supply-based feedback control and control loop reconfiguration scheme

Figure 4.2 illustrates the schematic of the air-conditioning system in consideration, the supply-based feedback control and the control loop reconfiguration scheme. In both control modes, the controller adopts the feedback control law as described in Chapter 4.1.2.1. In normal control mode (demand-based feedback control), the controlled variable (y_i) of an AHU control is the AHU supply air temperature as shown in Eq. (4.3). Its control setpoint is determined according to the needs of sensible and latent cooling demands, typically given as a fixed value such as 15 ℃, which might be optimized and reset according to changes in load conditions. When the demand limiting mode is activated, some operating chillers will be switched off immediately and only limited (cooling) supply is available. In such conditions, the cooling distribution among AHUs would be disordered if the same demand-based feedback control is used. To solve this problem, a supply-based feedback control is introduced. In supply-based feedback control mode, the controlled variable (y_i) of an AHU control is indoor air temperature in the corresponding zone represented by the returned air temperature from the zone, as shown in Eq. (4.4). In order to maintain a uniform temperature among different zones, which is the objective of adopting supply-based feedback control, a common control setpoint is used for the AHU control loops of all zones. As the cooling supply is insufficient to maintain a constant or preferable comfort temperature, the control setpoint in this mode is adjusted adaptively as elaborated in Chapter 4.1.2.3.

$$y_i(t) = T_{sup,i}(t) \tag{4.3}$$

$$y_i(t) = T_{zone,i}(t) \tag{4.4}$$

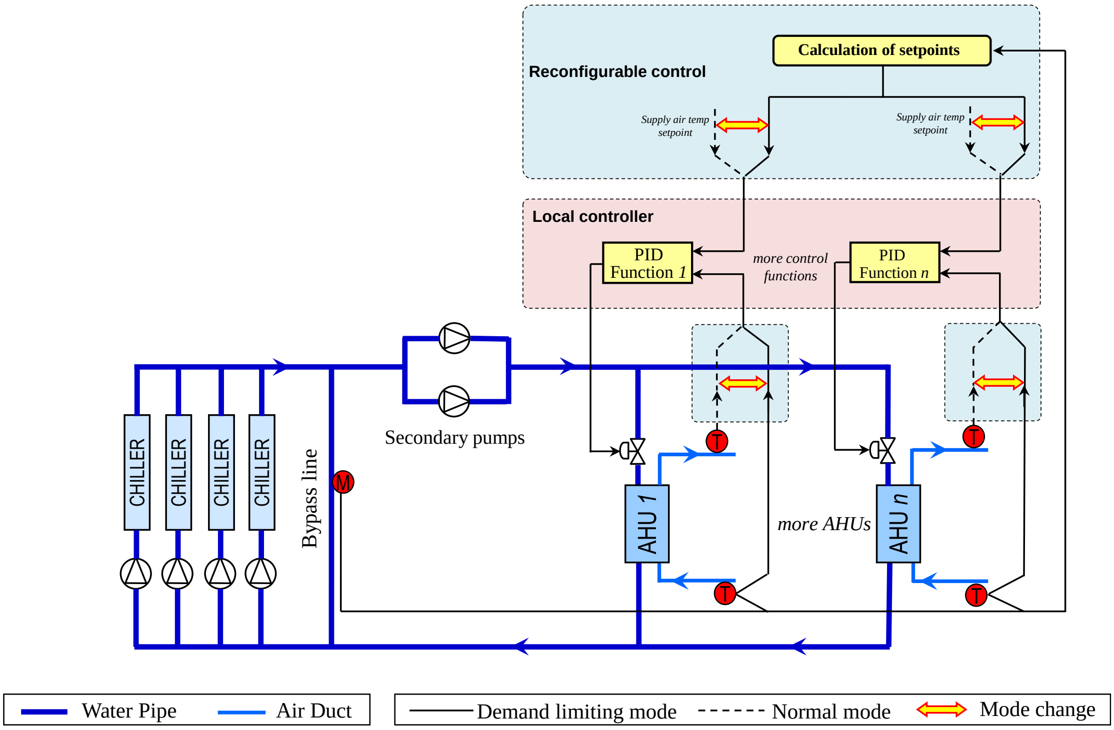

Figure 4.2 Schematic of the central air-conditioning system and the architecture of supply-based feedback control

4.1.2.3 Setpoint reset scheme

The setpoint for the AHU return air temperature control loops is reset according to Eq. (4.5), which consists of two terms. The first term is the average return air temperature. It aims to achieve uniform temperature among the zones. The second term is introduced as an adjustment term to consider the deficit water flow rate (i.e., M_{by}) in the bypass pipe, in order to eliminate the deficit flow in the demand limiting mode.

$$y_{sp}(t) = \frac{\sum_{i=1}^{n} T_{zone,i}(t)}{n} - a \cdot M_{by} \tag{4.5}$$

where, the coefficient a is adjustable to achieve better control performance for demand response. Figure 4.3 shows the process of control mode switching (i.e., transition from normal operation to demand response, and then reverts to normal operation). There are two transition processes (i.e., Switching 1 and Switching 2 in Figure 4.3) in the proposed control strategy switching from one mode to the other. Switching 1 denotes the transition from normal operation to demand response. At this moment, the control loop reconfiguration scheme is activated to enable demand limiting and proper distribution of limited cooling. Switching 2 denotes the transition from demand limiting mode back to normal mode, while the air-conditioning system ends the task of demand limiting. The chiller plant can now provide sufficient cooling supply as demanded to restore the indoor air temperature of the zones to their comfort setpoints. To ensure better control performance during the two switching moments and throughout the demand response and rebound periods, the parameter scheduling of coefficient *a* is implemented. The details for scheduling the parameter, i.e., coefficient *a*, are illustrated in Figure 4.4 and elaborated below.

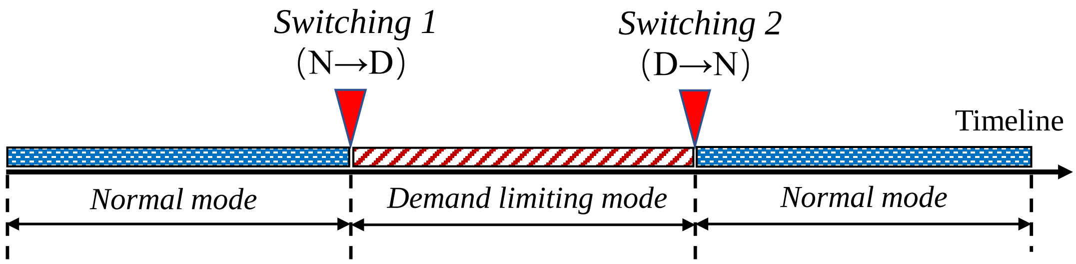

Figure 4.3 Process of the control mode switching

<u>*Parameter setting at Switching 1.*</u> At the switching moment from normal operation to demand response (i.e., Switching 1), the control loop reconfiguration scheme is activated to modify the inputs of the PID functions, as explained in Section 4.1.2.2. In the normal mode, the temperature in each building zone is regulated to the designated comfort setpoint of 24 °C, resulting in minimal deviation among zones. In order to eliminate the deficit flow as soon as possible, the initial value of coefficient *a* in Eq. (4.5) is set relatively high (i.e., a_0 in Figure 4.4).

Parameter setting during demand limiting mode. During the transition period following the switching 1, the purpose of setting coefficient a is to mitigate the deficit flow problem and prevent control instability. In order to achieve this, a decreasing parameter schedule is implemented for coefficient a starting from the initiation of the demand response event (i.e., t_A) for a short duration (from t_A to t_B). The parameter schedule is set by Eq. (4.6), where a_0 is the initial setting and r determines the decreasing speed. This approach ensures a gradual adjustment of coefficient a over the transition period following Switching 1, contributing to a controlled and stable system response during the demand response period.

$$a(t) = a_0 e^{-rt} \tag{4.6}$$

Parameter setting at Switching 2. At the switching moment from demand limiting mode to normal mode (i.e., Switching 2), the control objective is to properly distribute the available cooling supply in order to restore the temperature of these building zones to comfort setpoints. In this situation, coefficient a is set to 0 since the deficit flow problem is no longer a concern due to the sufficient cooling supply. However, considering the need to rapidly cool down the zones, the AHU valve openings should be relatively larger. Therefore, the reset of a back to 0 is delayed for a short period (i.e., from t_C to t_D in Figure 4.4) to facilitate a quicker cooling response.

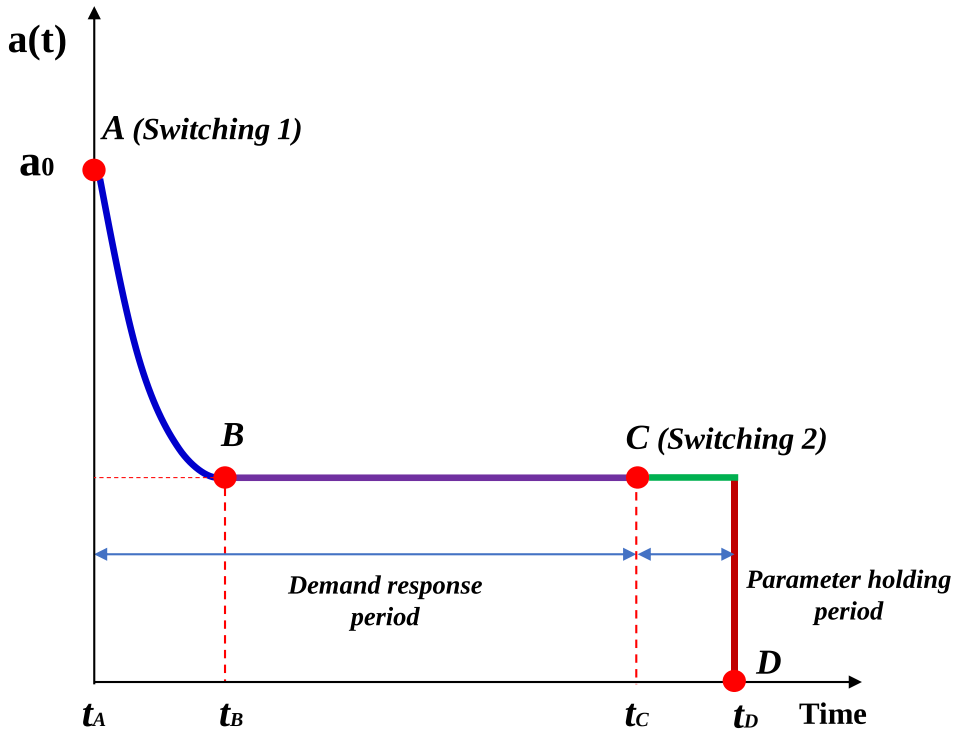

Figure 4.4 Parameter scheduling of coefficient *a*

4.1.2.4 Control performance indicators

To assess the control performance of cooling distribution, a temperature diversity indicator, denoted as *PI*, is proposed in Eq. (4.7). In this equation, PI_i represents the performance indicator for a specific zone *i* in the building, where, *n* denotes the total number of zones. The function of this indicator is to quantify the temperature diversity among the zones, aiming for a lower value to achieve the desired control objective of proper cooling distribution. Additionally, accumulated valve travel distance (AVTD) is utilized for quantifying the control stability of the AHU valves. AVTD is calculated using Eq. (4.8), where, Δu_t denotes the valve position modification during each sampling period *t*. *I* denotes the overall number of sampling periods within demand limiting mode.

$$PI_i(t) = \left| T_{zone,i}(t) - \frac{\sum_{i=1}^{n} T_{zone,i}(t)}{n} \right| \tag{4.7}$$

$$AVTD = \sum_{t=1}^{I} \Delta u_t \tag{4.8}$$

4.2 Arrangement of real-time hardware-in-the-loop tests

4.2.1 Hardware-in-the-loop test platform

To ensure the practical applicability regarding actual deployment and operation of the proposed control strategy, we have developed a hardware-in-the-loop experimental platform to closely simulate real-world conditions, as illustrated in Figure 4.5. This platform incorporates a physical programmable logic controller (PLC) as the feedback controller for regulating the valve openings of the AHUs within the central air-conditioning system. Specifically, we have employed a SIMATIC S7-1200 controller from Siemens as the hardware component of our platform. To accurately emulate the behavior of building thermal dynamics and various HVAC components (such as chillers, AHUs, hydraulic networks, etc.), we have constructed detailed physical models in TRNSYS. The simulated building represents a high-rise commercial structure located in Hong Kong. The software side is capable of managing dynamic processes associated with heat transfer, hydraulic properties, water balance, and energy conservation within the physical building and air-conditioning system.

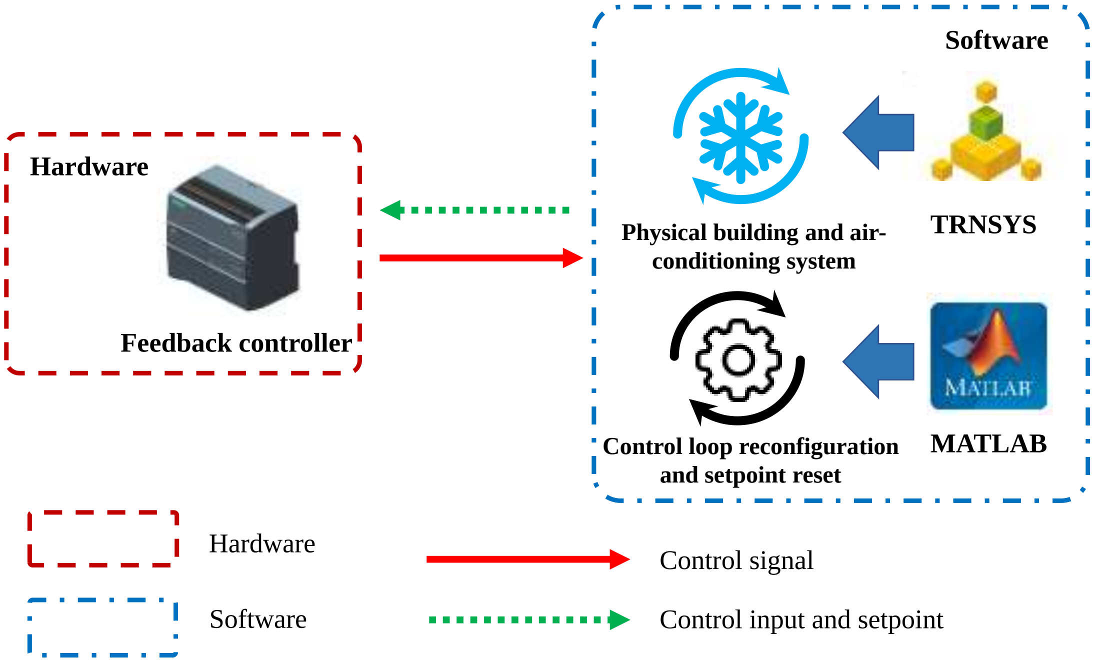

Figure 4.5 Hardware-in-the-loop test platform

Figure 4.2 illustrates the central air-conditioning system employed. It is a standard primary-secondary variable flow system. The chilled water system comprises four uniform-capacity duty chillers, each with a nominal capacity of 4,080 kW. The primary water pumps maintain a constant speed, each delivering a designated flowrate of 172.8 L/s. In the secondary chilled water circuit, two pumps with adjustable speeds are installed. These pumps allow for flexibility and control over the flowrate. The AHUs are in charge of delivering cooling to the various building zones. In this study, six typical building zones, each covering 1,600 m^2, are simulated to represent the entire air-side system of the building after multiplying their loads by a factor of 15. An AHU is installed to supply cool air to each zone. The building operates during office hours from 8:00 to 18:00. Throughout this period, all six zones maintain an indoor air temperature setpoint of 24 °C in normal operation.

4.2.2 Test arrangement

As shown in Figure 4.5, the hardware-in-the-loop platform establishes a connection between the physical hardware and the software component using the Modbus protocol. The hardware-in-the-loop test platform consists of a programmable logic controller (PLC) on the hardware side to deploy the reconfigurable control strategy, and software components including TRNSYS for building and air-conditioning system simulation and MATLAB. MATLAB is adopted for implementing supervisory schemes for the reconfigurable control, i.e., control loop reconfiguration and setpoint reset, which will typically be deployed in BAS network stations. The physical PLC receives control input and setpoint from the simulated virtual part of the platform. It then sends a control signal, specifically the AHU valve openings, back to relevant devices in the simulated virtual part of the platform. Half-day (12:00-24:00) real-time validation tests are conducted using the weather data on a typical summer day (July 23rd) in Hong Kong, while a two-hour demand response event from 14:00 to 16:00 is included. During this demand response event, two out of four operating chillers are switched off, while the two remaining chillers continue to operate. Comparative studies are performed to evaluate the performance of the control strategies.

Strategy I - Conventional control strategy. In this approach, conventional control is maintained. The AHU valve position is adjusted to maintain the same supply air temperature.

Strategy II - Reconfigurable control strategy without parameter scheduling. During the normal operating mode, the field digital controller adopts the conventional feedback control for AHU valve modulation. The feedback control loops for the six AHUs are set with the same proportional gain (K) of -0.005 and integral time (T_i)

of 50 seconds. The coefficient a in Eq. (4) is fixed at 0.05 throughout the demand response event.

Strategy III - Reconfigurable control strategy with parameter scheduling. This approach involves complete reconfigurable control as described in Chapter 4.1. The parameter scheduling method is employed to adjust the coefficient a (refer to Eq. (4)) according to the schedule outlined in Chapter 4.1.2.4. The duration of the decreasing parameter schedule (t_B - t_A) for coefficient a is set to 60 seconds, the duration for holding the value of coefficient a is set to 100 seconds (i.e., t_C - t_D), and the decreasing rate r in Eq. (4.8) is set to 0.05.

4.3 Test results of control performance, environmental and energy performance

4.3.1 Control performance

4.3.1.1 Valve opening

Figure 4.6 shows the valve opening profiles of the building zones under three different control strategies. Using the control strategy I, as shown in Figure 4.6 (a), the valve openings are increased to maintain the supply air temperature setpoints. All AHU valves reach their maximum opening positions within approximately 15 minutes and remain fully open throughout the two-hour demand response event. Furthermore, it is important to note that even after the demand response event ends, all valves continue to remain fully open for over 10 minutes. This indicates that when shutting down operating chillers for demand limiting, the cooling supply from the remaining chillers is insufficient to meet the cooling demand of terminal units.

Figure 4.6 (b) shows the valve opening profiles when using control strategy II. These test results indicate that, with fixed control parameters, strong oscillations occur in the valve opening control. The occurrence of such oscillations can be attributed to an excessive and fixed setting of coefficient *a*. Besides, the oscillations can cause mechanical wear and fatigue on these components, potentially reducing their lifespan and overall reliability.

On the contrary, the problem of control instability can be avoided under control strategy III, as shown in Figure 4.6 (c). The proactive adjustment helps alleviate the deficit flow problem very quickly. Moreover, the oscillation problem observed in control strategy II is effectively avoided through scheduling coefficient *a*. Once the demand response event ends at 16:00, the valve openings are generally adjusted to increase for a short period of 2 minutes. This adjustment ensures that more chilled water is provided to cool down the building zones effectively. Subsequently, the supply-based feedback control continues to adjust the valve openings for proper cooling distribution during the cooling down period. Figure 4.7 presents a comparison between the accumulated valve travel distances (AVTD) of control strategy II and control strategy III. The results show an average reduction of AVTD by 98% when replacing control strategy II with control strategy III. This reduction demonstrates the effectiveness of the proposed reconfigurable control strategy in achieving better control stability during fast demand response events.

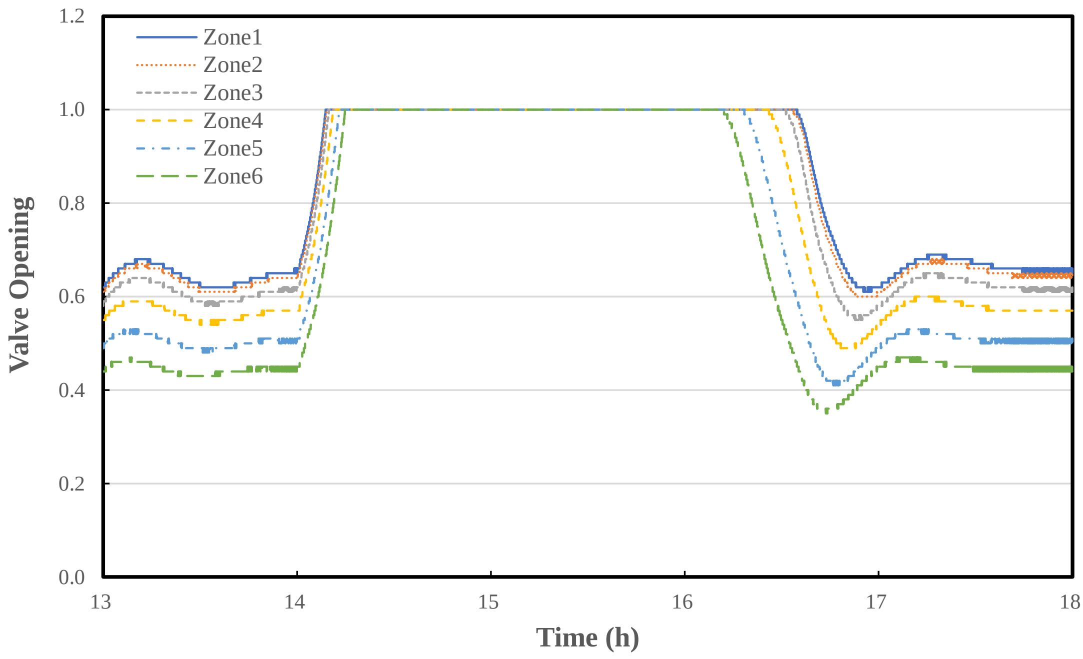

(a) Control strategy I

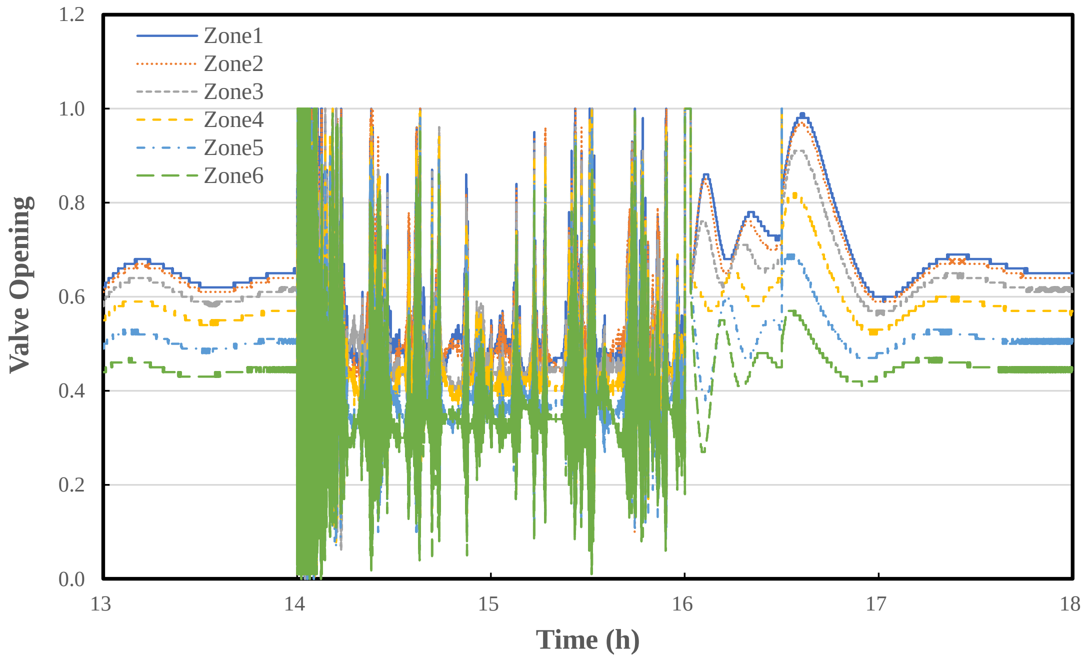

(b) Control strategy II

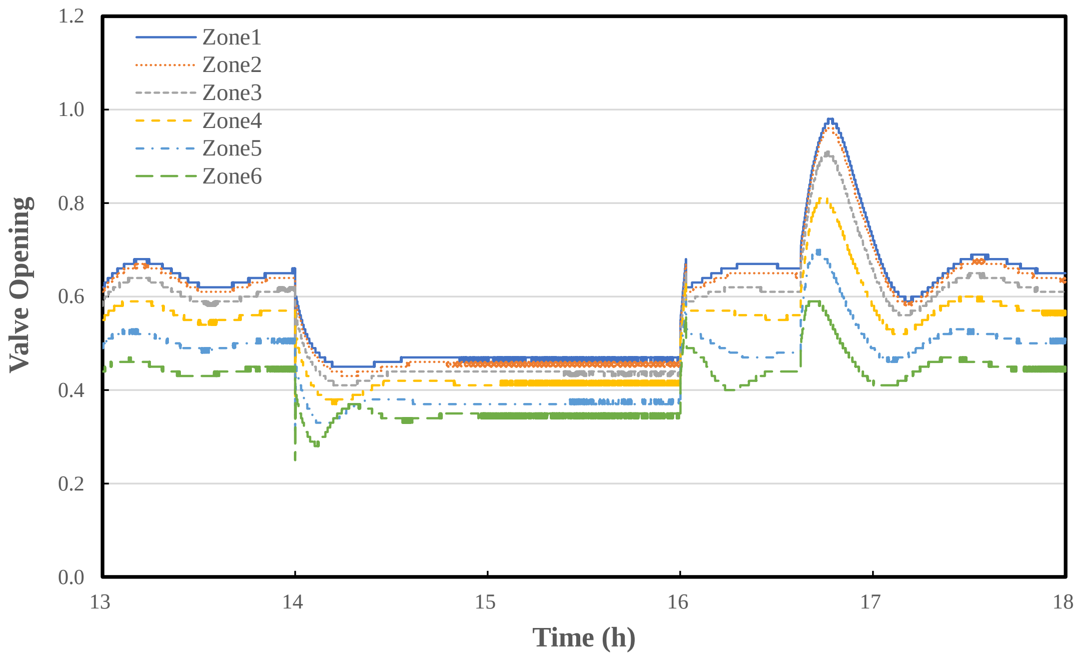

(c) Control strategy III

Figure 4.6 Valve opening profiles using different control strategies

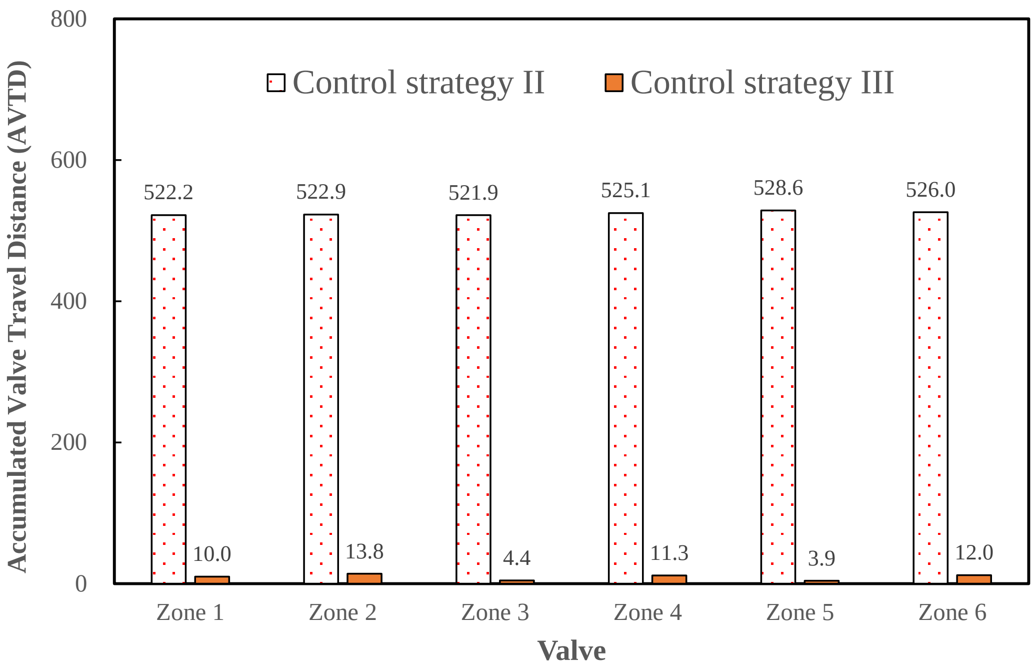

Figure 4.7 Comparation of accumulated valve travel distance between control strategy II and control strategy III

4.3.1.2 Chilled water distribution

Figure 4.8 shows the chilled water flowrates of different zones under different scenarios. Figure 4.8 (a) presents that the water flowrate distribution among zones is disordered when using conventional control. The chilled water flowrates of all zones begin to increase in correlation with the upward trend of the valve openings at 14:00. During this event, six AHU valves are controlled to be fully open. However, due to variations in hydraulic resistance among the AHUs, the distribution of chilled water becomes uneven. This disorderly distribution arises because the chilled water loop with lower resistance (e.g., AHU 6) receives a much larger share of chilled water than the distribution to other zones. Conversely, the chilled water loop at a more distant site (e.g., AHU 1) receives less chilled water, even when its valve has been already fully opened. The problem of uneven water distribution persists even after 16:00, during the rebound period. Figure 4.8 (b) presents the chilled water flowrate profiles using control strategy II. There are strong oscillations in valve opening control, resulting in oscillations in chilled water flowrate distribution. This instability in the system control leads to a decrease in the overall performance of the controlled process. However, the problem is eliminated in the test using control strategy III, as shown in Figure 4.8 (c). As discussed in Chapter 4.2.2, the proper adjustments in valve openings lead to a more appropriate distribution of chilled water.

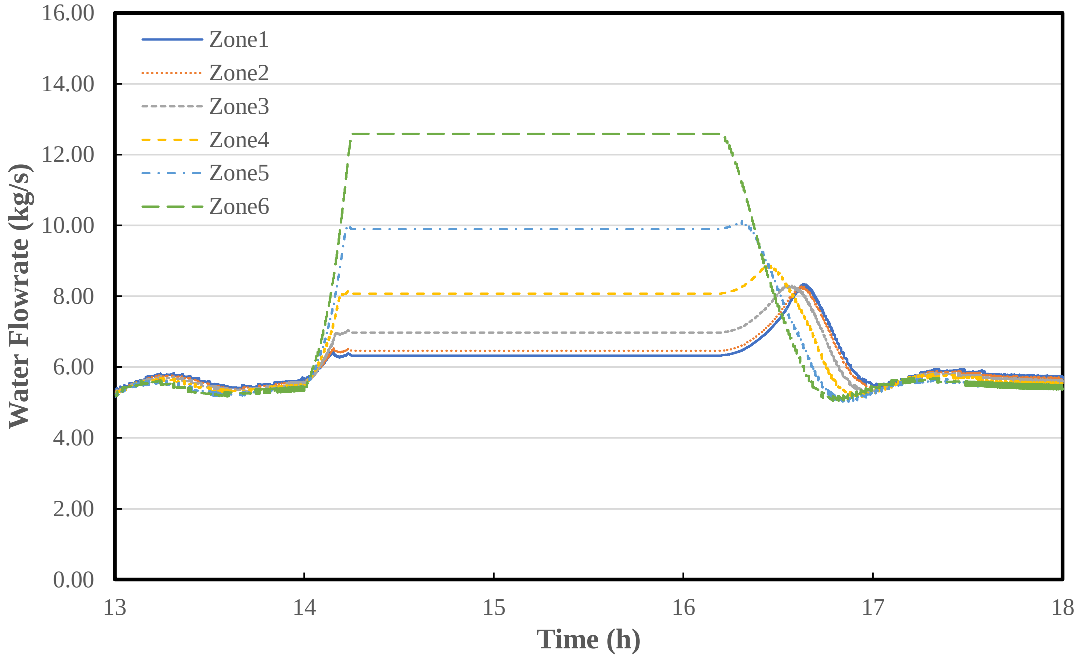

(a) Control strategy I

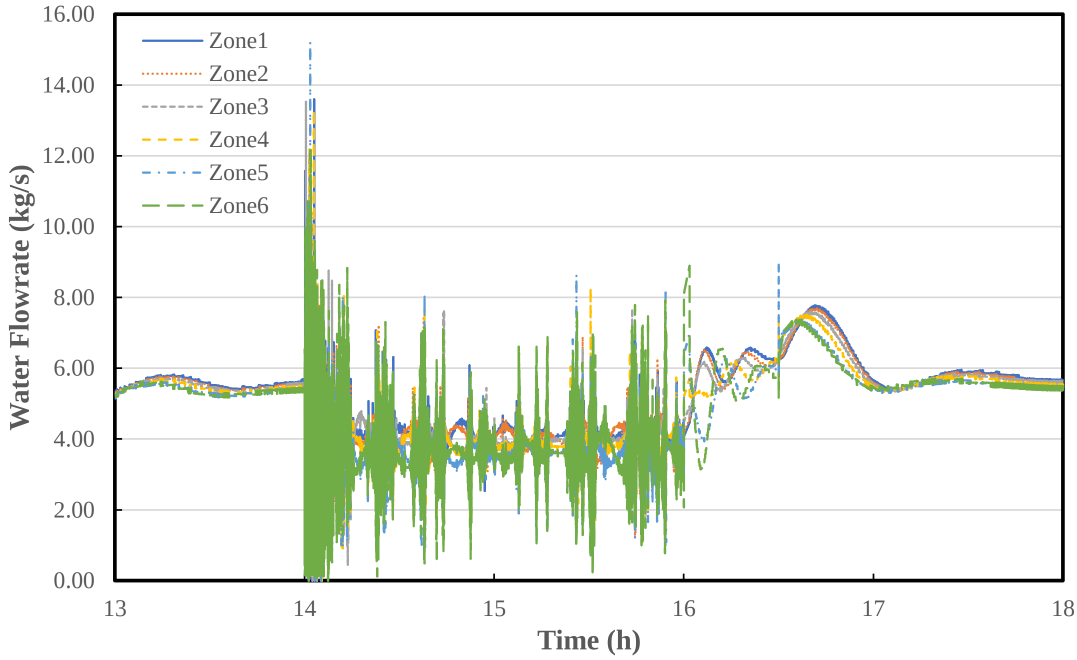

(b) Control strategy II

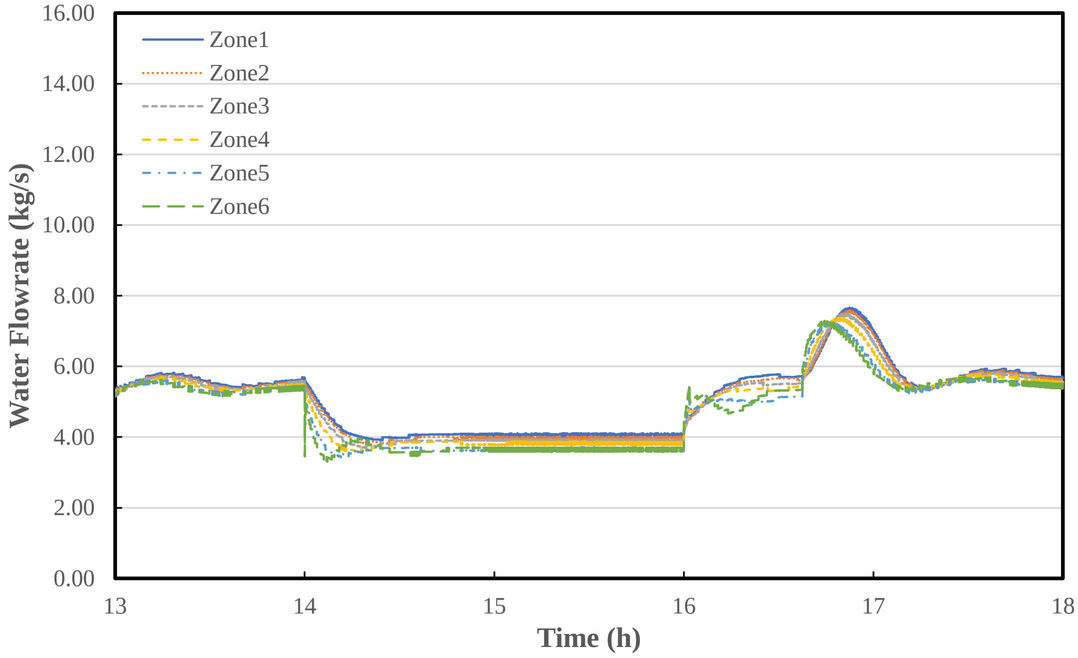

(c) Control strategy III

Figure 4.8 Chiller water flowrate profiles under different control strategies

4.3.1.3 Deficit flow in bypass pipe

Figure 4.9 shows the profiles of water flowrates in the bypass pipe using different strategies. There is a severe deficit flow problem from 14:00 to 16:00 when using control strategy I. Such deficit flow leads to a reduction in the temperature difference of the chilled water supplied to the building zones, resulting in decreased cooling effectiveness. Furthermore, the inability to meet the cooling demand of the building zones causes the secondary chilled water pumps to operate at full load. This, in turn, increases energy consumption and adds to the overall energy inefficiency of the system.

The bypass pipe water flowrate profile using control strategy II demonstrates strong oscillations during the demand limiting mode. This phenomenon is a result of the lack of proper parameter adjustment of coefficient *a*, which leads to oscillations in the bypass pipe water flowrate. On the other hand, when using control strategy III, the phenomenon of deficit flow gradually diminishes from 14:00. It takes approximately 12 minutes to eliminate the deficit flow. With this proposed supply-based feedback control, the deficit flow is effectively avoided throughout the demand response event, and no oscillations occur in the bypass pipe water flowrate.

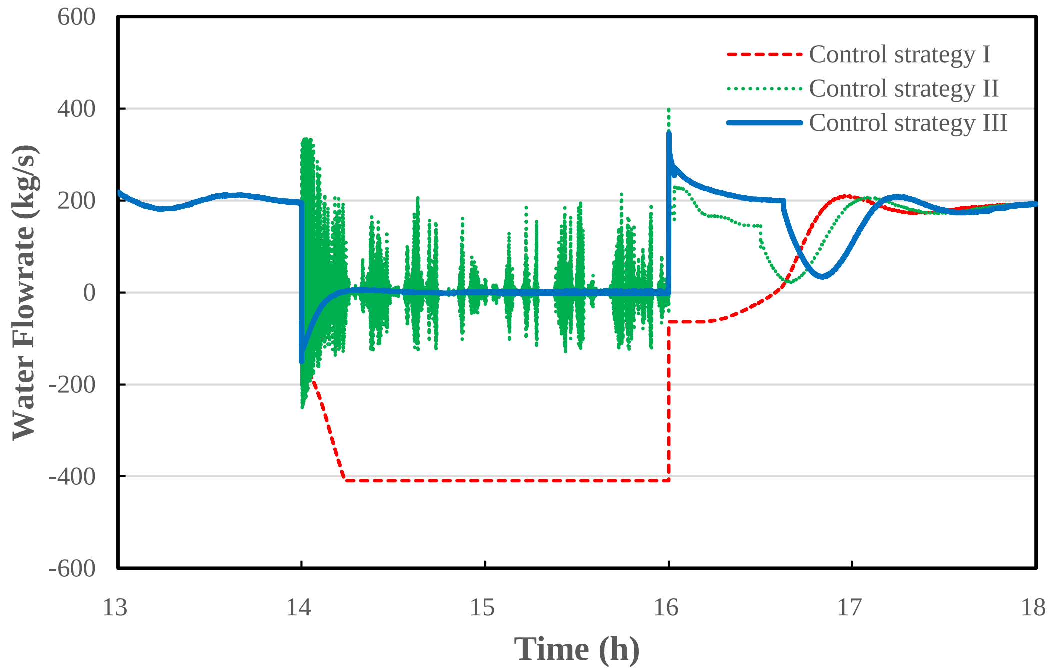

Figure 4.9 Bypass pipe water flowrate profiles using different control strategies

4.3.2 Environmental and energy performance

The previous section has highlighted the effectiveness of the proposed control in adjusting AHU valve openings to ensure proper chilled water distribution during fast demand response events. Test results confirm the importance of parameter scheduling in order to avoid control oscillations and achieve improved control performance. This section focuses on the comparison of the environmental and energy performance between conventional control (control strategy I) and the reconfigurable control (control strategy III).

4.3.2.1 Indoor air temperature

Figure 4.10 presents a comparison between the indoor air temperature profiles of conventional control and reconfigurable control. When using the conventional control, there are significant differences in temperature sacrifices among all building zones. In addition, the cooling down speeds also deviate significantly among the zones during the rebound period. Figure 4.11 (a) presents the temperature diversity performance indicators using conventional control. The test results demonstrate that for the majority of the zones, their temperature diversity indicators remain above 0.2 K for most of the time, indicating imbalanced thermal comfort sacrifices. This imbalance arises from improper chilled water distribution, as discussed in Chapter 4.3.1.2. However, when the proposed reconfigurable control is implemented, the problem of imbalanced thermal comfort sacrifices can be effectively addressed, as shown in Figure 4.11 (b). The diversity indicators of all six zones can be controlled within 0.2 K for most of the time.

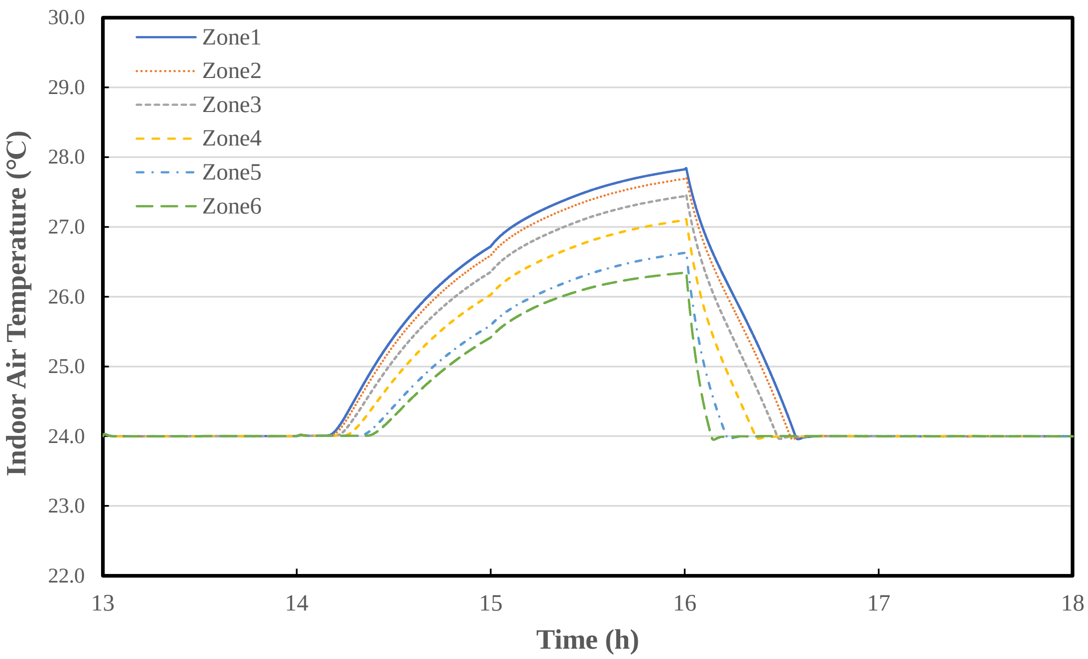

(a) Conventional control

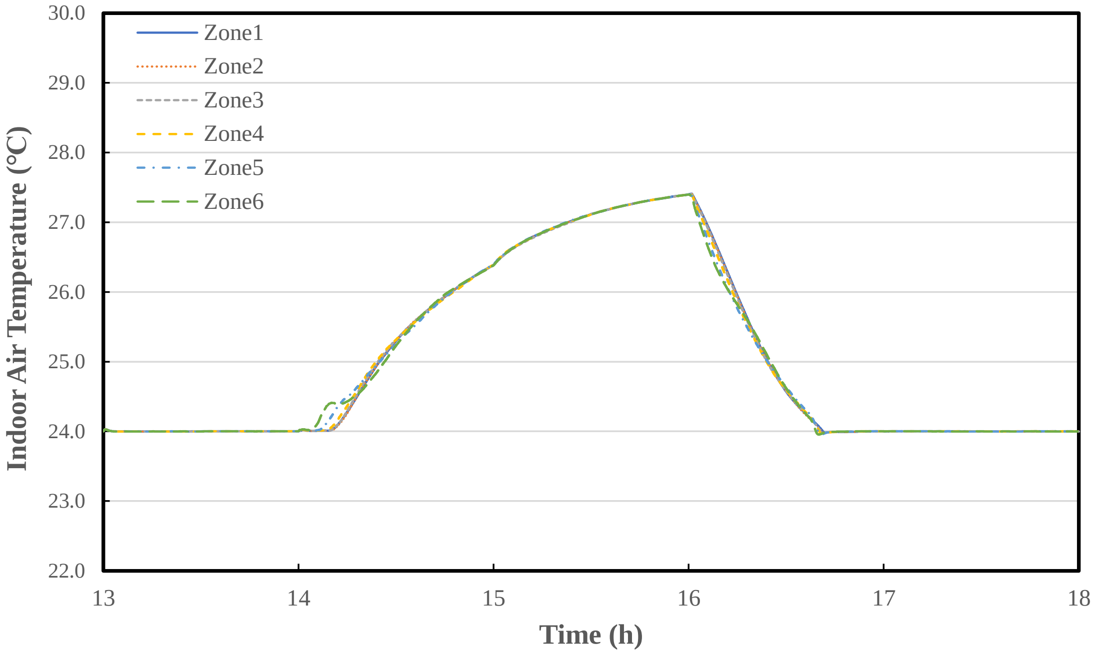

(b) Reconfigurable control

Figure 4.10 Comparation of indoor air temperature profiles using conventional control and reconfigurable control

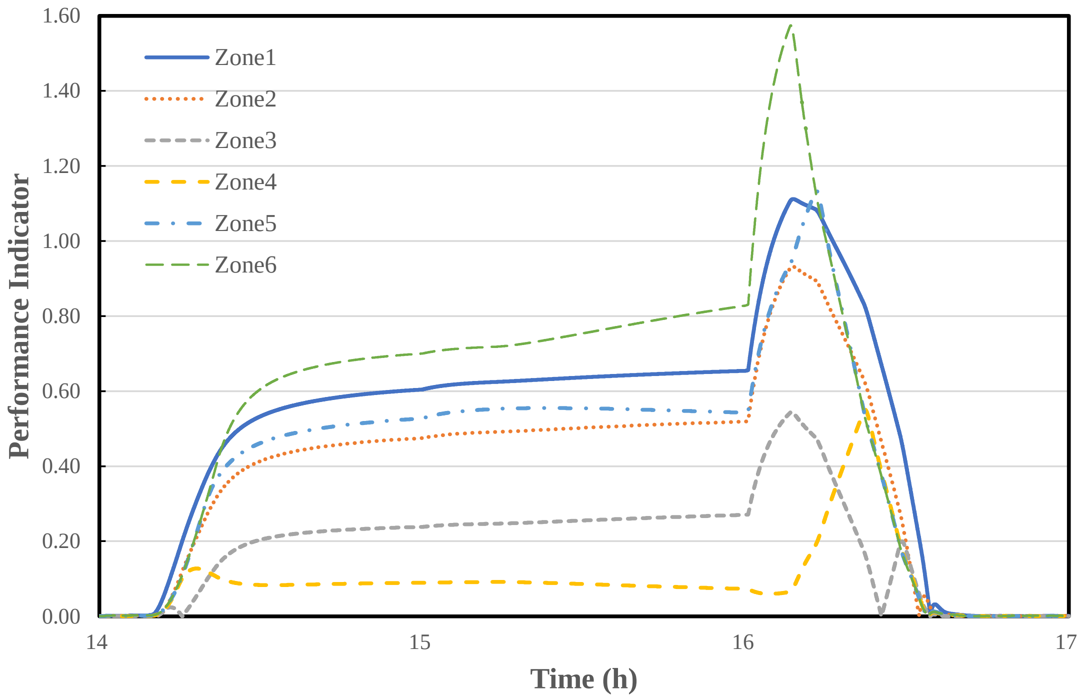

(a) Conventional control

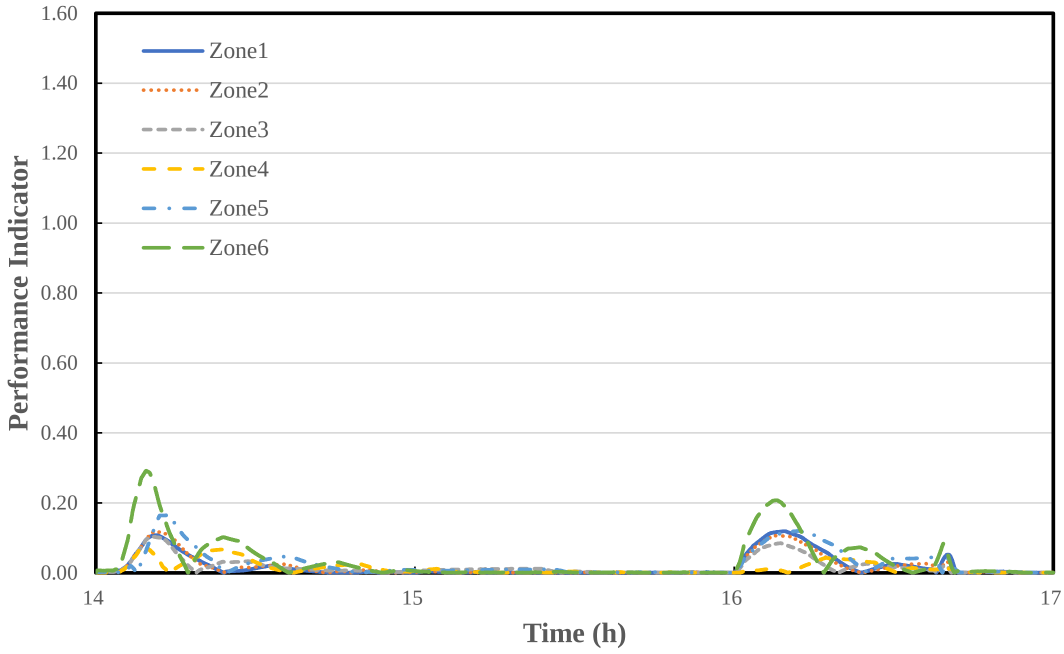

(b) Reconfigurable control

Figure 4.11 Comparation of temperature diversity performance indicators using conventional control and reconfigurable control

4.3.2.2 Energy consumption

Figure 4.12 shows the comparison between the secondary pump energy consumptions of conventional control and reconfigurable control. The energy consumption of the secondary pumps begins to increase at 14:00 due to the growing valve openings with the conventional control. The maximum energy consumption reaches 360 kW from 14:00 to 16:00. In contrast, the supply-based feedback control with proper valve opening adjustments significantly reduces the energy consumption of the secondary pumps. The maximum energy saving during the demand response event reaches 287 kW, which is crucial for achieving the desired effects of demand response. Figure 4.13 provides a comparison between air-conditioning system energy consumptions using conventional control and reconfigurable control respectively. In demand limiting mode, the power reduction of the chilled water system is 561.5 kWh, corresponding to a further reduction of 11.6%, when replacing the conventional feedback control with the supply-based feedback control. In addition, the power rebound is also reduced by 532 kW, corresponding to 27% of power rebound when using the conventional control.

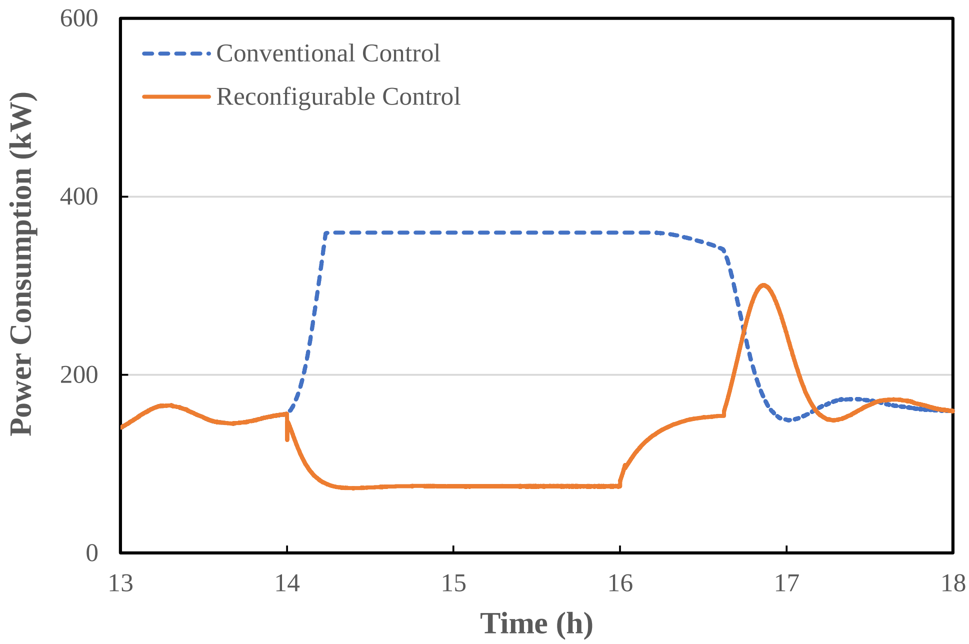

Figure 4.12 Comparation of secondary pumps energy consumption using conventional control and reconfigurable control

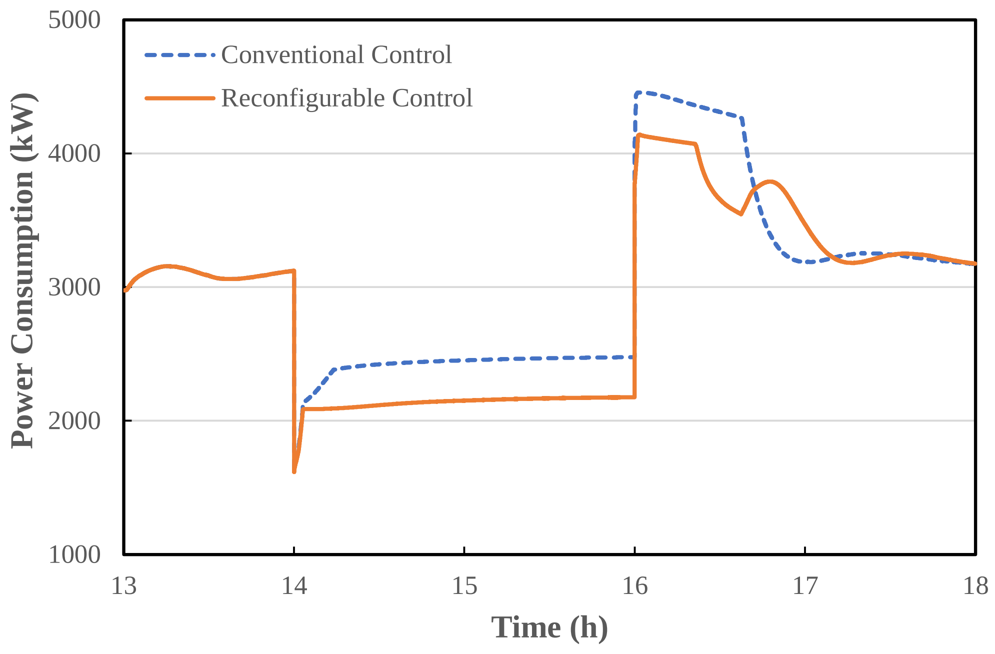

Figure 4.13 Comparation of air-conditioning system consumption using conventional control and reconfigurable control

4.4 Summary

Air-conditioning systems have the potential to provide valuable energy flexibility services, especially when faced with urgent power reduction requests from power grids. Adopting supply-based feedback controls and integrating them with demand-based feedback controls, as a reconfigurable control strategy, is proposed and recommended for air-conditioning systems to facilitate buildings in featuring fast demand response provision. Reconfigurable control strategy integrating supply-based feedback controls, for demand response and demand limiting events, and demand-based feedback controls for normal situation with sufficient cooling supply, should be the new norm for future buildings to facilitate the high renewable penetration of power system towards carbon neutrality. Based on the results of validation tests, the following major conclusions can be made:

- The conventional building automation systems adopting conventional feedback control face challenges in distributing cooling supply effectively during fast demand response while cooling supply is not sufficient after switching off some of the operating chillers. This results in disordered chilled water distribution, leading to imbalanced thermal comfort sacrifices among building zones. In addition, a severe deficit flow problem might arise, causing increased energy consumption in the secondary pumps.
- The proposed reconfigurable control strategy offers a solution for managing the distribution of cooling supply effectively to address the above issues. This strategy can be implemented on conventional building automation systems adopting digital controllers commonly used today, such as DDC and PLC.
- Test results show satisfactory control stability in valve opening control and proper chilled water distribution. This enables uniform space temperature distribution and thermal comfort control among the building zones during both demand response and rebound periods. The temperature deviation among the zones is controlled within 0.2 K for the majority of the time. Furthermore, proposed reconfigurable control achieves reductions of 11.6% and 27% of power demand during demand response and rebound periods respectively, compared to that using conventional controls.

CHAPTER 5 ITERATIVE LEARNING CONTROL STRATEGY FOR SHORTENED MORNING START PERIOD

To develop advanced control strategies for the special enhancement of the supply-based control at morning start period, this chapter proposes an iterative learning control strategy for building air-conditioning systems. This simple control strategy can determine the AHU water valve openings during the morning start period to achieve uniform cooling among building zones effectively, by updating the valve opening control values of individual AHUs using the iterative learning control. Section 5.1 presents the mechanism of iterative learning control and the operation procedure. The test platform and arrangement for the morning start period are elaborated in Section 5.2. Section 5.3 analyzes the control performance and energy saving potential. A summary of the work and results is given in Section 5.4.

5.1 Mechanism of iterative learning control and operation procedure

This study proposes an iterative learning control strategy for building air-conditioning systems for saving energy by shortening the morning start period, which is developed based on iterative learning control (Bristow et al., 2006). The daily precooling period is regarded as a repetitive process. The basic idea is to set the AHU valve openings corresponding to the actual cooling needs of individual zones during the precooling period. In this way, the conventional (PID) feedback control is temporarily taken over during this period. The fixed AHU valve opening control values are updated on a daily basis. An outline of the proposed control strategy is shown in Figure 5.1. The iterative learning controller adopts the iterative learning control strategy, and the control outputs are the AHU water valve opening control signals corresponding to individual building zones. The environmental variable measurements from the building zones are sent back to the iterative learning controller and used directly for iterative learning control. Two control performance indicators are proposed for evaluating the control performance and setting the control parameters. The Q-learning agent selects the control parameters of the iterative learning controller based on the control performance indicators.

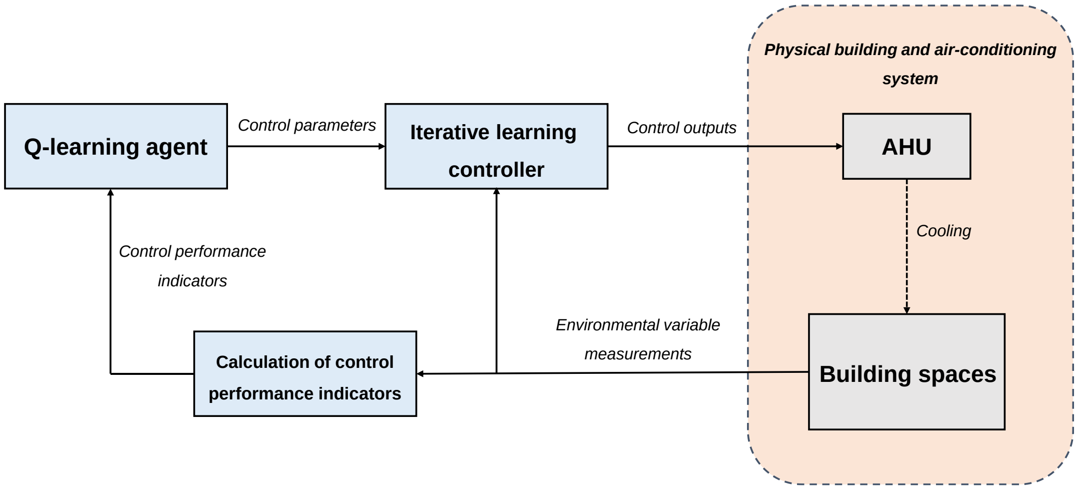

Figure 5.1 Outline of the proposed iterative learning control strategy

5.1.1 Basic control mechanism

Figure 5.2 illustrates the basic principle of the proposed control strategy. For building air-conditioning systems during the morning start period, the cooling demand is very high and individual air-conditioned building zones would compete for the limited cooling supply from the chillers. The iterative learning controller is proposed for the chilled water side to manage the distribution of the limited chilled water among the building zones aiming to keep indoor temperatures of all the building zones the same (approaching the temperature setpoint at the same time). The control objects are the

AHU water valve openings corresponding to individual building zones. The control outputs (valve opening control signals) are updated on a daily basis before the precooling start time, and remain the same during the precooling process. The iterative learning controller needs to collect data of two categories. The first category includes the control outputs at the last control interval (i.e., last day) and the control performance indicators at the last control interval. They are used to update the first term of the iterative learning control function at the current interval. The second category includes the environmental information (i.e., initial temperatures) of the building zones at the current interval, which are used to update the second term of the iterative learning control function at the current interval. As the time passes, the iterative learning controller can continuously track and approach the goal of consistent precooling lead time for different building zones at the morning start period.

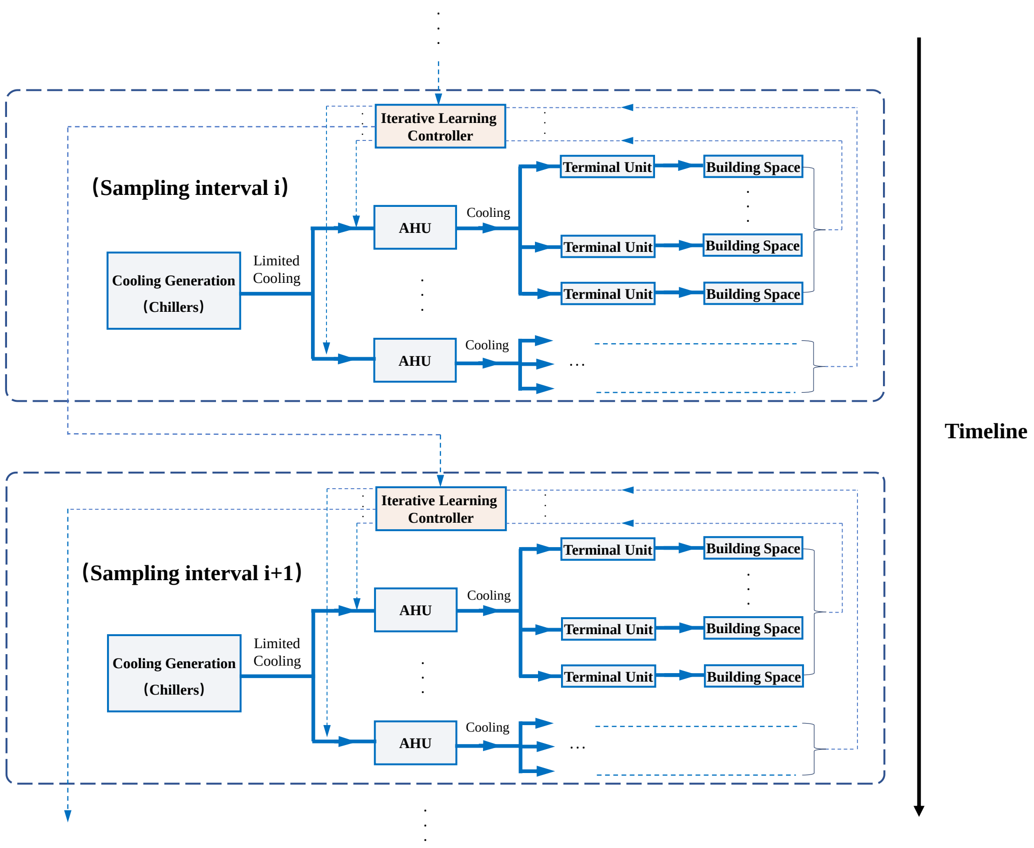

Figure 5.2 Basic principle of the proposed iterative learning control strategy

5.1.2 Control performance indicators

In order to evaluate the control performance, two control performance indicators are proposed based on the notion of consistent precooling lead time for different individual building zones.

The first indicator is the maximum return time among multiple zones from night setback (t_{max}), as shown in Eq. (5.1). Where, t_n represents the return time from night setback for zone *n*. Figure 5.3 illustrates the return time from night setback for an individual building zone. The precooling starts at time t_A, when the indoor air temperature is relatively high because the air-conditioning systems in commercial buildings are generally not operating during the night. The indoor air temperature of the zone then decreases and reaches the cooling setpoint at time t_B. The time difference between t_A and t_B (i.e., t_B - t_A) is defined as the return time from night setback.

$$t_{max} = max\{t_1, t_2 \cdots t_n\} \tag{5.1}$$

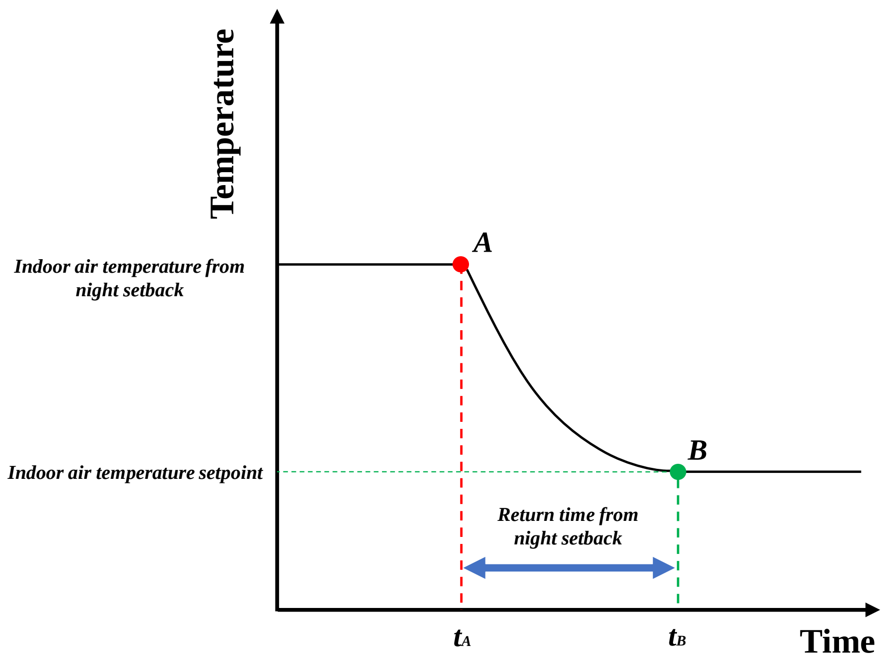

Figure 5.3 Illustration of the return time from night setback for an individual building zone

The goal of the proposed control strategy is to minimize the precooling lead time of building zones considering the distribution of limited cooling supply in the morning start period. In order to achieve consistent precooling lead time for different building zones, the maximum return time among all zones from night setback should be considered as a performance indicator and it represents the required precooling operation time of the chillers.

The second indicator is the cooling diversity indicator (*cdi*), as shown in Eq. (5.2).

$$cdi = \frac{\Delta t_{max}}{t_{max}} \tag{5.2}$$

$$\Delta t_{max} = max\{t_1, t_2 \cdots t_n\} - min\{t_1, t_2 \cdots t_n\} \tag{5.3}$$

The maximum deviation between the return time among all building zones from night setback (Δt_{max}) is defined in Eq. (5.3), which represents the largest precooling lead time deviation among the building zones during the morning start period. As the control objective is to minimize the maximum precooling lead time deviation under the limited cooling supply, the cooling diversity among the building zones should be consistent. The cooling diversity indicator defined in Eq. (5.2) is used as a performance indicator and its value is expected to be as low as possible.

5.1.3 *Operation procedure of iterative learning control strategy*

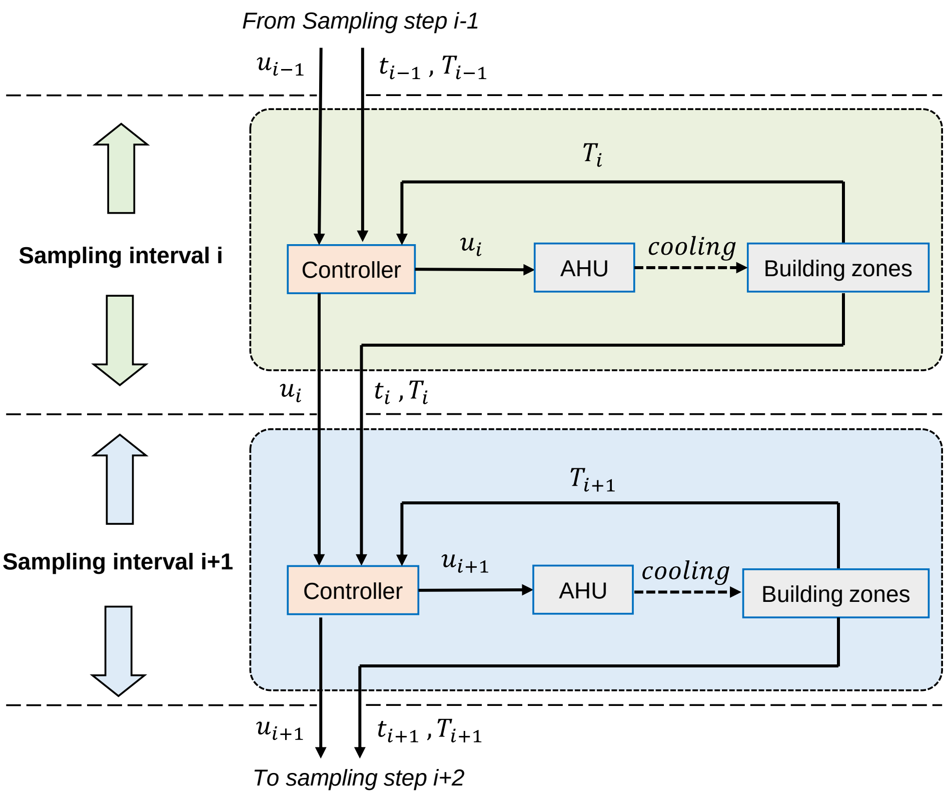

Figure 5.4 Schematic of the proposed control strategy

The schematic of the proposed control strategy is shown in Figure 5.4. The iterative learning control proposed in this study is based on daily operation data and measurements. The objects to be controlled are the AHU water valves corresponding to the building zones served. The control strategy attempts to continuously track the goal of consistent precooling lead time for different building zones during the morning start period. The control time interval (iterative step) is set to be one day. The control outputs are updated according to the daily learning results.

Initialization. At the start (e.g. the first day of the control operation), in order to accelerate the initial learning process, the initial control setting (u_1) is determined based on the previous operational data. At this step, the controller collects the following data information as defined from Eq. (5.4) to Eq. (5.6) during the morning start period, (1) return time (t_1) of the n building zones from night setback, (2) temperature (T_1) of the n building zones at the precooling start time, (3) AHU valve openings of the n building zones (u_1). These data are saved every day for the next day's learning control.

$$t_1 = [t_{1,1}, t_{2,1}, \cdots t_{n,1}] \tag{5.4}$$

$$T_1 = [T_{1,1}, T_{2,1}, \cdots T_{n,1}] \tag{5.5}$$

$$u_1 = [u_{1,1}, u_{2,1}, \cdots u_{n,1}] \tag{5.6}$$

Control updating at each control interval. In the day i, before the precooling start time, the proposed control algorithm is activated. The controller collects the zone temperatures (T_i) of building zones and execute the iterative learning control strategy as illustrated below.

- Calculate the average return time (t_{ave}) of the n building zones from night setback using Eq. (5.7).

$$t_{ave} = \frac{\sum_1^n t_{n,i-1}}{n} \tag{5.7}$$

- Calculate the AHU valve opening correction $\Delta u_{n,i}$, for each building zone n using Eq. (5.8).

$$\Delta u_{n,i} = k \cdot (t_{ave} - t_{n,i-1}) - b \cdot (T_{n,i} - T_{n,i-1}) \tag{5.8}$$

where, k and b can be recognized as the control parameters of the learning function, and they need to be adjusted according to the specific system.

- Calculate the corresponding AHU valve opening $u_{n,i}$, for each building zone n, using Eq. (5.9).

$$u_{n,i} = u_{n,i-1} - \Delta u_{n,i} \tag{5.9}$$

According to the control algorithm above, the AHU valve opening control signals of the n building zones (u_i) at day i could be determined. With time passes, the controller can handle the environmental difference every day and repeat the iterative learning control strategy to update the control outputs.

5.1.4 Control parameter setting using Q-learning agent

As illustrated in Eq. (8), the iterative learning control function has two key parameters (k, b) as the control parameters. The values of these two parameters have significant impacts on the overall control performance. If the values of k and b are high, the learning and correction process of the control strategy would be quick, but the system may be over tuned if they are too high. On the contrary, if the values of k and b are low, the system may avoid this problem; however, the learning process would be slow. For engineering practice, such control parameters could be manually determined by experienced engineers. To make the application of the proposed control strategy convenient and labor-saving, the tasks of selecting the control parameters can be formulated and treated as a basic reinforcement learning problem.

Q-learning is a classical reinforcement learning method. This method is model-free and the algorithm is based on a Q-table (Sutton & Barto, 2018). Compared with many network-based methods such as deep reinforcement learning, the Q-learning method is easier to converge and more feasible to apply in engineering practice (Qiu et al., 2020). The applications adopting Q-learning have been proven to be effective in many previous studies in the HVAC domain (Chen et al., 2018; Henze & Schoenmann, 2003; Qiu et al., 2020). In this study, this method is adopted for control parameter setting of the iterative learning controller.

The parameter identification and adjustment of the iterative learning controller are performed using an online adaptive approach with the proposed Q-learning agent, as shown in Figure 5.5. The inputs of the Q-learning agent are the control performance indicators, and the outputs are the control parameters. The detailed process of the Q-learning agent workflow for control parameter setting is elaborated below. By adopting the Q-learning method, the Q-learning agent can learn the process characteristics online and update in each control interval to select appropriate control parameters for the iterative learning controller, and therefore improve control performance.

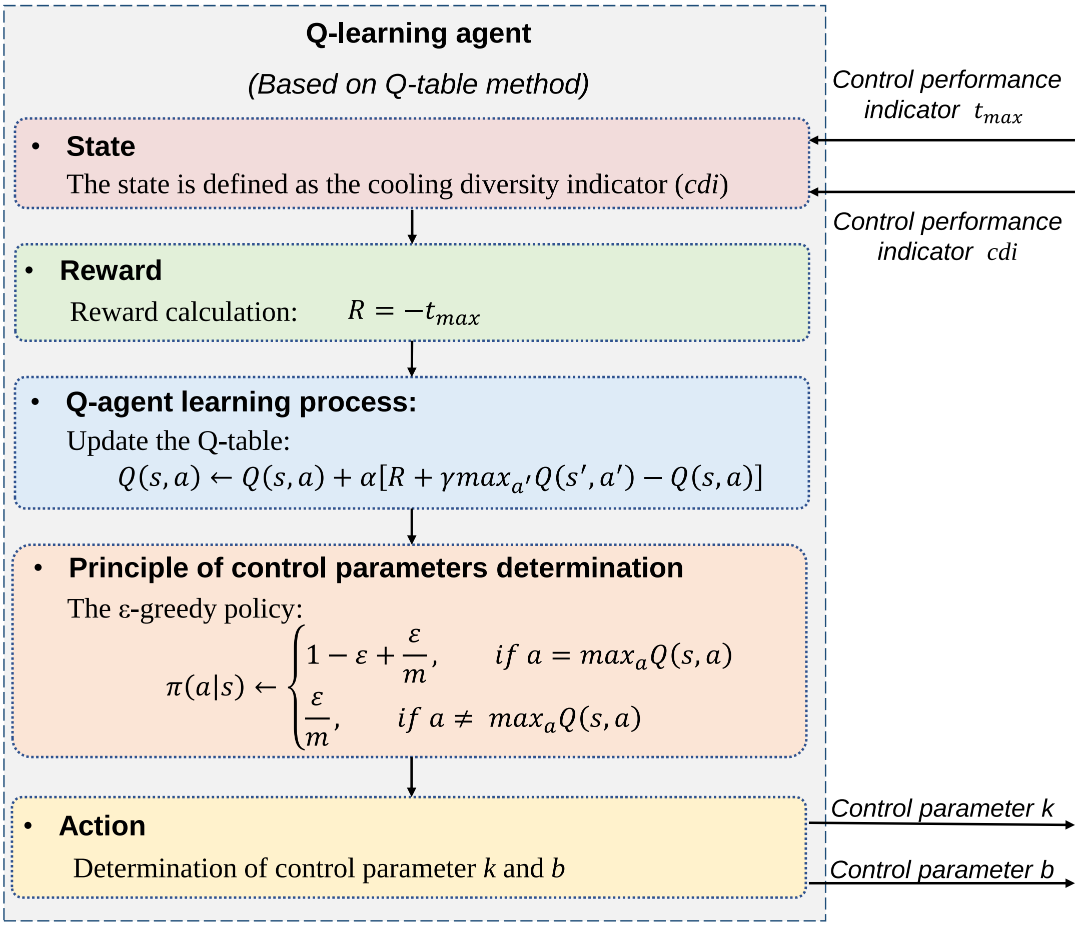

Figure 5.5 Outline of the Q-learning agent workflow for control parameter setting

Outline of Q-learning agent: For Q-learning agent design, the Q-table method is proposed as the policy to define the Q-learning agent's way of behaving at a given time. The control parameters (*k*, *b*) of the iterative learning controller are optimized by the Q-table in the Q-learning agent. For the Q-learning agent in this study, the Q-table provides a mapping from perceived states of the building zones to control parameter setting. Table 5.1 is the Q-table defined in this study for the iterative learning control strategy. The action (*A*) in this table represents the control parameters (*k*, *b*) to be determined, and the state (*S*) represents the calculated cooling diversity indicator (*cdi*) as introduced in Chapter 5.1.2. Each Q-value (e.g., *Q (S1 , A1)*) in Table 5.1 is updated through the Q-learning process, and its initial value is 0. All the Q-values formulate the Q-table, which is used to determine the control parameters (*k* , *b*). The learning process of the Q-learning agent using the Q-table is illustrated in the following five subsections.

Table 5.1 Format of the designed Q-table

Action (*k*, *b*) \ State (*cdi*)	[0,0.2)	[0.2,0.4)	[0.4,0.6)	[0.6,0.8)	[0.8,1]
(0.5, 0.0125)	*Q (S1 , A1)*	*Q (S2 , A1)*	*Q (S3 , A1)*	*Q (S4 , A1)*	*Q (S5 , A1)*
(1, 0.025)	*Q (S1 , A2)*	*Q (S2 , A2)*	*Q (S3 , A2)*	*Q (S4 , A2)*	*Q (S5 , A2)*
(2, 0.05)	*Q (S1 , A3)*	*Q (S2 , A3)*	*Q (S3 , A3)*	*Q (S4 , A3)*	*Q (S5 , A3)*

<u>Action</u>: The action is defined as the combination of the control parameters (*k*, *b*), and determining the action is the task of the Q-learning agent in this study. Discretization, as a classical and convenient method for action setting in Q-learning, is used in this study. The setting of the discretization precision for the action is flexible. Higher precision setting could make the state identification more accurate and the action selection more precise. But it would also lead to a larger Q-table and thus require longer period and more data for the operation of the Q-learning agent. In order to make

it easy for application, the action (k, b) is discretized into three combinations in this study, i.e., (0.5, 0.0125), (1, 0.025), and (2, 0.5). They are determined based on the expert judgement and the authors' experience. It is reasonable for such a setting because the three combinations of the control parameters could represent low, medium, and high learning rate, respectively for the iterative learning controller. The mission of the Q-learning agent is to determine the appropriate learning rate for the iterative learning control strategy.

State: The state in this study is defined as the cooling diversity indicator (*cdi*), because this control performance indicator can represent the consistency between the precooling lead times of different individual building zones. It reflects the iterative learning control performance of previous day, and the Q-learning agent should select the control parameters according to the state at current morning start period. The cooling diversity indicator is a continuous variable and for the convenience of application in Q-table, it is discretized into five intervals with equal length as shown in Table 5.1.

Reward: The reward is calculated using Eq. (5.10), based on the maximum return time among multiple zones (t_{max}) as described in Chapter 5.1.2. It is based on the notion that our expectation is to shorten the maximum return time among all building zones. For the Q-learning agent, the reward is higher when the maximum return time among all zones is lower.

$$R = -t_{max} \tag{5.10}$$

Q-agent learning process: During the learning process, the Q-learning agent accumulates experience by updating the Q-table, and the updating principle is shown in Eq. (5.11).

$$Q(s,a) \leftarrow Q(s,a) + \alpha[R + \gamma max_{a'} Q(s',a') - Q(s,a)] \tag{5.11}$$

where, Q (s, a) represents the Q-value with state (s) and action (a) as shown in Table 1, and the initial Q-values are set to 0. At each iterative learning control interval, the Q-value of Q (s, a) corresponding to the previous step is updated according to this principle. *R* is the reward calculated using Eq. (5.10), as the result of the action (a). α is the learning rate of the Q-learning agent; and γ is the impact of the reward at the next iterative learning control interval on the decision of action at the current step. In this study, the α and γ are set to 0.9 and 0.1, respectively. $max_{\alpha'} Q(s', a')$ is the max Q-value at state (s') with current Q-table.

Principle of control parameters determination: For every control interval, the Q-learning agent determines the control parameters (k, b) based on the ε -greedy policy in this study. The principle of the ε -greedy policy is shown in Eq. (5.12).

$$\pi(a|s) \leftarrow \begin{cases} 1 - \varepsilon + \dfrac{\varepsilon}{m} & , if\ a = max_a Q(s,a) \\ \dfrac{\varepsilon}{m} & , if\ a \neq max_a Q(s,a) \end{cases} \tag{5.12}$$

where, $\pi(a|s)$ is the probability of the action (a) when it is chosen at the state (s). It means that, for each control step, the probability for Q-learning agent to choose the known best action is $1 - \varepsilon + \frac{\varepsilon}{m}$ according to the Q-table, while the probability for Q-learning agent to choose another action is $\frac{\varepsilon}{m}$. ε is a predefined parameter representing the balance between exploration and exploitation, and ε is set to 0.3 in this study. *m* is the number of available actions to be chosen, which is set to 3 in this study. In this way, the Q-learning agent would choose an action most of the time, which has maximum estimated action value for exploitation, but there is probability for the Q-learning agent to select another random action for exploration.

5.2 Test platform and arrangement for morning start period

To test the applicability and performance of the proposed iterative learning control strategy, a virtual dynamic simulation platform is developed using TRNSYS. The real-time simulation platform of the building and its air-conditioning system is constructed, referring to the actual system of a super-high-rise commercial building (International Commerce Centre) in Hong Kong, and the main parameters are presented in Table 5.2.

Table 5.2 Main parameters of central air-conditioning system

Chiller	Cooling capacity (kW)	Rated flow (evaporator)(L/S)	Rated flow (condenser) (L/S)	Rated power (kW)	Number
	4080	172.8	205.3	960	4
Pump	Rated flow (L/S)	Rated power (kW)	Head (m)	Efficiency (%)	Number
Primary pump	172.8	110	45.1	72.5%	4
Secondary pump	345	163	41.4	85.7%	2

To make it simple and clear for control performance evaluation and demonstration, the dynamic test platform is developed by simplifying the actual energy system of the International Commerce Centre. The air-conditioning system for six typical and standard floors is concerned only in this study. The area of each building floor is 1,600 m^2.The detailed physical models of the air-conditioning system in this test platform are calibrated using real data (Tang, Wang, Shan, et al., 2018; S. Wang, 1998). The test platform is a typical primary constant-secondary variable chilled water system, and the schematic is shown in Figure 5.6. It consists of four identical chillers, and each chiller's rated capacity is 4080kW. For the primary chilled water pump side, each chiller is interlocked with a water pump with the constant speed of 172.8 L/s. For the secondary chilled water loop, two variable speed water pumps are employed and the chilled water is circulating in the AHUs to provide a cooling source. The building is simulated using a multizone model (Type 56) in TRNSYS. The six typical floors concerned are considered as six individual building zones, respectively (i.e., each floor is considered as a building zone). These zones have different cooling loads since the heat gains (including occupants, electrical devices, etc.) in these zones are different. Each building zone is cooled by an individual AHU. Each of the six air-conditioned zones is cooled by the supply air temperature from its corresponding AHU to its zone temperature setpoint. Each AHU cools down the supply air temperature to the pre-defined setpoint.

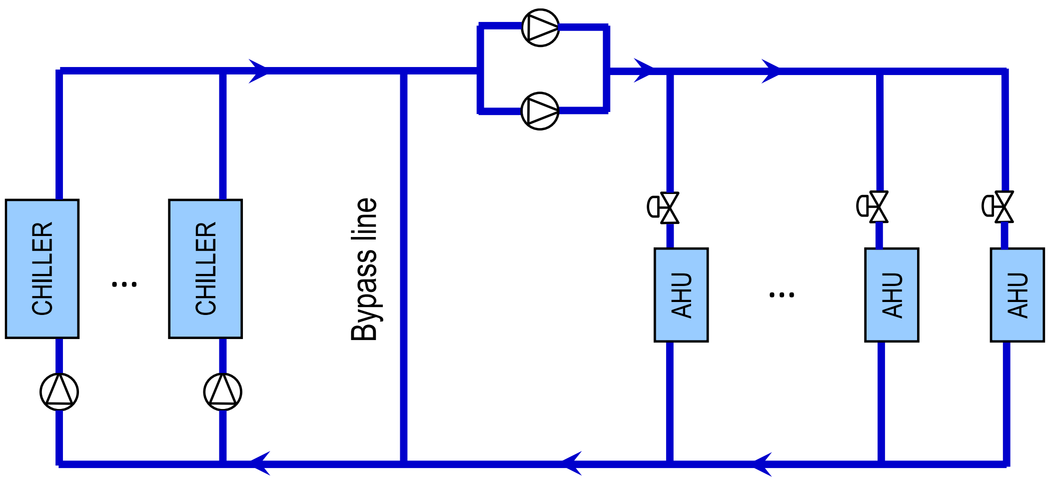

Figure 5.6 Schematic of central air-conditioning system concerned

In this study, a TRNSYS-MATLAB co-simulation test platform is constructed, as shown in Figure 5.7. The iterative learning controller and other models (i.e., the building models and the air-conditioning system models) are built on TRNSYS 18 (32-bit) while the Q-learning agent is built on MATLAB 2014a (32-bit). Fig. 8 shows the overview of the simulation studio file for the TRNSYS-MATLAB co-simulation. Type 155 (in the TRNSYS library) is used for calling the MATLAB component. The weather data for a typical year in Hong Kong is adopted in the test. The office hours of the building are from 08:00 to 18:00, from Monday to Saturday, and the air-conditioning system is switched off during the non-office hours.

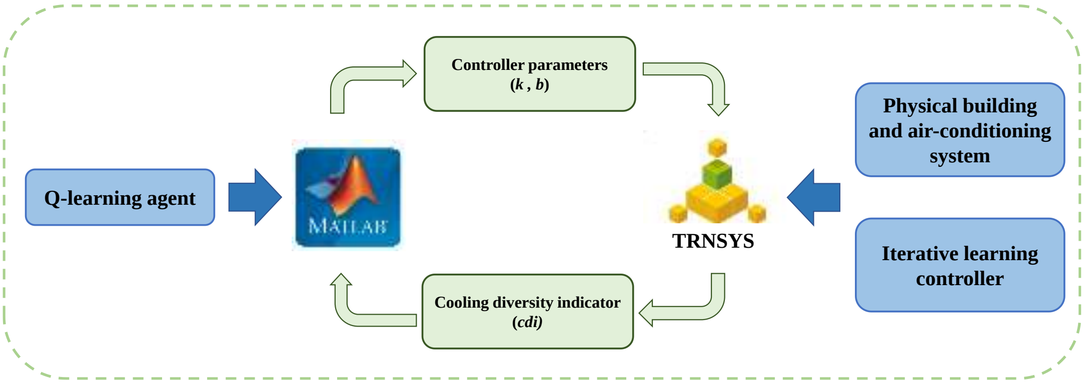

Figure 5.7 Outline of TRNSYS-MATLAB co-simulation test platform

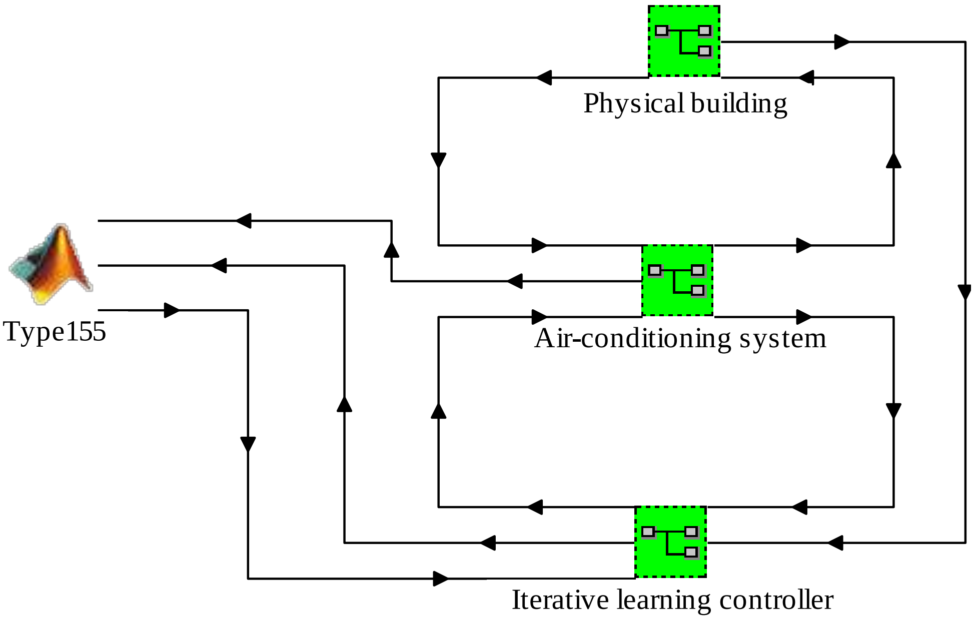

Figure 5.8 Overview of the simulation studio file for the TRNSYS-MATLAB co-simulation

Prior to the morning start period in each working day, the iterative learning controller is activated, adpoting the proposed method as introduced earlier in Chapter 5.1. For the validation tests, the number of building zones n is set to 6, and a hot month (July) in Hong Kong is selected as the experimental operation period. A test period of four weeks, i.e., from July 2nd to July 29th, is selected. The control parameters (k, b) are determined and updated online using the Q-learning agent, as described in Chapter 5.1.4.

5.3 Control performance and energy saving potential

The control performance, precooling time reduction, and energy saving are tested and analyzed to evaluate the feasibility and performance of the proposed control strategy. Two proposed indicators (t_{max} and cdi) are used to evaluate the control performance of the proposed iterative learning control strategy at morning start period, and this performance is also compared with that of the conventional feedback control. The precooling period starts before the office hours (8:00) every working day, and the air-conditioning system is switched off after the office hours (18:00). And the indoor air temperature setpoints for all the six building zones are 24 °C. The energy saving of the chilled water system (chillers, primary pumps, and secondary pumps) by adopting the proposed control strategy is quantitatively analyzed in the following sections.

5.3.1 Control operation and control performance

5.3.1.1 Valve opening control outputs

The AHU valve opening control outputs for the six zones were determined by the proposed iterative learning control strategy every day at morning start period, and the results are shown in Figure 5.9. For Day 1 (02/July), the initial valve openings were manually determined based on the normal operation data of the six AHUs before the test period. The initial valve openings for the six AHUs were 1, 0.87, 0.82, 0.76, 0.65, and 0.6 correspondingly. Figure 5.10 compares the AHU valve openings under the conventional control and the proposed control, on a typical summer day (23/July). Unlike the conventional feedback control, all the AHU valves are set to be fully open to compete for the limited chilled water supply. It can be seen from the results that, when using the proposed strategy, the AHU valve openings corresponding to the six building zones were adjusted and then remained unchanged every day during the morning start period. It can be seen from Figure 5.9 that the valve opening for AHU 1 was controlled at 1 during morning start period in all test days under the proposed control. This indicates that zone 1 is at a disadvantage for chilled water distribution among the six building zones. On the contrary, the valve opening of AHU 6 was controlled to be the lowest among the six AHUs during morning start period in all the test days. It indicates that the zone 6 has the advantage in competing for the limited chilled water supply. In summary, using the proposed iterative learning control strategy, the control outputs could be updated at each control interval (everyday morning start period) to continuously track the goal of consistent precooling lead time for different building zones.

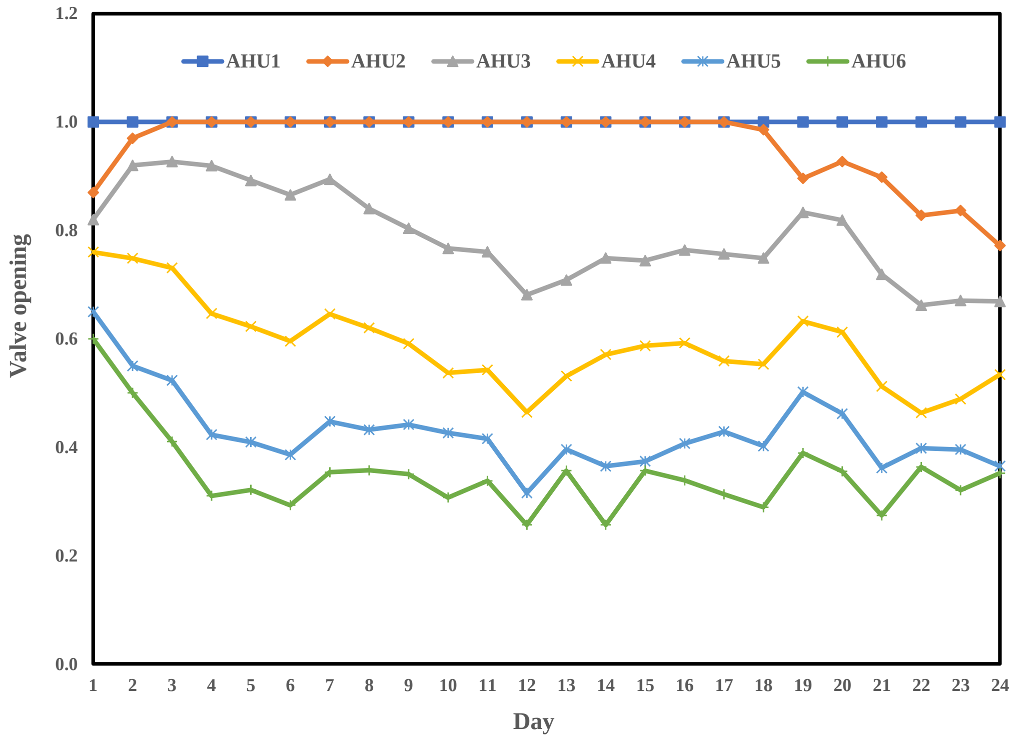

Figure 5.9 AHU valve opening control outputs of the six building zones during morning start period

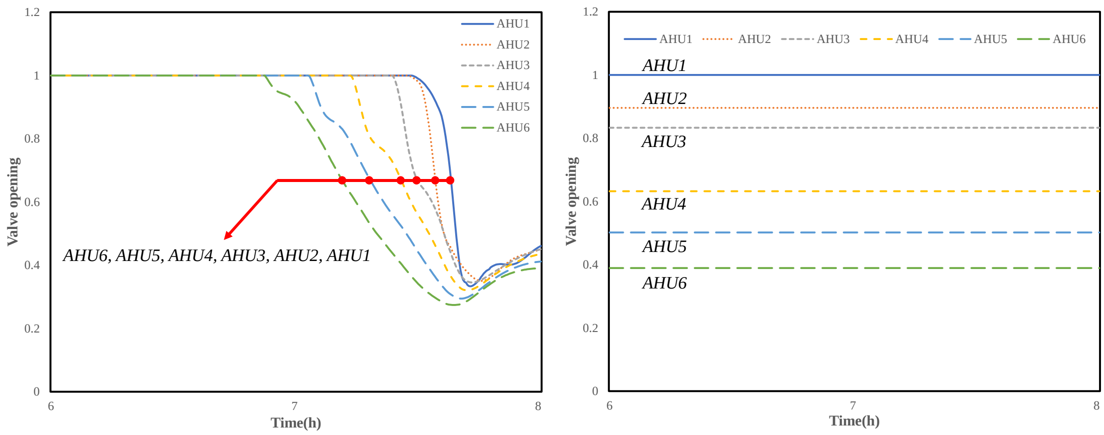

(a) Valve opening profiles using the conventional control

(b) Valve opening profiles using the proposed control

Figure 5.10 Comparison of AHU valve openings under the conventional control and the proposed control on a typical summer day

5.3.1.2 Maximum return time among multiple zones

The maximum return time among multiple zones from night setback (t_{max}) is defined as a control performance indicator, as illustrated in Chapter 5.1.2. It indicates the required precooling time for all building zones to reach their temperature setpoint. The value of t_{max} is expected to be as low as possible. Figure 5.11 presents the t_{max} under the proposed iterative learning control and the conventional feedback control. It can be observed that under the proposed iterative learning control, the t_{max} was lower than that under the conventional control for the four-week test period. Among the test results, the maximum reduction of t_{max} was 0.19 hour on Day 19 (23/July) and the maximum reduction percentage of t_{max} was 15.6% on Day 23 (27/July). For the convenience of comparison, the daily t_{max} over a week was summed up and the accumulated t_{max} for four weeks in the test period is shown and compared in Table 5.3. It can be seen from Table 5.3 that the t_{max} reduction in Week 1 was 8.3%, and for the following three weeks the t_{max} reduction effect was over 11%. The results show that the proposed iterative learning control strategy reduced the maximum return time among the six building zones. This means that the required precooling time under the conventional feedback control was reduced when applying the proposed iterative learning control.

Table 5.3 Maximum return time among multiple zones (t_{max}) comparation of the four-week test period

Week		1	2	3	4
Accumulated t_{max} (hour)	Conventional control	4.47	6.45	5.38	6.55
	Proposed control	4.10	5.68	4.77	5.82
t_{max} reduction (%)		8.3	11.9	11.3	11.1

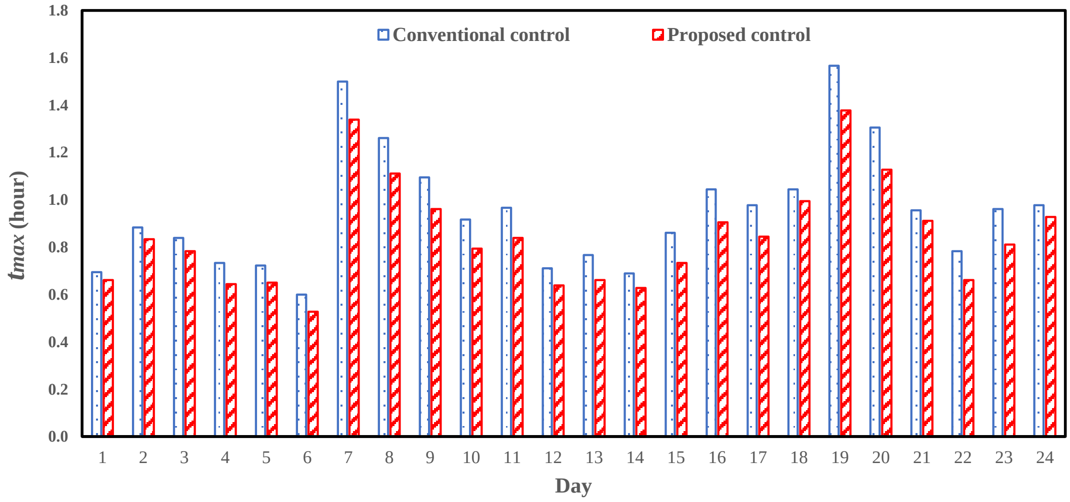

Figure 5.11 Maximum return time among multiple zones (t_{max}) during the test period

5.3.1.3 Cooling diversity

The cooling diversity indicator (*cdi*) is another control performance indicator, as introduced in Chapter 5.1.2. It represents the cooling diversity among the building zones during the morning start period, and it is expected to be as lower as possible. The results of *cdi* under the conventional feedback control and the proposed iterative learning control are compared in Figure 5.12. It can be observed from Figure 5.12 that the *cdi* under the proposed control strategy is much lower than that of conventional control.

The reduction of *cdi* was not very significant on Day 1 (02/July). However, after the first three test days, the *cdi* was significantly lower under the proposed control strategy than that under the conventional control. During the test period, the maximum reduction of *cdi* by applying the proposed control strategy was on Day 17 (20/July), with a reduction of 0.47. The percentage of maximum *cdi* reduction was 86.8% on Day 23 (27/July). For the convenience of comparison, the daily average *cdi* over a week of the four weeks in the test period is shown and compared in Table 5.4. The results show that for the first week, the *cdi* reduction was 49.1%, and for the following three test weeks, the *cdi* reduction was over 70%. The test results indicate that the proposed iterative learning control strategy significantly reduced the cooling diversity indicator (*cdi*). By applying the proposed control strategy, the consistency of precooling lead time among the six building zones was improved significantly.

Table 5.4 Cooling diversity indicator (*cdi*) comparation of the four-week test period

Week		1	2	3	4
Average *cdi*	Conventional control	0.57	0.52	0.53	0.52
	Proposed control	0.29	0.15	0.14	0.14
cdi reduction (%)		49.1	71.2	73.6	73.1

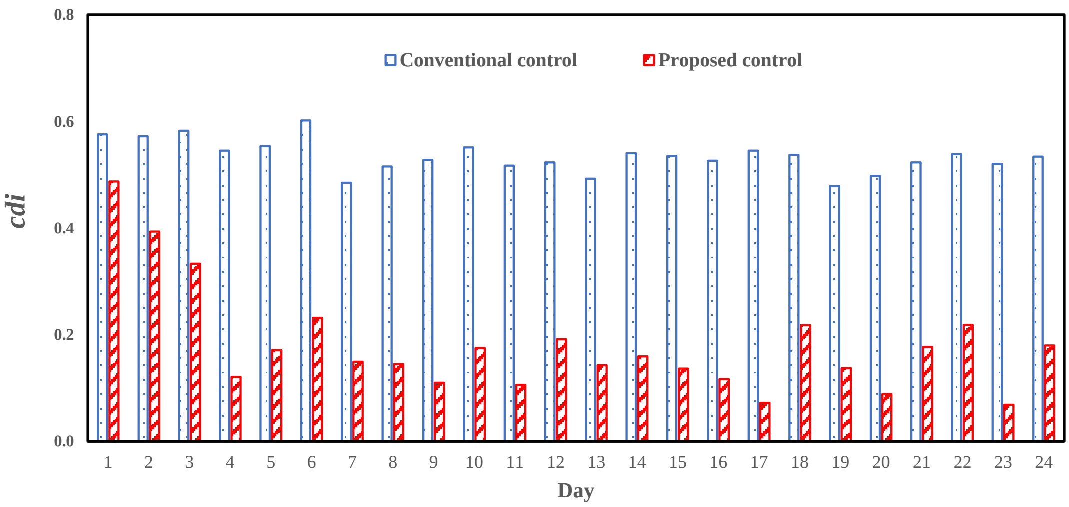

Figure 5.12 Cooling diversity indicator (*cdi*) during the test period

5.3.1.4 Reduction of precooling time

Based on the above control performance analysis, it is evident that the proposed iterative learning control strategy could achieve better control performance than conventional feedback control on distributing the limited chilled water supply during the morning start period. By applying the proposed iterative learning control strategy, the maximum return time (t_{max}) among different building zones and the cooling diversity indicator (*cdi*) of different building zones were reduced significantly. In this way, the consistency of precooling lead time among different building zones was achieved by adjusting the AHU valve openings corresponding to individual building zones. The precooling time reduction was therefore achieved.

Figure 5.13 presents the precooling time reduction using the proposed control strategy on a single day, i.e., Day 19 (23/July). Figure 5.13 (a) shows the temperature profiles of the six building zones under the conventional feedback control, it is clear that the cooling-down speeds of indoor air temperature among the zones were significantly different. Precooling starts at around 6:26 AM under conventional feedback control. By 8:00 AM, all zones reach the temperature setpoint, with Zone 6 reaching its setpoint 0.75 hour earlier than Zone 1. The t_{max} was 1.57 hours and the *cdi* was 0.48 under conventional feedback control, indicating that conventional precooling took 1.57 hours.

When the proposed strategy was used at the same conditions, the cooling-down speeds among the different building zones were much more similar, as shown in Figure 5.13 (b). Precooling starts at around 6:38 AM under the proposed control. Allzones reached the temperature setpoint almost synchronously at 8:00 AM. The t_{max} was 1.38 hours and the *cdi* was 0.14, with the precooling time reduced to 1.38 hours. Compared to using the conventional control strategy, the precooling time was reduced by 0.19 hour (from 1.57 hours to 1.38 hours). The potential precooling time was thus reduced by 12.1% on a typical summer day (23/July) in Hong Kong.

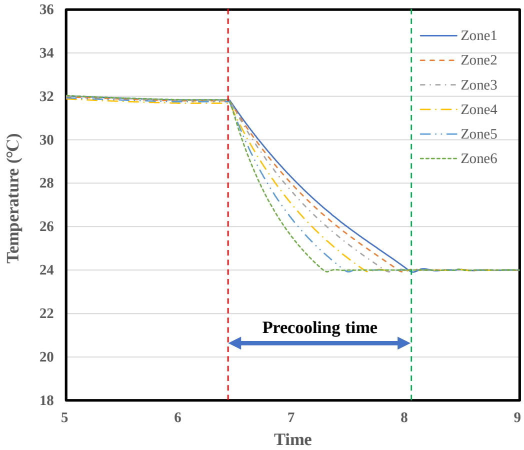

(a) Temperature profiles using the conventional control

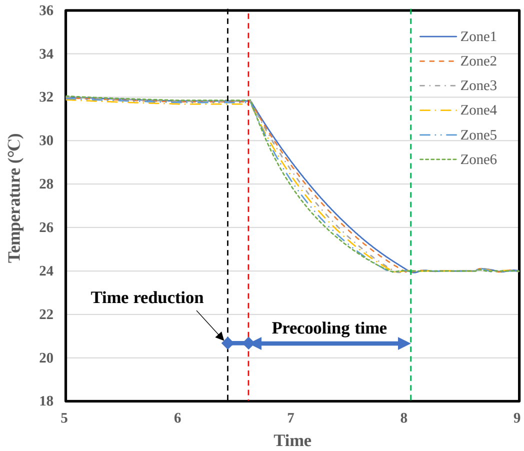

(b) Temperature profiles using the proposed control

Figure 5.13 Precooling time reduction evaluation of a typical summer day

The daily reductions of the precooling time over the four-week test period are shown in Table 4.5 and Figure 5.14. It can be observed that the maximum daily reduction was 0.19 hours on Day 19 (23/July). The average daily reduction of precooling time was 0.1 hours (10.9%), and the accumulated precooling time reduction over the test period was 2.48 hours.

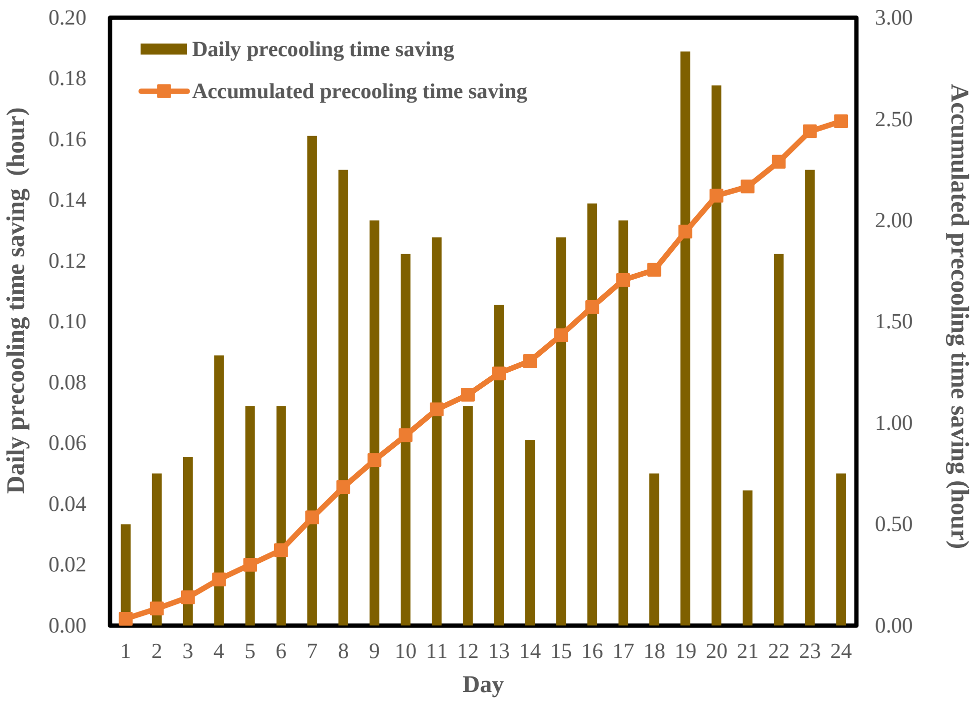

Figure 5.14 Reduction of precooling time during the test period

Table 5.5 Reduction of precooling time during the test period

	Day	Daily potential precooling time reduction (hour)	Daily potential precooling time reduction (%)
Week 1	1	0.03	4.8
	2	0.05	5.7
	3	0.06	6.6
	4	0.09	12.1
	5	0.07	10.0
	6	0.07	12.0
Week 2	7	0.16	10.7
	8	0.15	11.9
	9	0.13	12.2
	10	0.12	13.3
	11	0.13	13.2
	12	0.07	10.2
Week 3	13	0.11	13.8
	14	0.06	8.9
	15	0.13	14.8
	16	0.14	13.3
	17	0.13	13.6
	18	0.05	4.8
Week 4	19	0.19	12.1
	20	0.18	13.6
	21	0.04	4.7
	22	0.12	15.6
	23	0.15	15.6
	24	0.05	5.1
Accumulated potential precooling time reduction (hour)		2.48	

5.3.2 Energy saving using proposed control strategy

Based on the reduction of the precooling time obtained from the tests, the energy savings of the proposed iterative learning control strategy can be quantified. In the system, the energy consumption of the main chilled water plant includes that of the chillers, primary pumps, and secondary pumps. Table 5.6 shows the comparision between the energy consumptions using the proposed iterative learning control and conventional control on a typical summer day (23/July). The reduction of precooling time was 0.19 hours when adopting the proposed iterative learning control. As shown in Table 5.6, the major energy saving came from the chillers, and the overall energy savings were 695 kWh (12.8%) by using the proposed control strategy.

Table 5.6 Energy consumption comparation of a typical summer day

	Overall (kWh)	Chillers (kWh)	Primary pumps (kWh)	Secondary pumps (kWh)
Conventional control	5415	4341	519	555
Proposed control	4720	3834	454	432
Reduction (kWh)	695	507	65	123
Reduction (%)	12.8	11.7	12.5	22.2

The energy savings during the entire four-week test are shown in Table 5.7 and Figure 5.15. It can be seen that the maximum daily overall energy savings were 695 kWh on Day 19 (23/July). The average daily overall energy saving was about 400 kWh (12.4% savings) and the accumulated overall energy saving over the test period (four weeks) was 9,615 kWh.

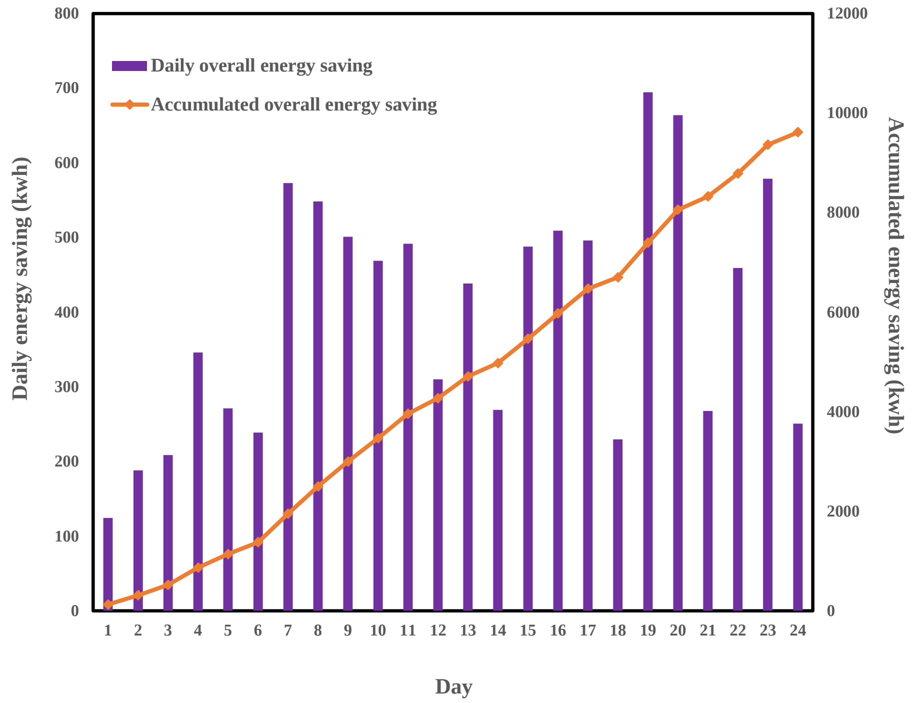

Figure 5.15 Energy saving in the test period

Table 5.7 Energy saving during the test period

	Day	Daily overall energy saving (kWh)	Daily overall energy saving (%)
Week 1	1	124	5.1
	2	188	6.3
	3	208	7.4
	4	346	14.0
	5	271	11.2
	6	239	12.0
Week 2	7	573	11.0
	8	548	12.8
	9	501	13.5
	10	469	15.2
	11	492	15.0
	12	310	13.1
Week 3	13	438	16.5
	14	269	11.7
	15	488	16.8
	16	509	14.4
	17	496	15.0
	18	230	6.5
Week 4	19	695	12.8
	20	664	14.9
	21	268	8.3
	22	459	17.5
	23	579	17.8
	24	251	7.6
Accumulated overall energy saving (kWh)		9615	

5.4 Summary

For commercial buildings, the precooling time is significantly extended due to the varied cooling rates of different zones leading to significant energy waste. To address this common operational issue, a new iterative learning control strategy has been proposed to optimally distribute the limited cooling supply during the morning start period. The control outputs, such as valve openings, are updated daily. This iterative learning control strategy continuously tracks the goal of achieving consistent precooling lead time across different building zones each morning. A Q-learning agent has been developed to select and tune the parameters of the iterative learning controller based on the Q-table method. Based on the experiences and results from validation tests, several key findings are summarized as follows:

- The proposed iterative learning control strategy updates the control outputs at each control interval (daily) to consistently achive the goal of uniform precooling lead times across different building zones.
- The strategy has successfully reduced the maximum return time among multiple zones from night setback (t_{max}) and the cooling diversity indicator (*cdi*). The average daily reduction in precooling time was 0.1 hour (10.9% reduction), with a total reduction of 2.48 hours over the four weeks test period.
- The strategy has significantly enhanced energy savings. The average daily energy savings of the chilled water plant was 400 kWh, with a total of 9,615 kWh over the four weeks test period.

CHAPTER 6 EVENT-DRIVEN CONTROL STRATEGY FOR FAST DEMAND RESPONSE

To address the challenges associated with building grid-interaction, this chapter proposes an event-driven control strategy of air-conditioning systems aimed at facilitating fast demand response for smart grids. The proposed control strategy determines the optimal AHU (Air Handling Unit) water valve openings based on real-time indoor environment data from various air-conditioned zones. This ensures even distribution of the limited cooling supply after part of the operating chillers are shut down during the demand response period. Section 6.1 illustrates the mechanism of event-driven control and operation procedure. Section 6.2 elaborates on the test arrangement for fast demand response. Section 6.3 presents the performance of the chilled water distributionand the power limiting effect. Conclusive remarks are provied in Section 6.4.

6.1 Mechanism of event-driven control and operation procedure

6.1.1 Outline of the proposed event-driven control strategy

Figure 6.1 shows the outline of the proposed event-driven control strategy to address the disordered water flow distribution problem that occurs after shutting down some of the operating chillers for fast demand response. The basic idea is to adjust the AHU valve opening associated with each air-conditioned zone to allow for even cooling distribution (i.e., evenly-spread thermal comfort) among all air-conditioned zones. The developed control strategy is activated after part of the operating chillers are shut down. It mainly consists of two parts: the event-driven control scheme and the cooling distribution control scheme, as shown in Figure 6.1.

The term "event" refers to the scenario in which the degree of indoor air temperature imbalance among different building zones reaches the preset threshold defined in this study. Environmental variable measurements (i.e., zone air temperatures) are collected and sent to the event-driven control scheme module. This module analyzes the real-time data and determines whether a predefined event has occurred (i.e., whether the degree of indoor air temperature imbalance exceeds the threshold), as illustrated in Chapter 6.1.2. Based on the judgment, the event-driven scheme would then decide whether to activate the cooling distribution control scheme, as illustrated in Chapter 6.1.3, to adjust the control outputs (i.e., AHU valve openings) for even cooling distribution. At each sampling interval, the event-driven control scheme makes an appropriate decision on whether to adjust the AHU valve openings.

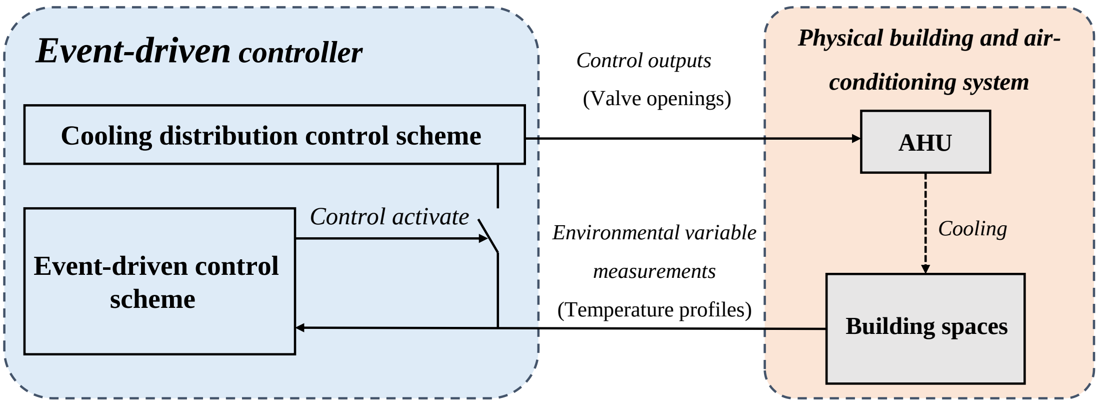

Figure 6.1 Outline of the proposed event-driven control strategy

Unlike existing time-driven control strategies, which trigger control actions at a fixed time interval (*P*) as shown in Figure 6.2 (a), the proposed event-driven control strategy only triggers control actions (i.e., AHU valve opening adjustment) when necessary, based on the real-time indoor environment. As shown in Figure 6.2 (b), the control outputs of the proposed event-driven control strategy are implemented at variable time intervals (P_1, P_2, P_3, etc.). An additional step is included in the event-driven control strategy compared to existing time-driven control strategies: it involves assessing whether the predefined event occurs and determining whether adjustments to the AHU valve openings are needed at the current sampling interval. In this way, the proposed control strategy only triggers necessary valve opening adjustments, leading to significantly reduced unnecessary wear and tear on the AHU valves compared to existing time-driven control strategies.

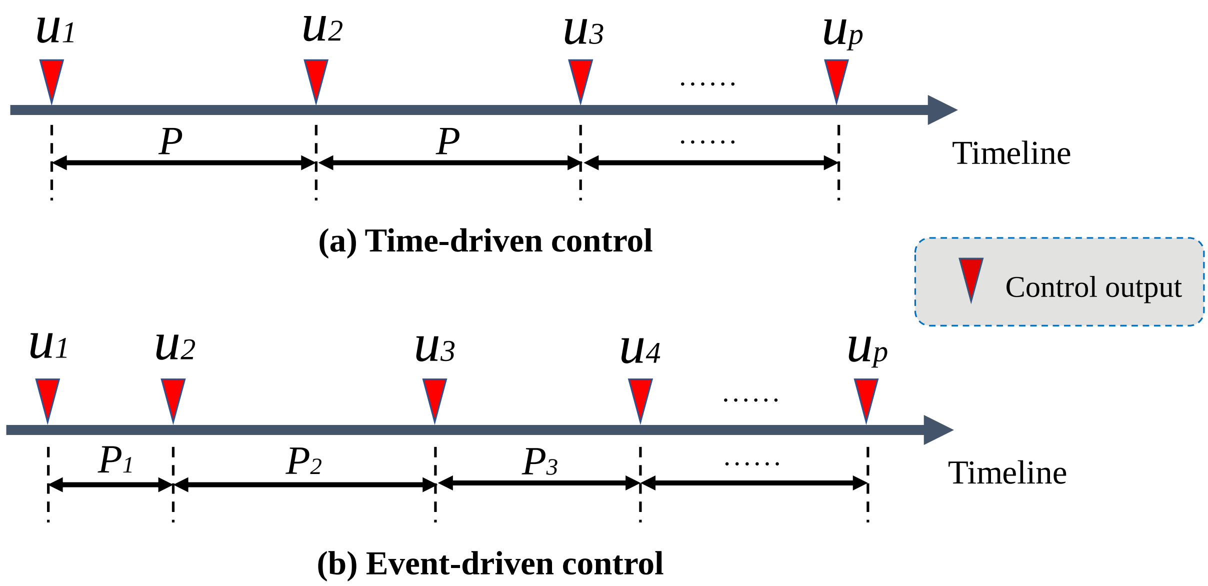

Figure 6.2 Comparation between the proposed event-driven control strategy and existing time-driven control strategies

6.1.2 Event-driven control scheme

The framework of the event-driven control scheme is depicted in Figure 6.3. The event-driven controller first analyzes real-time indoor environment data and then determines whether the pre-defined event has occured. The event determination is a crucial pre-defined step in the event-driven control scheme. This control scheme operates on the premise that the higher the degree of indoor air temperature imbalance among different building zones, the higher the necessity for AHU valve opening adjustments. A Temperature Imbalance Indicator (*TII*) is proposed in this study to facilitate event determination, as illustrated by Eq. (6.1). Here, T_{ave} represents the average indoor temperature of the *n* building zones and can be calculated using Eq. (6.2). T_m represents the temperature of building zone *m*.

$$TII_m = \left| T_{ave} - T_m \right| \tag{6.1}$$

$$T_{ave} = \frac{\sum_{m=1}^{n} T_m}{n} \tag{6.2}$$

The Temperature Imbalance Indicator (*TII*) canrepresent the degree of temperature imbalance for each building zone relative to the average zone temperatures. If the TII for a building zone exceeds the pre-defined event threshold (e.g., 0.1℃ in this study), an event will be detected, and the AHU valve opening will be adjusted according to the control output provided by the cooling distribution control scheme for that zone. Otherwise, the AHU valve will maintain its previous valve opening setpoint. It is worth mentioning that the pre-defined event threshold is adjustable for real-world applications, depending on on-site implementation situations (e.g., considering sensor accuracy).

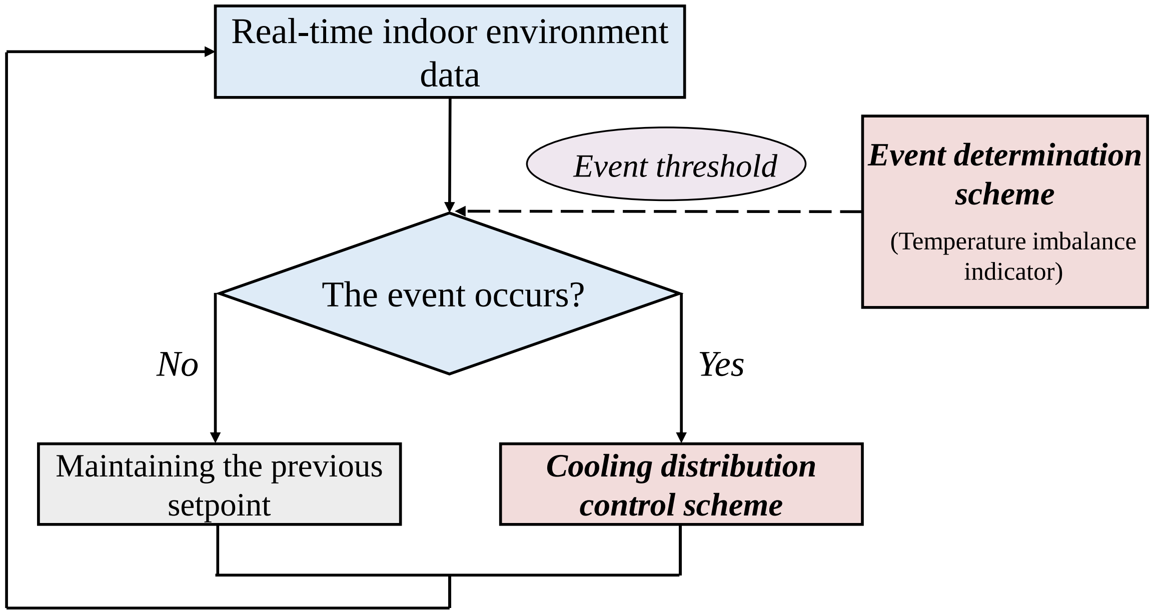

Figure 6.3 Framework of the event-driven control scheme

6.1.3 Cooling distribution control scheme

Figure 6.4 illustrates the basic principle of the proposed cooling distribution control scheme used in the event-driven control strategy. After some of the operating chillers are shut down for fast demand response, the cooling supply becomes limited and insufficient to satisfy the building's cooling demand. To avoid the unbalanced cooling distribution problem typical of conventional cooling demand-based controls, the event-driven controller is deployed on site to manage the distribution of the limited cooling supply. If necessary, the event-driven controller adjusts the AHU valve openings based on indoor environment conditions to achieve even cooling distribution under limited cooling supply, thus maintaining consistent temperature rises across all air-conditioned zones.

At each sampling interval, the event-driven controller collects the measured space temperatures of all air-conditioned zones. The control action of the event-driven controller is triggered by the occurrence of a specific event rather than by the passing of time, as illustrated in Chapter 6.1.2. When this specific event occurs at sampling interval *i*, the control action is activated, and the event-driven controller adopts the proposed cooling distribution control scheme. The control outputs calculated at sampling interval *i* are maintained for the AHU valves until sampling interval *j*, when the specific event is detected again. With proper design of the specific event-driven control strategy, the event-driven controller can achieve efficient chilled water distribution with minimal AHU valve opening adjustments.

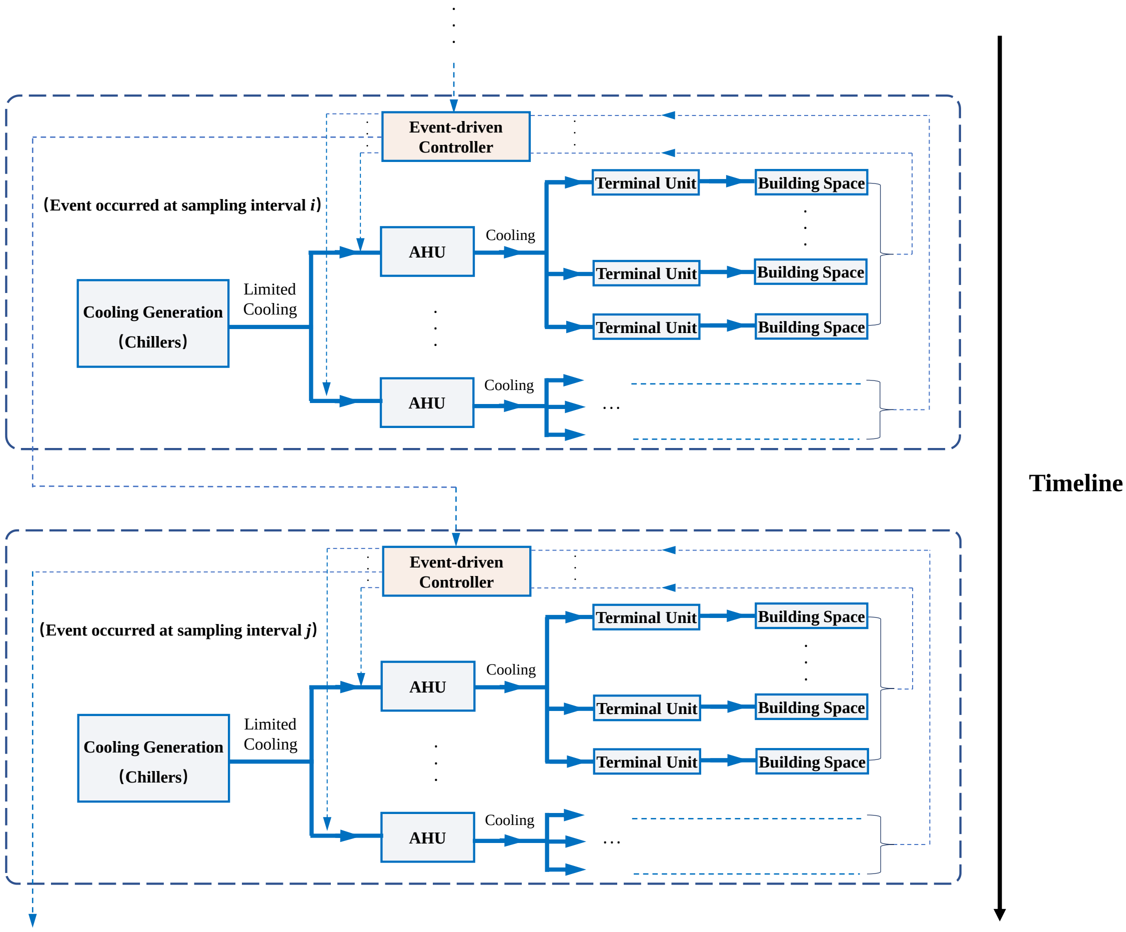

Figure 6.4 Basic principle of the proposed cooling distribution control scheme

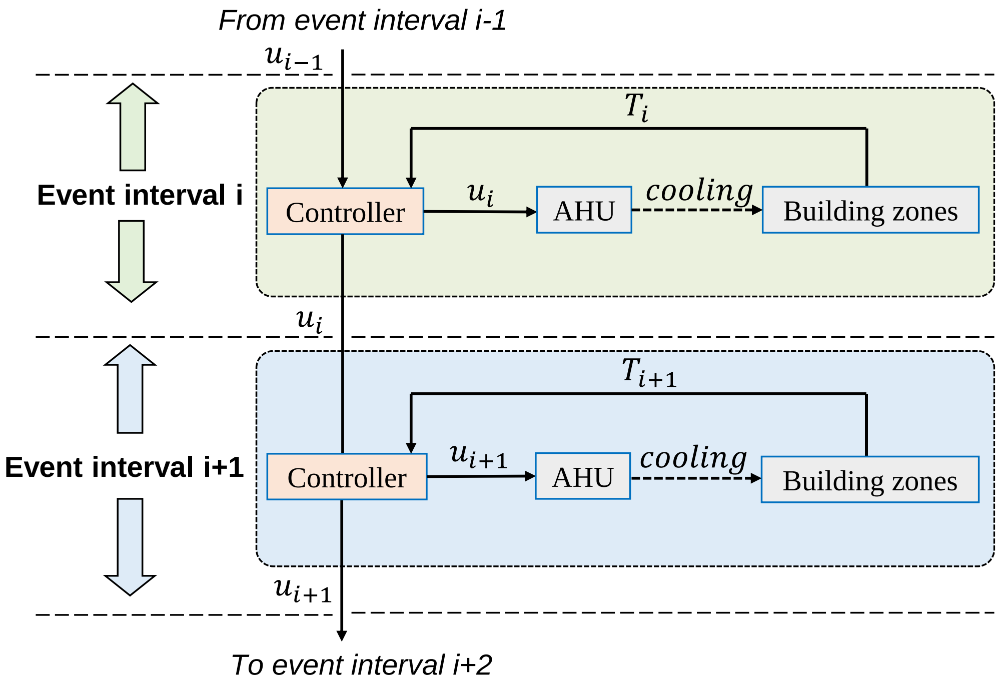

Figure 6.5 Operation procedure of cooling distribution control scheme

The detailed operation procedure of the cooling distribution control scheme is illustrated in Figure 6.5. The event interval refers to the time between detections of a predefined event, during which the control outputs are adjusted. At each event interval, the controller collects the indoor air temperature profiles of all building zones. Then, the controller calculates the control outputs based on the current indoor air temperature profiles and the previously calculated control outputs from the last event interval. The detailed operation procedure is outlined below.

- At event interval *i*, the event-driven controller collects the following data as inputs as defined in Eq. (6.3) and Eq. (6.4), including: (1) indoor temperatures (T_i) of the *n* building zones at the event interval *i* and (2) AHU valve openings of the *n* building zones at the event interval *i-1* (u_{i-1}).

$$T_i = [T_{1,i}, T_{2,i}, \cdots T_{n,i}] \tag{6.3}$$

$$u_{i-1} = [u_{1,i-1}, u_{2,i-1}, \cdots u_{n,i-1}] \tag{6.4}$$

- Calculate the average temperature ($T_{ave,i}$) of the *n* building zones at event interval *i* using Eq. (6.5).

$$T_{ave,i} = \frac{\sum_{m=1}^{n} T_{m,i}}{n} \tag{6.5}$$

- Calculate the AHU valve opening correction $\Delta u_{m,i}$, for the building zone concerned using Eq. (6.6).

$$\Delta u_{m,i} = k \cdot \left(T_{ave,i} - T_{m,i}\right) \tag{6.6}$$

Where, *k* is the control parameter of the event-driven controller. The setting of *k* affects the control efficiency and stability. A high *k* value can speed up the control process but may induce oscillation. Conversely, a low *k* value results in slower response. However, since the control action at each step is activated by the event-driven control and only when the temperature difference among zones exceeds the threshold, the risk of overshooting is then much lower if the k value is not set too high, making the choice of control parameter setting less challenging. In this study, *k* is set to 0.1 based on expert judgment and the authors' experience.

- Calculate the corresponding AHU valve opening $u_{m,i}$, for the building zone concerned, using Eq. (6.7).

$$u_{m,i} = u_{m,i-1} - \Delta u_{m,i} \tag{6.7}$$

According to the control algorithm above, the AHU valve opening control signals for the *n* building zones (u_i) at event interval *i* could be determined to achieve even cooling distribution.

6.1.4 Performance indicators for evaluating the demand response control

Tto evaluate the control performance of the event-driven control and compare it with the time-driven control, two control performance indicators are proposed in this study. The first one is the Temperature Diversity Indicator (*TDI*) as shown in Eq. (6.8). Here, T_{max} represents the highest temperature among the *n* building zones as shown in Eq. (6.9), and T_{min} represents the lowest temperature among the *n* building zones as shown in Eq. (6.10).

$$TDI = T_{max} - T_{min} \tag{6.8}$$

$$T_{max} = max\{T_1, T_2 \cdots T_n\} \tag{6.9}$$

$$T_{min} = min\{T_1, T_2 \cdots T_n\} \tag{6.10}$$

The Temperature Diversity Indicator (*TDI*) is designed to measure the degree of maximum temperature deviation among the zones, considering that the control objective is to maintain consistent ndoor air temperature rises across all building zones. The TDI is expected to be as low as possible for achieving this control objective.

The second performance indicator is the Accumulated Valve Travel Distance (*AVTD*) as shown in Eq. (6.11). Here, Δu_i represents the valve opening adjustment at control interval i, and I represents the total control intervals during the demand response period. The goal is to use the minimum valve opening adjustment necessary to maintain consistent indoor air temperature rises across all building zones. Thus, the AVTD is also expected to be as low as possible to meet the control objective. A trade-off between these two performance indicators may need to be considered in real implementation.

$$AVTD = \sum_{i=1}^{I} \Delta u_i \tag{6.11}$$

6.2 Test arrangement for fast demand response

In this study, a virtual dynamic simulation platform is developed using TRNSYS to test the applicability and performance of the proposed event-driven control strategy for fast demand response. The developed virtual test platform adopts detailed physical models of the building and its air-conditioning system, including chillers, pumps, hydraulic networks, and AHUs. These detailed physical models of the air-conditioning system are calibrated using real data. Figure 6.6 illustrates the schematic of the central air-conditioning system on this test platform. The chilled water distribution system of the air-conditioning system is a typical primary constant-secondary variable chilled water system. The chiller plant consists of four identical chillers, each with a rated capacity of 4,080 kW. The chillers and the primary chilled water pumps are designed on a one-to-one matching basis. Each primary chilled water pump operates at a constant speed and has a design flowrate of 172.8 L/s. Two variable speed water pumps are installed in the secondary chilled water loop. The chilled water is distributed to the AHUs to provide cooling for the building zones. A multizone model (Type 56) in TRNSYS is used to simulate the building zones, referencingto a super-high-rise commercial building in Hong Kong. Six typical air-conditioned zones with different cooling load profiles are involved. Each building zone has an area of 1,600 m^2, and is cooled by the cool air supplied by its corresponding AHU. The office hours of the building are from 8:00 to 18:00, and the indoor air temperature setpoints for all six building zones during the office time are 24℃. Disturbances such as. weather and internal load variations are considered in the simulation. The internal load variations include the heat generated by occupants, electrical devices, etc., in the commercial building concerned. The real-time weather data is derived from a typical summer day (i.e. July 23th) in Hong Kong for the validation tests.

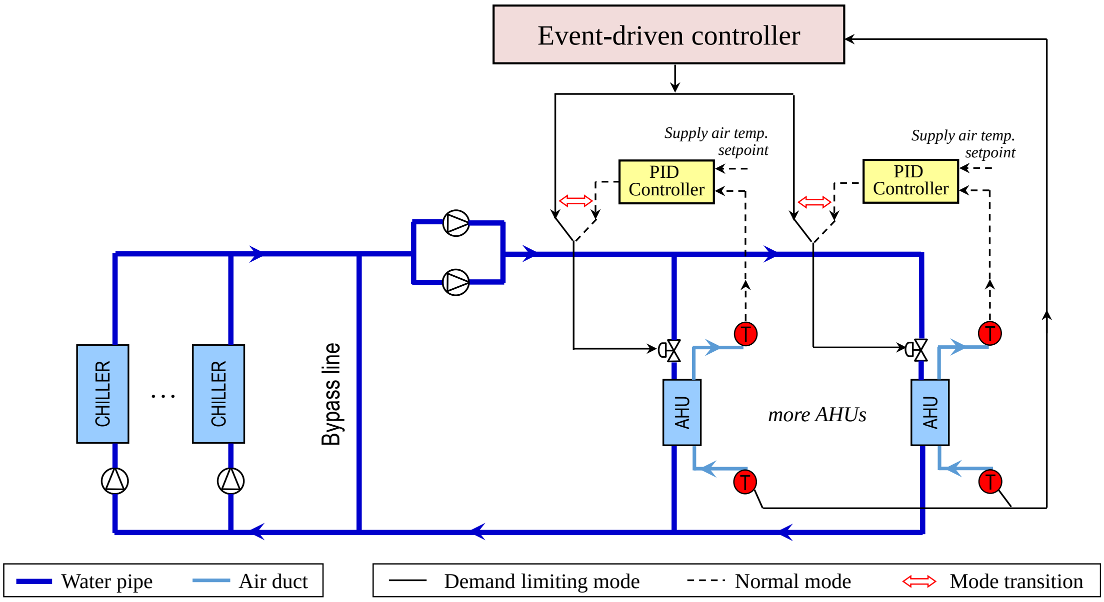

Figure 6.6 Schematic and test arrangement of central air-conditioning system concerned

The test arrangement is also presented in Figure 6.6. The normal mode refers to the operation mode during non-demand-response period when conventional feedback control is adopted, while the demand limiting mode refers to the operation mode during the demand response period when the proposed event-driven control strategy is activated. In normal mode, each PID controller collects the supply air temperature of the corresponding AHU and outputs control signals to adjust the AHU water valve opening. The control objective of each local PID controller is to maintain the AHU supply air temperature at the pre-determined setpoint. In the demand limiting mode, after shutting down part of the operating chillers, the event-driven controller is activated to override conventional feedback control. The event-driven controller first collects the AHU return air temperature profiles of all building zones. Then, it calculates the Temperature Imbalance Indicator (*TII*) and conducts the event-driven control scheme as illustrated in Chapter 6.1.2. Once the event occurs (i.e., the temperature imbalance indicator exceeds the event threshold), the event-driven controller outputs the control signals for adjusting the AHU valve openings, given by the cooling distribution control scheme as illustrated in Chapter 6.1.3. The control objective of the event-driven controller is to achieve uniform temperature rises among the building zones after shutting down some operating chillers for fast demand response. The demand response period is set for two hours in this study from 14:00 to 16:00 on a summer day in Hong Kong. The event-driven controller is set to continue to operate for some time (e.g., around half an hour) after the demand response ends to avoid competition for cooling supply among building zones with high cooling demands immediately after the demand response period.

In this test, two operating chillers are shut down, and two chillers continue to operate during the demand response event. Additionally, a comparative study of the proposed event-driven control and the existing time-driven control is conducted to validate and demonstrate the advantages of the proposed control strategy. The control actions are periodically triggered at a fixed time interval for time-driven control in this test. The fixed time interval is set to be the same as the controller's sampling interval (i.e., 2s). In this study, the simulation time step is set as short as 2 seconds to realistically simulate the dynamic operation processes of the system/components involved, including those of fast dynamic (e.g., sensors and actuatora). More importantly, it is very common for the control interval of digital controller to be rather short, such as 1 or 2 seconds for modern building automation systems (BASs). In addition, as the program of the strategy is simple and the computing load is very low, it does not impose any burden in running the control routines at each sampling interval of the controller. Therefore, we choose to use a short sampling interval, similar to the sampling interval of typical digital controllers, as the sampling interval of the proposed control strategy for the convenience of implementation in practical BASs. The event threshold for event determination under the event-driven control is set to 0.1℃. It is important to note that such a low threshold is adopted to provide a high demand and challenging test condition to validate the control performance of the event-driven strategy for cooling distribution. The event threshold is adjustable according to on-site implementation situations (e.g., considering the sensor accuracy and practical needs).

6.3 Chilled water distribution performace and power limiting effect

6.3.1 Indoor air temperature

Figure 6.7 shows the indoor temperature profiles of six building zones under conventional and proposed controls. As shown in Figure 6.7 (a), the indoor air temperature profiles of the six building zones differ significantly when conventional feedback control is used during the demand response period (from 14:00 to 16:00) and immediately after. This variance primarily results from the limited cooling supply following the shut down of half of the operating chillers. Despite high cooling demands, each zone must compete for the limited supply. Zones with relative low cooling demand and high priority in chilled water distribution manage to maintain relatively low temperature rises during the demand response period (e.g. Zone 6). Conversely, zones with relatively high cooling demand and low priority in chilled water distribution experience significant indoor air temperature increase during this period (e.g. Zone 1). Two zones report indoor temperatures increases exceeding 4 ℃ by the end of the demand response period: Zone 1 reaches 28.2 ℃ at 16:00, while Zone 6 reaches 26.7 ℃. Different cooling rates among the building zones are also evident immediately after the demand response period due to the continued limitation of cooling supply, requiring zones with high cooling demands to compete for the limited supply to return to their indoor air temperatures to their original setpoints.

Figure 6.7 (b) shows the temperature profiles of the six building zones under the proposed event-driven control. The temperature profiles of these zones are nearly identical during the demand response period, with an average indoor air temperature of 27.5 °C at the end. The zones also maintain similar cooling rates immediately after the demand response period. These results demonstrate that the proposed event-driven control strategye effectively maintains uniform indoor air temperature rises across different building zones after some of the operating chillers are shut down for fast demand response.

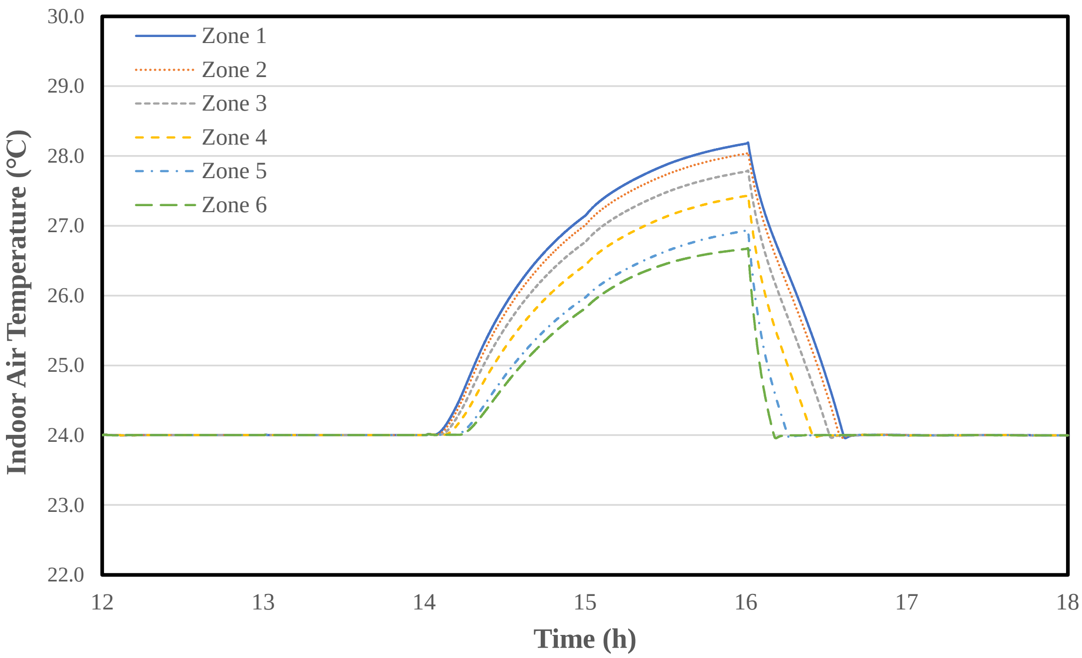

(a) Temperature profiles under the conventional control

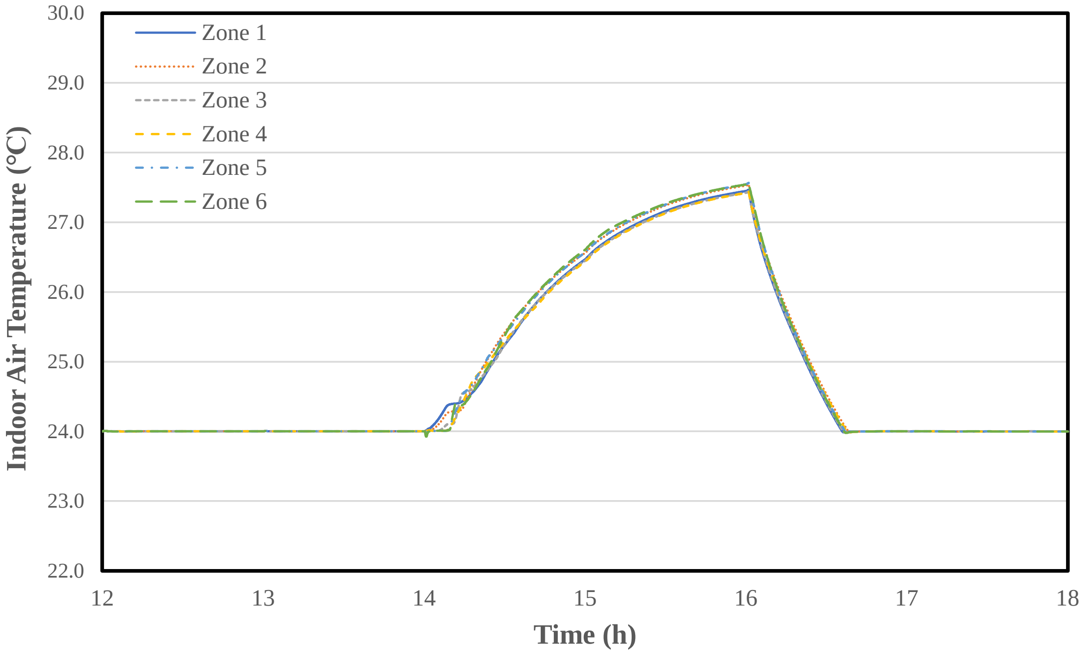

(b) Temperature profiles under the proposed event-driven control

Figure 6.7 Indoor temperature profiles of building zones under the conventional control and the proposed event-driven control

6.3.2 Water flowrate adjustment

Figure 6.8 displays the chilled water flow profiles of the six building zones under both the conventional control and the proposed event-driven control. As illustrated in Figure 6.8(a), the chilled water flowrates are notably high during the demand response period when using conventional feedback control. After two of the operating chillers are shut down at 14:00, the building zones begin to compete for the limited colling supply. The water valves of the air handling units (AHUs) are controlled to maintain their maximum openings in an effort to secure more chilled water. Zones with lower water-loop hydraulic resistances, such as Zone 6, received more chilled water supply, with flowrates reaching over 12 kg/s. Conversely, zones with higher hydraulic resistances, like Zone 1, receive less chilled water.

This disordered water flow distribution becomes a significant issue during the demand response period under conventional control. It ultimately leads to uneven indoor air temperature increases across the zones, as shown in Figure 6.7(a). Moreover, the problem of disordered water flow distribution persists even after the demand response period ends at 16:00.

Figure 6.8 (b) shows the chilled water flow profiles of the six zones under the proposed event-driven control. The disordered water distribution problem is almost completely avoided with this strategy. After two of the operating chillers are shut down, the water flowrates distributed to the six zones are quickly and properly adjusted. These flowrates remain relatively stable throughout the demand response period and immediately thereafter. As a result, the limited cooling supply is distributed effectively, leading to even indoor air temperature rises across the zones, as shown in Figure 6.7 (b).

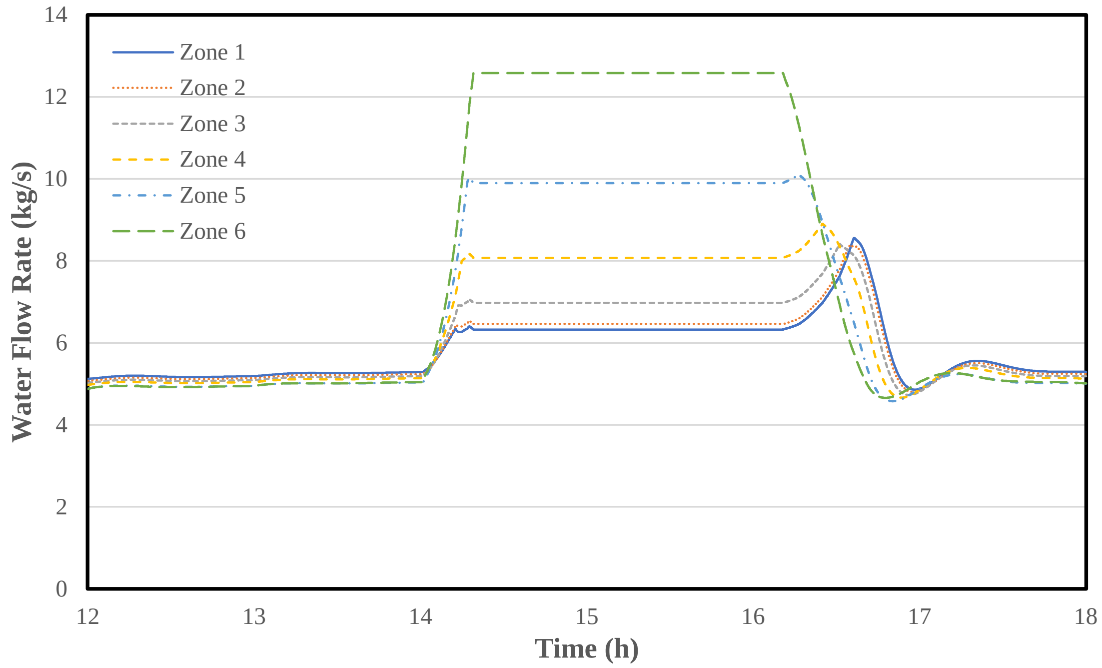

(a) Chilled water flow rate under the conventional control

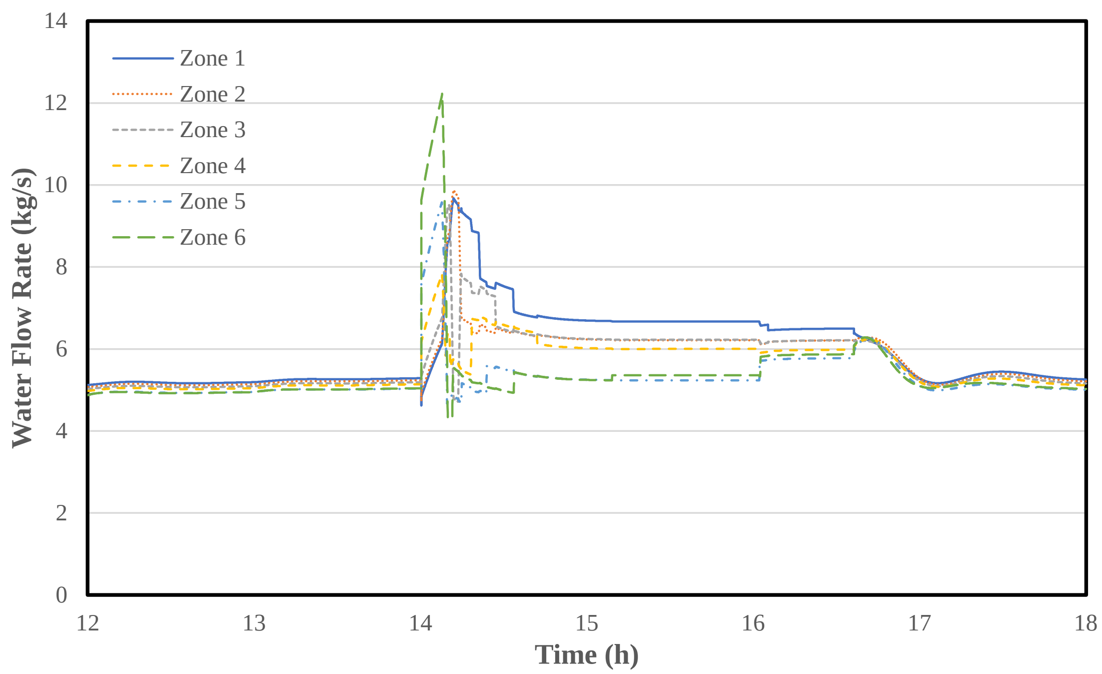

(b) Chilled water flow rate under the proposed event-driven control

Figure 6.8 Chilled water flow profiles of zones under the conventional control and the proposed event-driven control

6.3.3 Power limiting effect

Considering that a major objective of demand response control is to meet the power reduction needs of the smart grid, the power limiting effect of the proposed event-driven control is evaluated and compared with that of conventional control. Figure 6.9 illustrates the power consumption of the chiller plant (including the chillers, primary pumps, and secondary pumps) under both conventional and proposed event-driven control for fast demand response.

It is evident that while shutting down part of the operating chillers can achieve immediate power reduction, conventional feedback control compromises the power limiting effect during the demand response period and causes a more severe rebound effect immediately after. Under convention control, the power reduction of the chiller plant is approximately 735 kW, which accounts for 23% of the power consumption just before the demand response period. In contrast, the power reduction under the proposed event-driven control is greater, at 905 kW, achieving a 5% of power reduction and saving a total of 246 kWh electricity during the demand response period by shifting from conventional control to proposed event-driven control. This improvement is largely due to the fact that under conventional control, secondary chilled water pumps operate at full speeds to compete for the limited cooling supply, thereby compromising the power limiting effect. The proposed event-driven control addresses the issue of full-speed operation of the secondary pumps. Additionally, it is observed that the power rebound effect could be mitigated to some extent (i.e., by 170 kW in the test) using the proposed event-driven control.

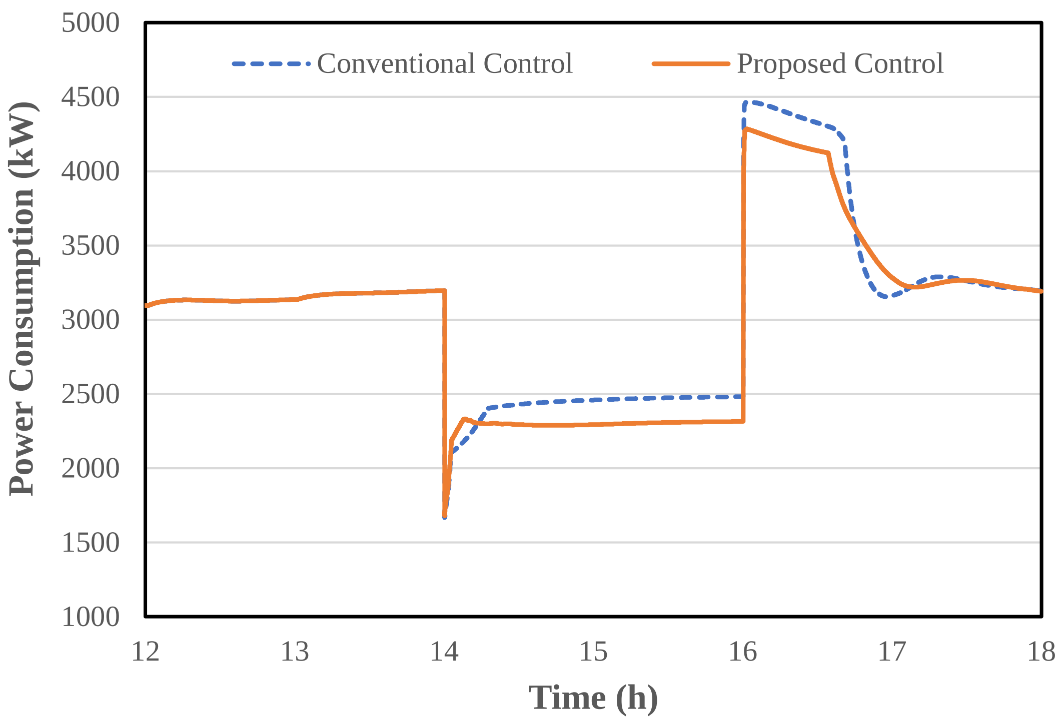

Figure 6.9 Power consumption of the chiller plant under the conventional control and the proposed event-driven control

6.3.4 Performance comparation between time-driven control and event-driven control

6.3.4.1 Temperature diversity indicator

Figure 6.10 shows the temperature profiles of the six building zones under both time-driven control and proposed event-driven control. Both control methods manage to maintain even indoor air temperature rises among all zones during the demand response period and exhibits similar cooling down speeds immediately after. The temperature profiles under the time-driven control are more consistent compared to those under the event-driven control. This consistency is due to control outputs being implemented at each sampling interval under conventional control.

As illustrated in Figure 6.11, the temperature diversity indicators for both control methods are compared. Under the time-driven control, the temperature diversity indicators remainlower than 0.1℃ most of the time during the demand response period. Initially, there is an increase in the temperature diversity indicator, but as time progress, the indicator decreases to nearly 0 under. This indicates that the indoor air temperatures of the six zones are almost identical under the time-driven control.

As for the event-driven control, the temperature diversity indicator follows a similar trend to that under the time-driven control. However, the temperature diversity indicator under the event-driven control is slightly higher, reaching up to 0.37℃, though it remains below 0.2℃ for most of the demand response period.

In conclusion, both the time-driven and event-driven control successfully achieve the control objective during the demand response period. However, the time-driven control exhibits slightly better performance regarding the temperature diversity indicator.

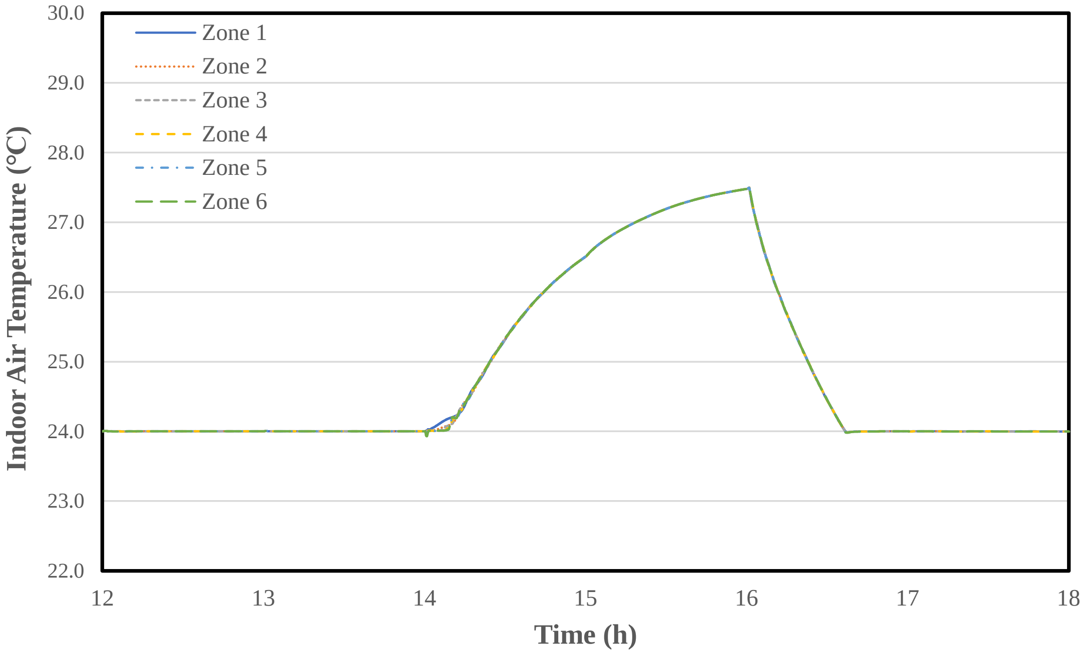

(a) Temperature profiles under the time-driven control

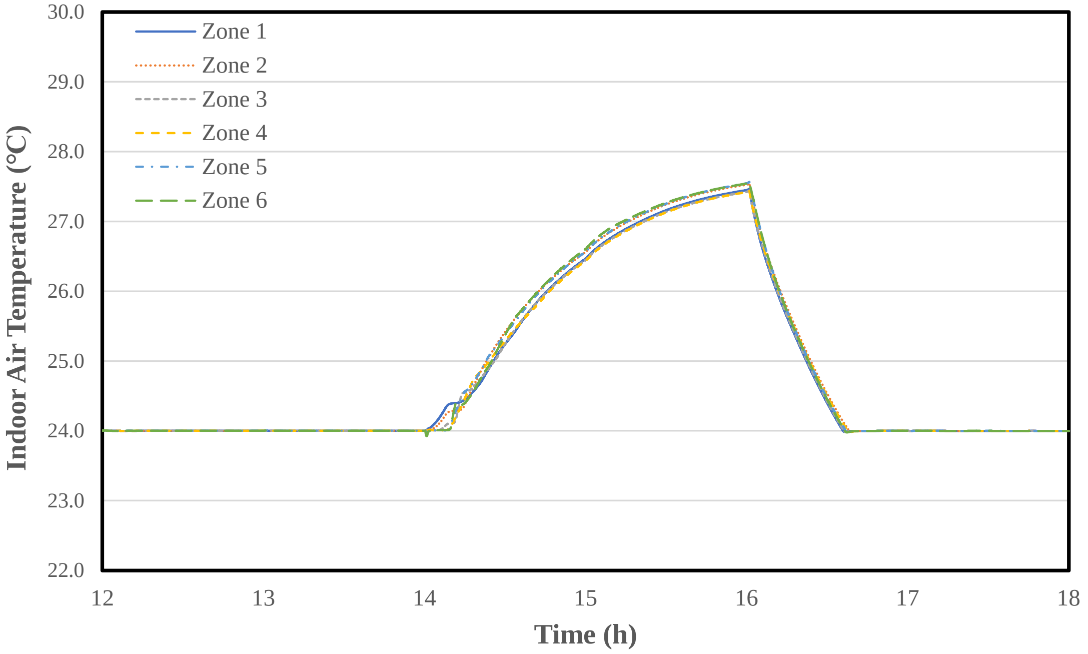

(b) Temperature profiles under the event-driven control

Figure 6.10 Temperature profiles of zones under the time-driven control and the proposed event-driven control

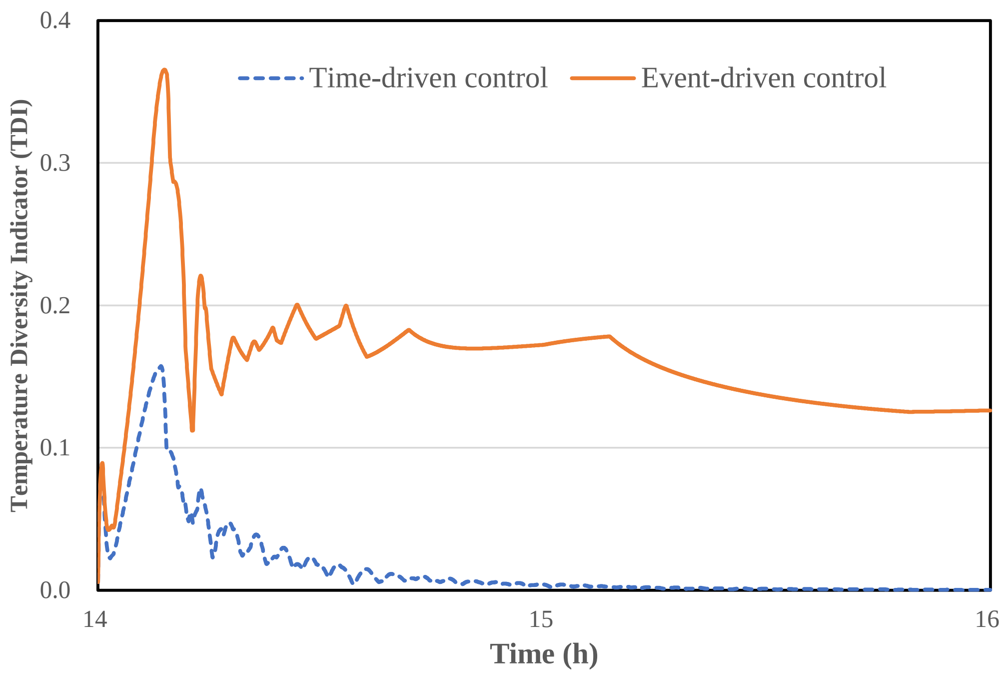

Figure 6.11 Temperature diversity indicator under the time-driven control and the proposed event-driven control

6.3.4.2 Accumulated valve travel distance

Figure 6.12 shows the valve opening profiles of six zones during the demand response period under the time-driven control and the proposed event-driven control. Under the time-driven control, the valve openings of the six zones are oscillatory within the first hour of the demand response period, as shown in Figure 6.12 (a). This oscillation occurs because the valves are adjusted at every sampling interval to track the control objective. In contrast, with the proposed event-driven control strategy is adopted, the valve openings are much more stable, as seen in Figure 6.12 (b). There are only a few adjustments to the valves throughout the demand response period, indicating that adjustments are made only when necessary under the event-driven control.

Figure 6.13 presents the accumulated valve travel distances for both strategies. It can be observed that the accumulated valve travel distance is significantly reduced for all six zones when switching from the time-driven to the event-driven control. The maximum reduction inaccumulated valve travel distance occurs in zone 1, reaching as high as 79.6%, with an average reduction of 54.6% across all zones. This reduction significantly decreases the wear and tear on the AHU valves under the demand response control.

Therefore, the proposed event-driven control strategy is more advisably for real-world applications compared to existing time-driven controls.

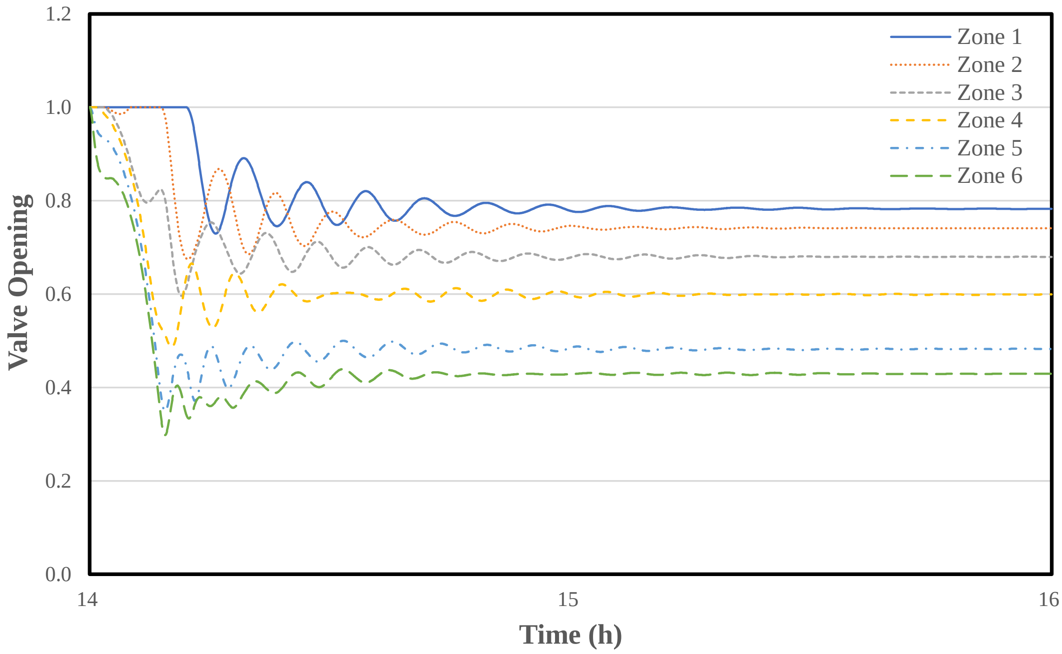

(a) Valve opening profiles under the time-driven control

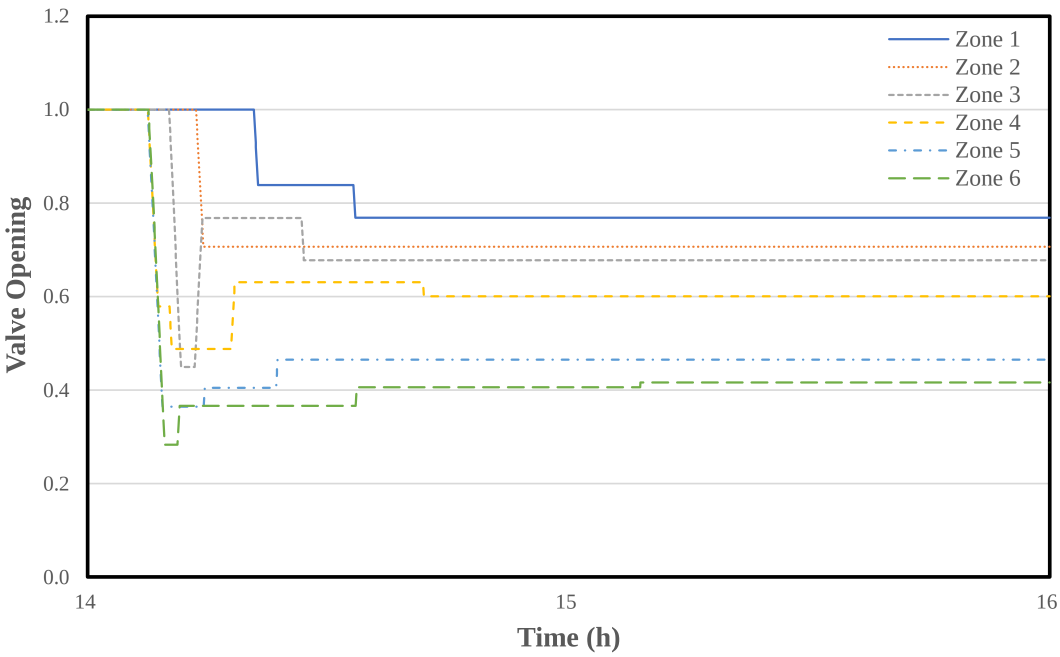

(b) Valve opening profiles under the event-driven control

Figure 6.12 AHU valve opening profiles of zones under the time-driven control and the proposed event-driven control during demand response period

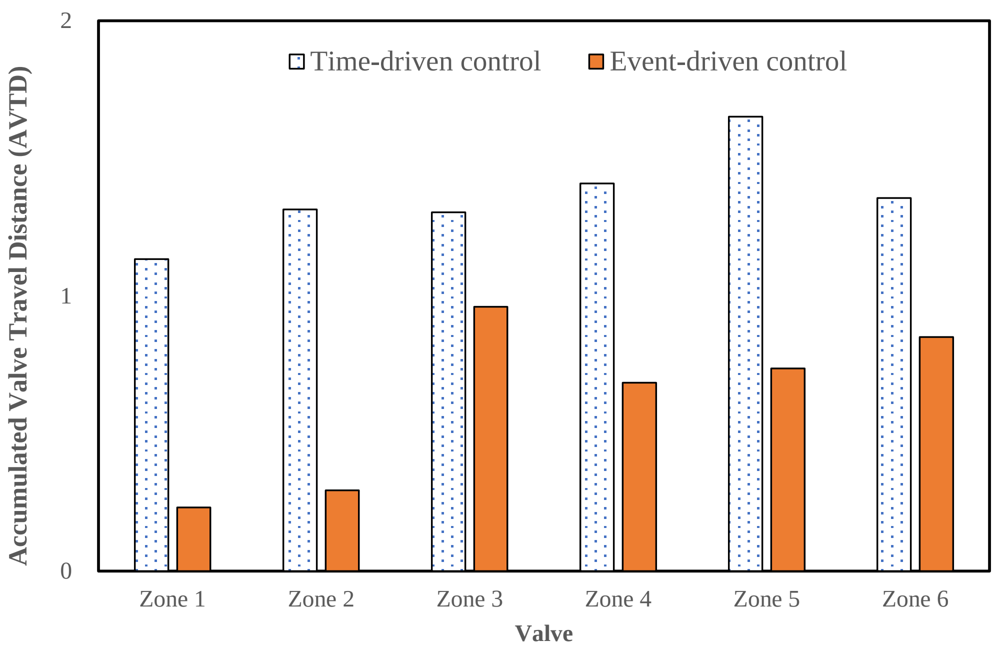

Figure 6.13 Accumulated valve travel distances under the time-driven control and the proposed event-driven control during demand response period

6.4 Summary

Buildings can play a significant role in addressing the power imbalance problem of power grids with high penetration of intermittent renewable energy in a cost-effective manner by utilizing their air-conditioning systems. Shutting down some operating chillers has proven to be an effective method. However, this approachcan lead to disordered chilled water flow distribution and uneven indoor thermal comfort degradation across different building zones. To address the issues, an event-driven control strategy for air-conditioning systems is proposed in this study. This strategy includes a cooling distribution control scheme for even cooling distribution and an event-driven control scheme to minimize valve adjustments during the control process. It requires no additional sensors nor additional experimental work for the identification of thermodynamic characteristic parameters. Besides, the proposed strategy helps avoid unnecessary wear and tear on the AHU valves. The major findings from the test results are summarized as follows:

- The proposed event-driven control strategy can maintain uniform indoor air temperature rises among different building zones during the demand response period. Proper distribution of the limited cooling supply ensures that similar indoor air temperature profiles among the zones can ultimately be achieved.
- The power demand and energy consumption of the chiller plant can be significantly reduced during the demand response period using the proposed event-driven control strategy, for example, a power demand reduction of 170 kW (approximately 5%) and a reduction in electricity consumption by 246 kWh (5%). Furthermore, the power rebound effect immediately after the demand response period can also be mitigated to some extent.

- Both the proposed event-driven and the time-driven controls can achieve the control objective during the demand response period. However, the accumulated valve travel distance of AHUs for different building zones can be reduced by an average of 54.6% under the event-driven control compared with the time-driven control.

CHAPTER 7 MULTI-AGENT BASED DISTRIBUTED COOPERATIVE CONTROL STRATEGY FOR ENHANCED SCALABILITY

To further improve the control generality and scalability, this chapter proposes a distributed cooperative control strategy of air-conditioning systems based on the multi-agent system to perform building fast demand response. Section 7.1 illustrates the mechanism of multi-agent-based distributed cooperative control strategy. Validation platform and arrangement are presented in Section 7.2. Section 7.3 presents the test results and analysis on the chilled water system and air-side system. The conclusions are made in Section 7.4.

7.1 Mechanisum of multi-agent based distributed cooperative control strategy

7.1.1 Outline of the distributed cooperative control strategy

Figure 7.1 illustrates the outline of multi-agent-based cooperative control strategy. It is implemented at field control stations. A multi-agent system is constructed by multiple agents, which are designed as local controllers of corresponding terminals (i.e., AHU valves and VAV dampers) in the central air-conditioning system. These agents work together to achieve an even distribution of limited cooling among building spaces during a demand response event. The agents determine the cooling distributed to individual building spaces by managing the chilled water flow rate through AHUs and the supply air flowrate of VAV terminals. Each agent is enabled to collect the environmental variable measurement (i.e., temperature profile) of its corresponding building space, send its collected information to its neighbors, and receive information from them through the field network. At each control interval, the agents perform information collection and communication, and determine the individual control outputs in a distributed, self-organizing way. In the event of an urgent power reduction request from the power grid, a portion of operating chillers will be shut down to enable power limiting. This proposed distributed cooperative control strategy will then be activated to override conventional control to properly distribute the limited cooling supply.

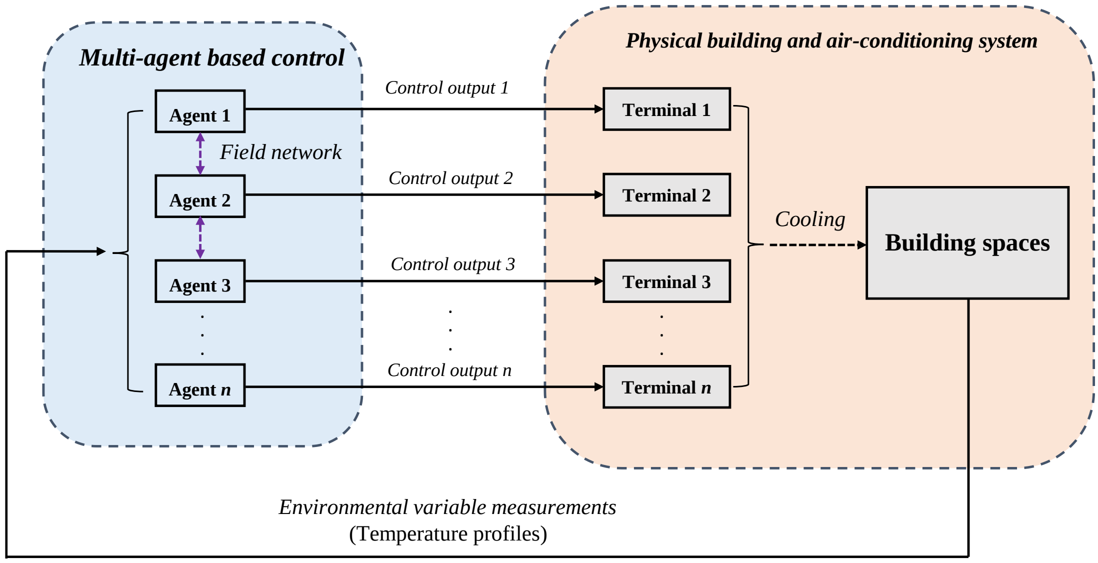

Figure 7.1 Outline of the distributed cooperative control strategy

7.1.2 Basic principle of the control algorithm

7.1.2.1 Problem formulation

Achieving even cooling distribution among different air-conditioned zones/spaces can be regarded as a consensus problem. Therefore, the proposed control adopts principles from algebraic graph theory (Godsil & Royle, 2001), which is widely used to address consensus problems in computer science. Algebraic graph theory is commonly employed in the fields of multi-agent systems and distributed control to study and solve issues related to consensus control. In computer science, consensus algorithms aim to solve the problem of reaching agreement among a group of distributed nodes or processes in a network. These algorithms ensure that all nodes in the network agree on a single value or decision. They typically involve a series of rounds where nodes exchange messages, propose values, and attempt to converge on a common agreement. Consensus control aims to coordinate the behavior of multiple agents in a networked system so that they can reach an agreement or consensus on a particular value or state. The fundamentals of algebraic graph theory for consensus control involve the following key concepts and techniques:

- Graph Representation: The network of agents is represented using a graph, where each agent is a node and the communication links between agents are represented by edges. The graph can be represented using an adjacency matrix or an adjacency list.
- Laplacian Matrix: The Laplacian matrix of the graph, derived from the adjacency matrix, captures important information about the graph's connectivity.
- Consensus Algorithm: This iterative process allows agents in a network to reach an agreement on a common value or state.

A graph G is composed of a set of vertices V and a set of edges E, as shown in Eq. (7.1). The vertex set V can be described using Eq. (7.2), where n represents the number of nodes in the graph. The edge set E of a graph can be described using Eq. (7.3), where e_{ij} represents the specific edge pointing from v_i to v_j. The edge e_{ij} indicates that v_i and v_j are adjacent (i.e., v_j is a neighbor of v_i). The set of neighbors of the node v_i is denoted by N_i as shown in Eq. (7.4). In algebraic graph theory, nodes can be viewed as agents. If agent v_j is a neighbor of agent v_i, then agent v_i will exchange information with agent v_j.

$$G = (V, E) \tag{7.1}$$

$$V = \{v_1, v_2, \cdots, v_n\} \tag{7.2}$$

$$E = \{e_{ij} = (v_i, v_j)\} \in V \times V \tag{7.3}$$

$$N_i = \{v_j \in V | (v_i, v_j) \in E\} \tag{7.4}$$

The adjacency matrix $A=[a_{ij}]$ is used to describe the structure of the graph G. A is a $n \times n$ matrix, and its elements a_{ij} are shown in Eq. (7.5).

$$a_{ij} = \begin{cases} 1, (v_i, v_j) \in E \\ 0, otherwise \end{cases} \tag{7.5}$$

Figure 7.2 illustrates a typical simple graph G with six vertices. The adjacency matrix A of this graph can be derived as shown in Eq. (7.6) according to the algebraic graph theory.

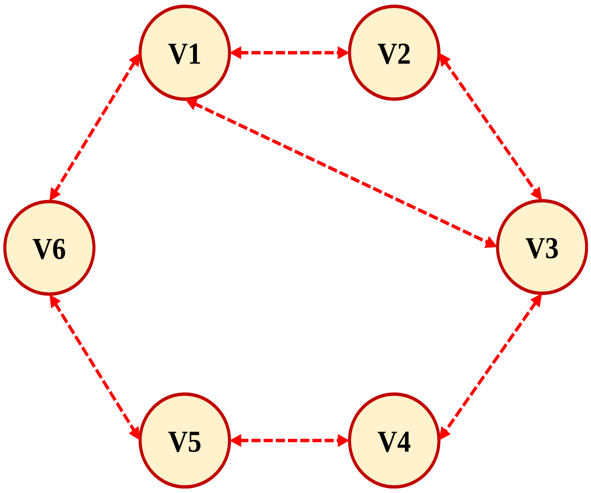

Figure 7.2 Illustration of a typical graph G with six vertices

$$A = \begin{bmatrix} 0 & 1 & 1 & 0 & 0 & 1 \\ 1 & 0 & 1 & 0 & 0 & 0 \\ 1 & 1 & 0 & 1 & 0 & 0 \\ 0 & 0 & 1 & 0 & 1 & 0 \\ 0 & 0 & 0 & 1 & 0 & 1 \\ 1 & 0 & 0 & 0 & 1 & 0 \end{bmatrix} \tag{7.6}$$

The problem of proper cooling distribution during fast demand response event can be formulated using Eq. (7.7). Where, x_i represents the corresponding temperature profile of the building zone/space for agent v_i. Figure 7.3 depicts the schematic of the agent deployment in the air-conditioning system concerned. Each AHU valve is equipped with a valve agent working as the controller for proper cooling distribution at the chilled water side. Similarly, each VAV damper is equipped with a damper agent at the supply air side. During a fast demand response event, agents are able to exchange collected state information with their neighboring agents. This communication occurs between agents in the chilled water system and the supply air system, forming corresponding graphs. The ultimate control objective is to ensure that thermal comfort sacrifices are evenly distributed across all building zones and spaces.

$$x_1 = x_2 = \cdots = x_n \tag{7.7}$$

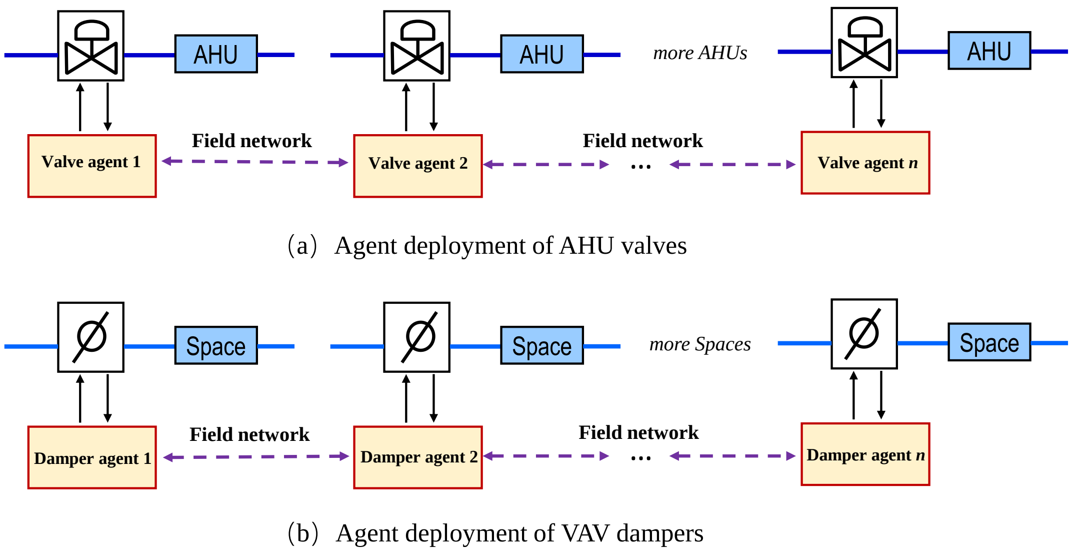

Figure 7.3 Schematic of the agent deployment in the air-conditioning system

7.1.2.2 Consensus algorithm

To address the aforementioned problem, the consensus algorithm (Olfati-Saber et al., 2007) is adopted in this study. The consensus algorithm for this multi-agent system involves the use of a graph laplacian matrix $L=[l_{ij}]$, which is a mathematical construct that describes the relationships between the agents in the system. The elements l_{ij} of the laplacian matrix are shown in Eq. (7.8), where $|N_i|$ denotes the number of neighbors for agent v_i. For instance, the laplacian matrix of the graph demonstrated in Figure 7.2 is presented in Eq. (7.9).

$$l_{ij} = \begin{cases} -1, v_j \in N_i \\ |N_i|, v_j = v_i \\ 0, otherwise \end{cases} \tag{7.8}$$

$$\mathrm{L} = \begin{bmatrix} 3 & -1 & -1 & 0 & 0 & -1 \\ -1 & 2 & -1 & 0 & 0 & 0 \\ -1 & -1 & 3 & -1 & 0 & 0 \\ 0 & 0 & -1 & 2 & -1 & 0 \\ 0 & 0 & 0 & -1 & 2 & -1 \\ -1 & 0 & 0 & 0 & -1 & 2 \end{bmatrix} \tag{7.9}$$

The algorithm for achieving consensus on the states of n agents (i.e. Eq. (7.7)) can be represented by Eq. (7.10). Where, X is the set of state information of the n agents as shown in Eq. (7.11). U represents the set of control inputs for the n agents as shown in Eq. (7.12). The control output for agent v_i can be derived as shown in Eq. (13) in the continuous-time situation. It has been proven that a consensus can be asymptotically reached.

$$U = -\mathrm{LX} \tag{7.10}$$

$$\mathrm{X} = [x_1, \cdots, x_n]^T \tag{7.11}$$

$$\mathrm{U} = [u_1, \cdots, u_n]^T \tag{7.12}$$

$$u_i(t) = -\sum_{v_j \in N_i} a_{ij} \left(x_i(t) - x_j(t) \right) \tag{7.13}$$

7.1.3 *Control strategy operation procedure*

Figure 7.4 illustrates the diagrams of the control operation procedures for the chilled water system and the supply air system, respectively. The operation procedure follows the consensus algorithm described in Chapter 7.1.2. The detailed control operation is presented below.

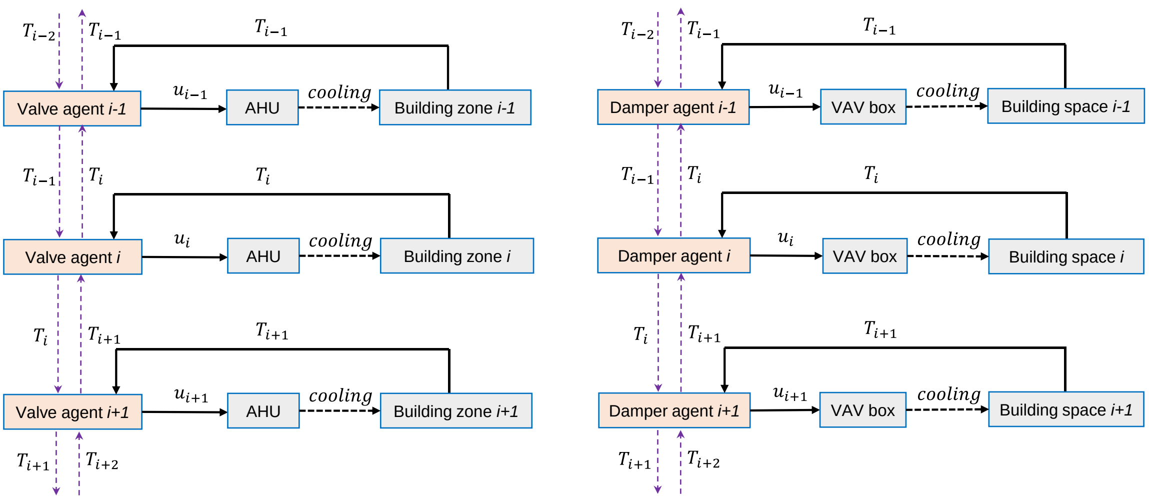

(a) Operation procedure for AHU agents (b) Operation procedure for VAV agents

Figure 7.4 Diagram of the control operation procedure

In normal operation, each agent functions as a local feedback controller (i.e., PID controller) to regulate the supply air temperature and space temperature at their setpoints. Once fast demand response control is initiated, which involves shutting down the chillers, the agents begin to exchange information with one another. At each control interval *t*, valve agent *i* (as depicted in Figure 7.4(a)) follows the detailed control operation procedure shown below.

- Collect the measured indoor air temperature profile ($T_i(t)$) from the AHU serving building zone *i*.
- Communicate with neighboring agents through the field network, including sending and receiving temperature profiles (i.e., $T_i(t)$ *and* $T_{i-1}(t)$ & $T_{i+1}(t)$

respectively) to and from all connected neighboring agents (i.e., valve agent *i-1* and valve agent *i+1*).

- Calculate the incremental control setting ($\Delta u(t)$) using Eq. (7.14). based on the agent inputs (i.e., the collected indoor air temperature profiles of its own and its neighbors).
- Calculate the AHU valve opening value ($u(t)$) using Eq. (7.15), and output for control.

$$\Delta \mathrm{u(t)} = -\sum_{j \in N_i} a_{ij} \left(T_i(t) - T_j(t) \right) \tag{7.14}$$

$$\mathrm{u(t)} = \mathrm{u(t-1)} + \Delta \mathrm{u(t)} \tag{7.15}$$

where, N_i represents the set of neighbors for agent i as defined in Eq.(7.4). j represents each of the single neighbors of agent i in N_i. For the valve agent i, as shown in Figure 7.4(a), its neighbors consist of valve agent i-1 and valve agent i+1. a_{ij} is the element of the adjacency matrix as defined in Eq.(7.5). It is worth pointing out that the value of a_{ij} does not need to be constant (i.e., 1 in Eq. (7.5)). It can be adjusted according to the real application.

The damper agent i on the supply air side also follows the same operation procedure (Figure 7.4(b)) as illustrated above. The proposed distributed cooperative control strategy enables valve agents and damper agents to collaborate and distribute the limited cooling supply effectively. It is accomplished by managing the flow rates of chilled water and supply air following the shutdown of part of the operating chillers. The multi-agent system operates in a self-organizing manner, ensuring the uniform thermal comfort sacrifices are asymptotically achieved among all building zones and spaces during the power limiting events.

7.2 Validation platform and arrangement

7.2.1 Test platform

In order to test the proposed control strategy, a virtual dynamic simulation platform has been constructed by TRNSYS. This platform models a super-high-rise commercial building in Hong Kong, incorporating detailed physical models of building envelope and major components of the central air-conditioning system, such as chillers, pumps, AHUs, fans, and hydraulic networks. The physical models are calibrated using real data sources.

The central air-conditioning system comprises four identical chillers, each with a rated capacity of 4,080kW. Each chiller is interlocked with a primary chilled constant speed pump, which has a rated water flow rate of 172.8L/s. The system utilizes a primary constant-secondary variable chilled water distribution system and air-side systems. Figure 7.5 depicts the diagram of the central air-conditioning system.

The secondary chilled water loop is equipped with two variable speed water pumps that circulate chilled water in the AHUs, responsible for cooling supply air temperature to a predetermined degree. The building is divided into six air-conditioned zones, each covering an area of 1,600 m^2. The cooling load profiles of these zones vary, and each zone is cooled by a corresponding AHU (e.g., zone1 is cooled by AHU1).

The multi-zone model (Type 56) in TRNSYS is used in this study to simulate this building. The air-side systems employ typical variable air volume systems. Figure 7.5 *(b)* illustrates an air-side system schematic for one of the air-conditioned zones. Eight spaces with varying load profiles are involved in the VAV system. It is assumed that the indoor air is well mixed and the temperature is uniformly distributed in each single space in the TRNSYS simulation. During office hours (i.e., 8:00-18:00), the temperature setpoint is set at 24 °C.

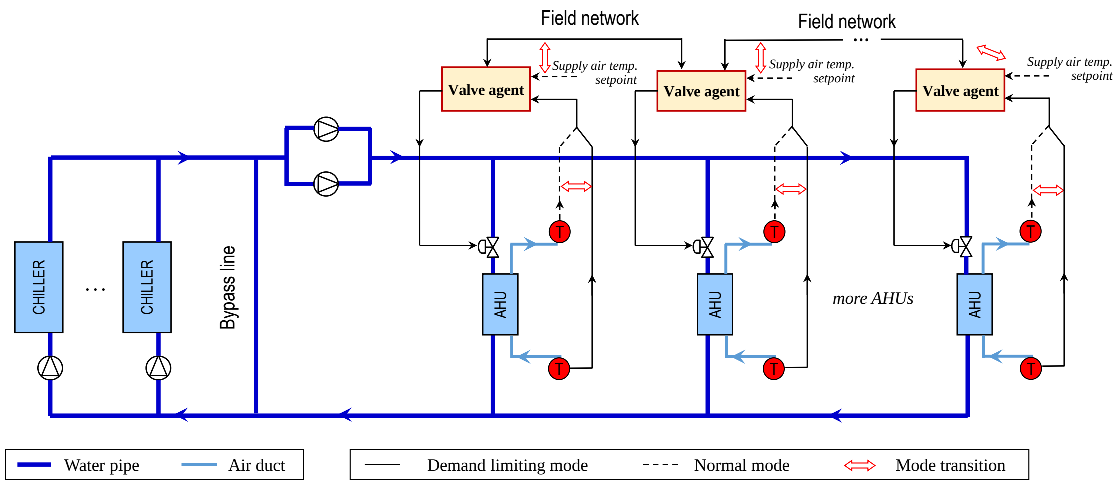

(*a*)

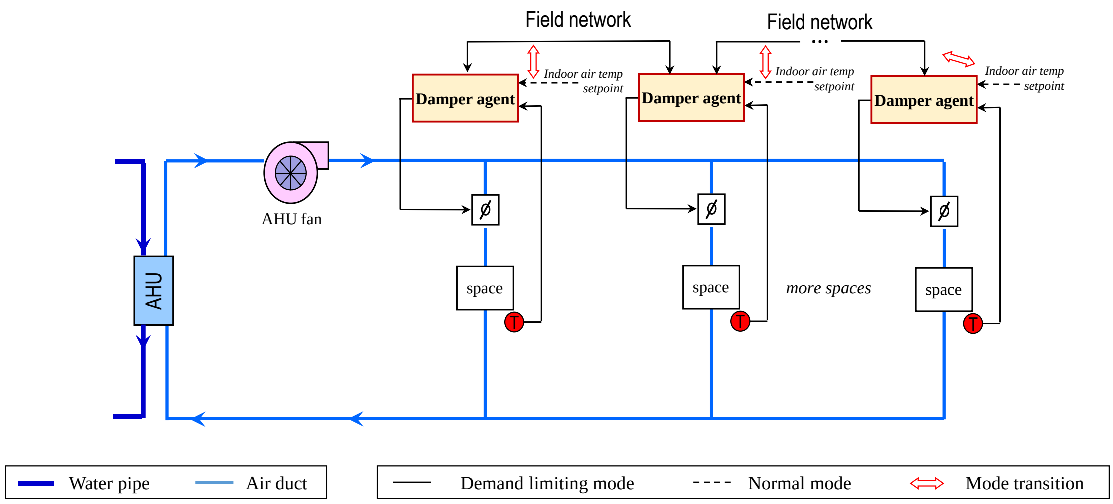

(*b*)

Figure 7.5 Diagram of the proposed control for chilled water side (*a*) and air side (*b*) of the central air-conditioning system

7.2.2 Test arrangement

Figure 7.5 depicts the schematic of the test arrangement. During normal mode (i.e., when there is no urgent need for load reduction), the valve and damper agents execute standard feedback control using the PID control algorithm. The valve agents manage the AHU valve openings to maintain the supply air temperature at predetermined setpoints (Figure 7.5(*a*)), while the damper agents control the VAV dampers to maintain the indoor air temperature at its predetermined setpoints (Figure 7.5(*b*)).

Upon receiving an urgent load reduction request from the power supply side, the building air-conditioning system switches from normal mode to demand limiting mode. The first step involves immediately shutting down two operating chillers to meet the demand limiting threshold. Then, the developed cooperative control approach takes over conventional control. As depicted in Figure 7.5(*a*), the valve agents regulate the AHU valve opening to manage the zone air temperature using return air temperature profiles collected from corresponding building zones and received from neighboring agents through the field network. Similarly, as shown in Figure 7.5(*b*), the damper agents control the opening of VAV dampers to adjust the indoor air temperature for corresponding building spaces using the space air temperature profiles collected from corresponding building spaces and received from neighbor agents.

The total airflow rates of individual AHUs remain constant since the start of demand response to prevent high fan energy consumption and high humidity in building spaces. This study focuses on a two-hour demand response event from 14:00 to 16:00 on the typical summer day of Hong Kong. The element of adjacency matrix a_{ij} in Eq. (7.14) is set to 0.1 for the validation test. The proposed control strategy continues to operate for a short period (around 20 minutes in this study) after the demand response event to prevent competition for cooling supply among the building zones and spaces. The extra operation process should last until the indoor air temperatures among the building zones and spaces return to their original setpoints after the demand response event.

7.3 Test results and analysis on the chilled water system and air-side system

7.3.1 Central cooling system test results

7.3.1.1 Indoor air temperature

The indoor air temperature profiles, adopting conventional proposed controls during the power limiting test, are shown in Figure 7.6. The results show that all six zones experience sacrifices in thermal comfort under both control methods during thedemand response event. Using conventional control, the six zones experience varying levels of thermal comfort sacrifices, as shown in Figure 7.6(a). This variation occurs becasue the AHUs serving different zones compete for a limited cooling supply to satisfy the high cooling demand after shutting down chillers. Zones with higher cooling demand and lower chilled water distribution priorities, such as Zone 1, experience greater thermal comfort sacrifice., At 16:00, the temperature profile of Zone 1 and Zone 6 are 28.2 ℃ and 26.7 ℃, respectively. The unbalanced temperature rise continues for about half an hour after the demand response event because the high cooling demand cannot be fully met by all the operational chillers, causig individual zones to still compete for chilled water to return to their original temperature setpoints.

However, when using the proposed multi-agent distributed cooperative control, all zones experience the same temperature rise during the demand response event, as shown in Figure 7.6 (b). The average temperature a six building zones is 27.7 ℃ at 16:00. Additionally, the temperature profiles of the zones after this power limiting event are also similar. Test results indicate that the proposed control can effectively address unbalanced temperature rises for building zones during the power limiting event.

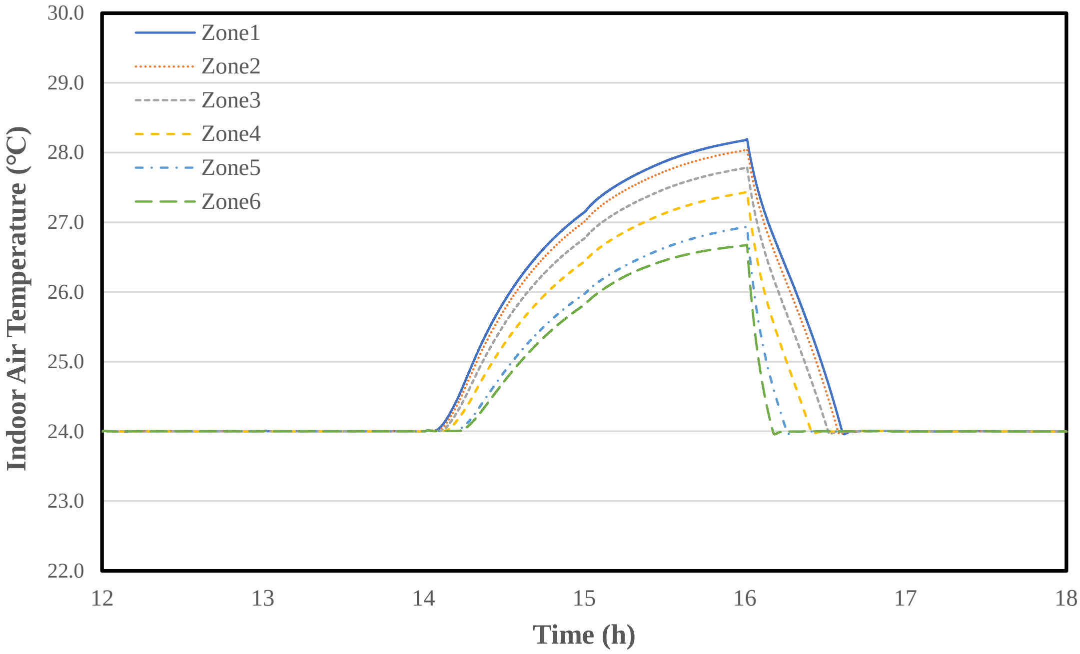

(a) Conventional control

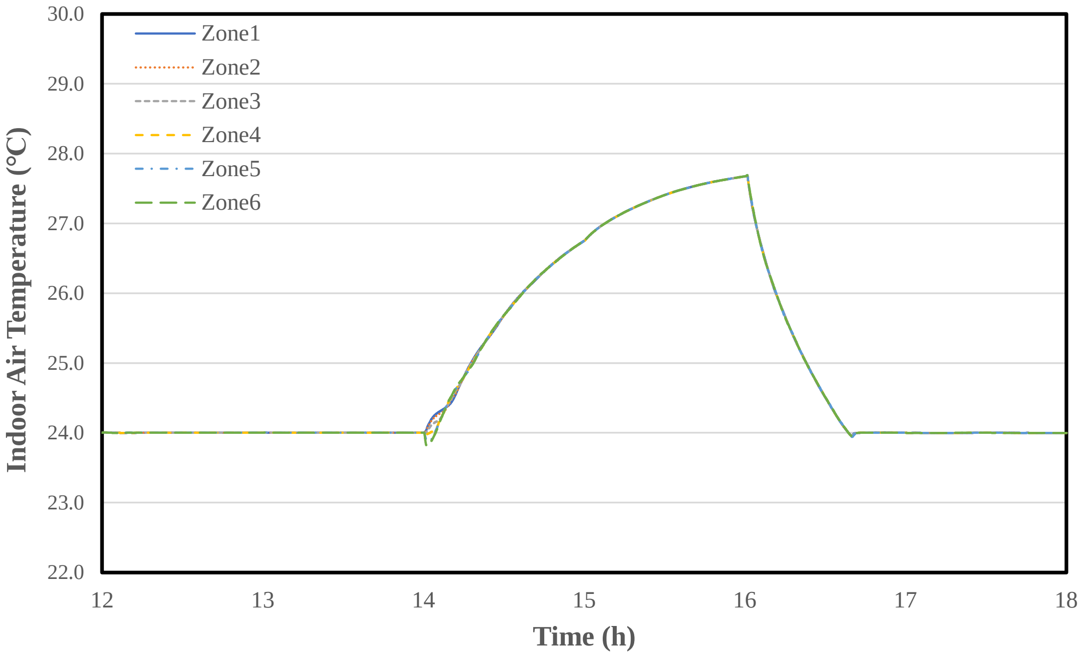

(b) Proposed control

Figure 7.6 Indoor temperature profiles using conventional and proposed controls during the test

7.3.1.2 Chilled water flowrate

Figure 7.7 depicts the chilled water flowrate profiles during the demand response test, comparing different control strategies. Figure 7.7(a) shows that the conventional control leads to high and uncontrolled chilled water flowrates in individual AHUs, resulting in disordered chilled water distribution. This occurs becasue the demand-based feedback control forces AHU valves to remain fully open, leading to competition for limited cooling supply. In this scenario, AHUs with lower hydraulic resistance, such as AHU 6, have higher priority for chilled water supply, causing their chilled water flowrates to gradually increase and reach maximum values when all AHU valves are fully open. Zone 6 records the highest flowrate of 12.6 kg/s, while Zone 1 only achieves a flow rate of 6.3 kg/s even with the valve fully open, indicating significant disordered water distribution both during and after the power limiting event.

However, when the proposed multi-agent distributed cooperative control strategy is adopted, as illustrated in Figure 7.7 (b), the water flowrates of the six zones are adjusted by the valve agents during and after the power limiting event, mitigating the disordered chilled water distribution among the zones. The multi-agent system achieves proper water distribution, maintaining the same temperature rises for the six zones in this power limiting event, as demonstrated in Figure 7.7 (b).

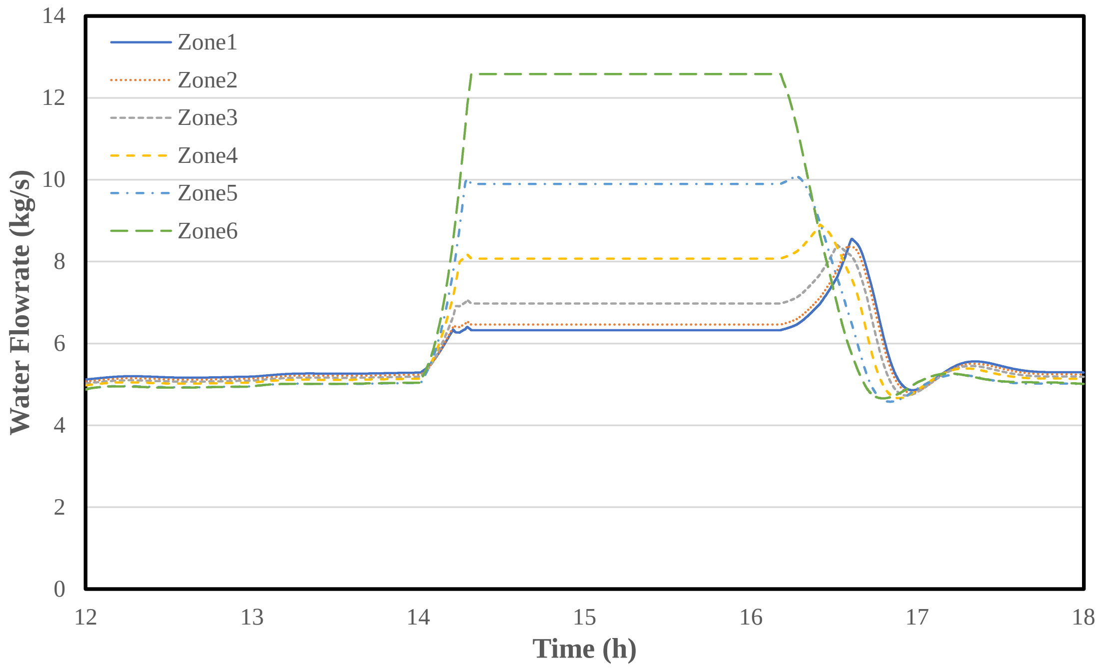

(a) Conventional control

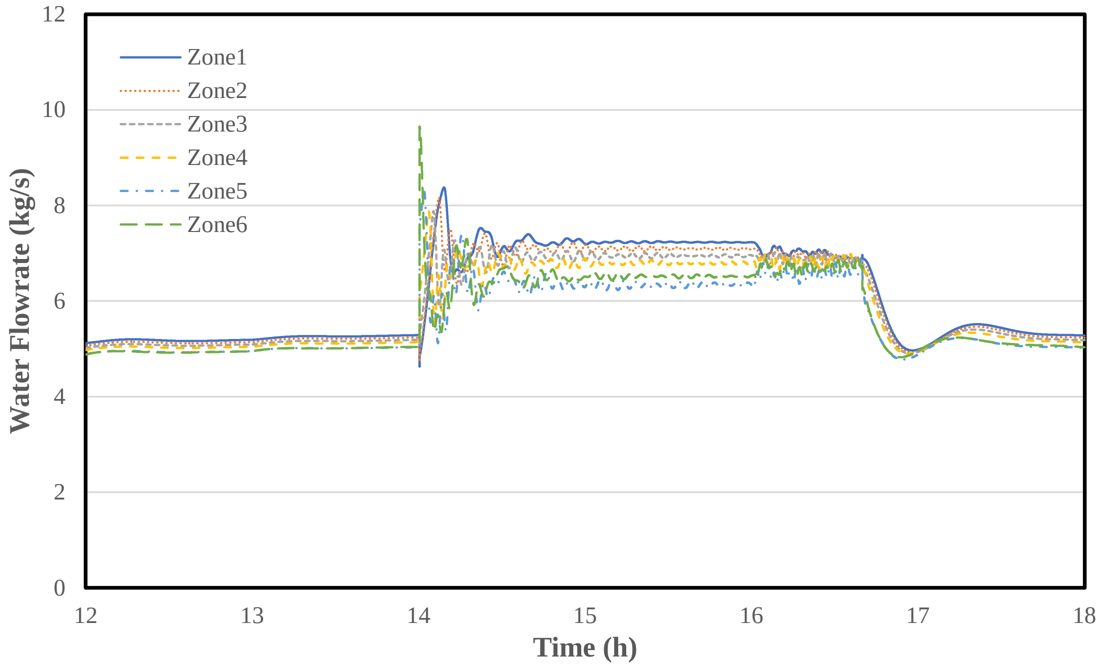

(b) Proposed control

Figure 7.7 Chilled water flowrate profiles under the conventional and proposed controls during the test

7.3.2 Air-side system test results

7.3.2.1 Indoor air temperature

Figure 7.8 presents the temperature profiles of eight spaces during this demand response test, comparing the conventional and proposed controls. With the conventional control, the temperature profiles of eight spaces differ significantly during and after this demand response event, as shown in Figure 7.8 (a). This occurs because the pressure losses associated with the terminal units of different spaces result in different priorities for accessing the limited cooling supply. Space 8 has the lowest thermal comfort sacrifice, with its indoor air temperature reaching 26.1 ℃ at the end of the demand response event, while space 1 experiences the highest thermal comfort sacrifice, with its indoor air temperature reaching up to 28.5 ℃. The uneven temperature rises among the eight spaces are significant.

However, the proposed control effectively addresses the unbalanced temperature rises in these building spaces in the power limiting event, as depicted in Figure 7.8 (b). These temperature profiles are only slightly different right after the start of the demand response event (i.e., 14:00), and even temperature rise among the different building spaces is achieved shortly afterward. The average temperature of all spaces served by the AHU is 27.6 ℃ at the end of the power limiting event, and uniform temperature variation is maintained after the event.

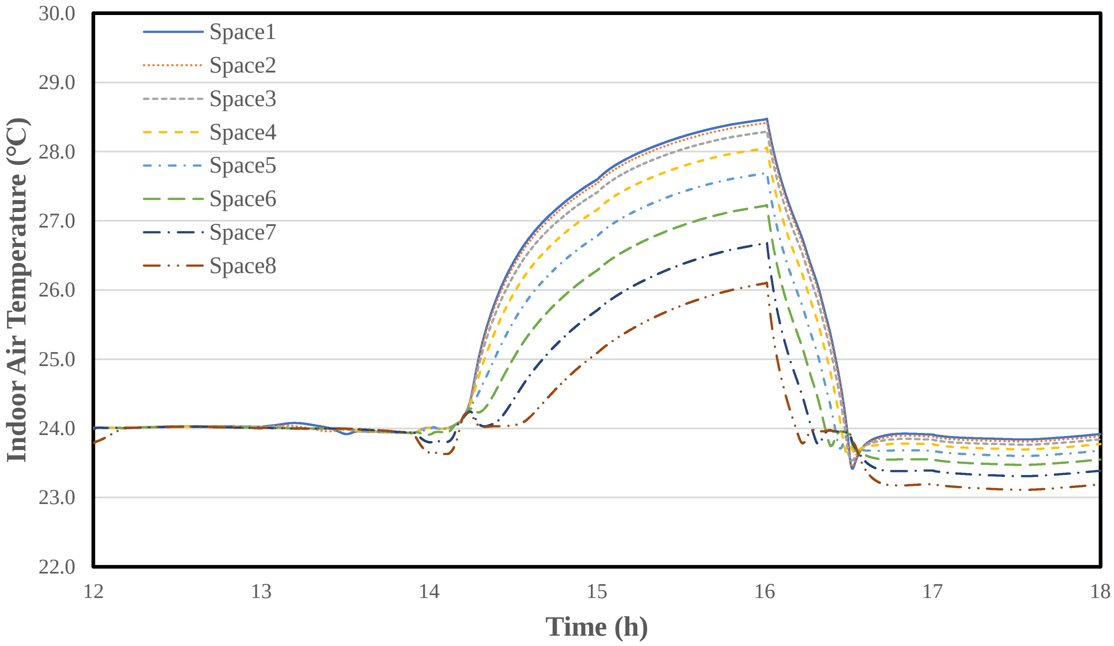

(a) Conventional control

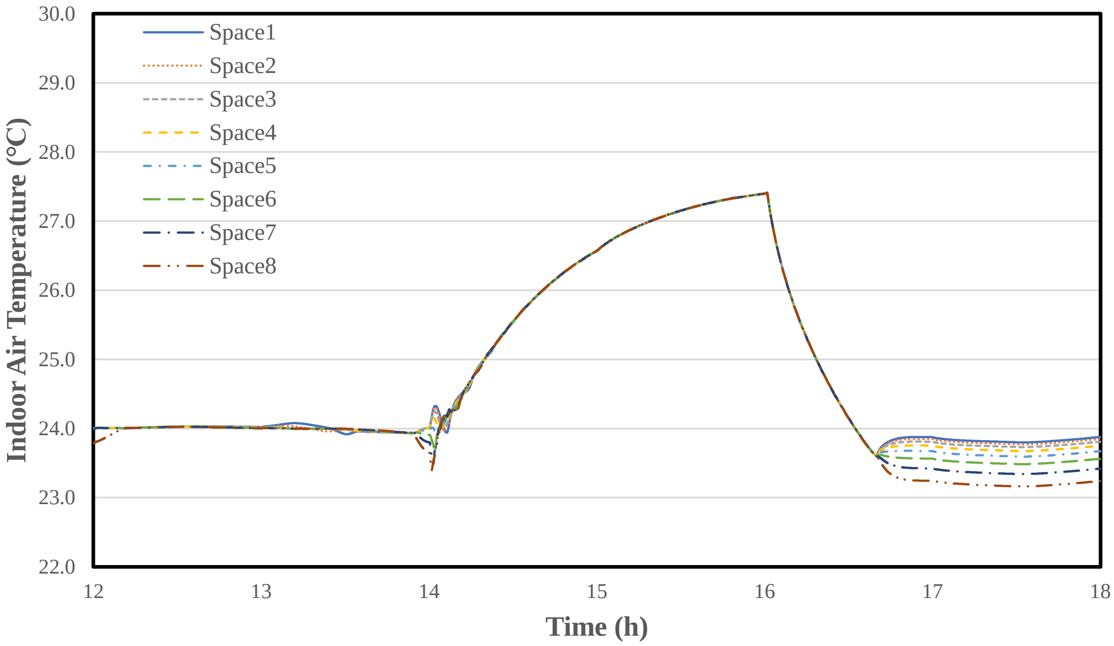

(b) Proposed control

Figure 7.8 Indoor temperature profiles under the conventional and proposed controls during the test

7.3.2.2 Supply air flowrate

The supply air flowrate profiles of eight spaces using the two different controls during the demand response test are depicted in Fig.9. Similarly, it can be observed from Figure 7.9(a) that the problem of disordered and uneven supply air distribution is significant when using the conventional control during and immediately after the demand response period, for the same reason explained above. The results show that space 8 has the highest priority in competing for the limited cool air. The air flowrate of space 8 reaches its maximum value at 2.3 kg/s during the rapid demand response event, while the maximum air flowrate of space 1 is as low as 1.3 kg/s.

In contrast, Figure 7.9 (b) shows that the proposed control adjusts the supply air flowrates through damper agents, resulting in almost complete avoidance of disordered and uneven air flow distribution among the spaces. As a result depicted in Figure 7.8 (b), this proposed control strategy maintains uniform thermal sacrifices among these building spaces.

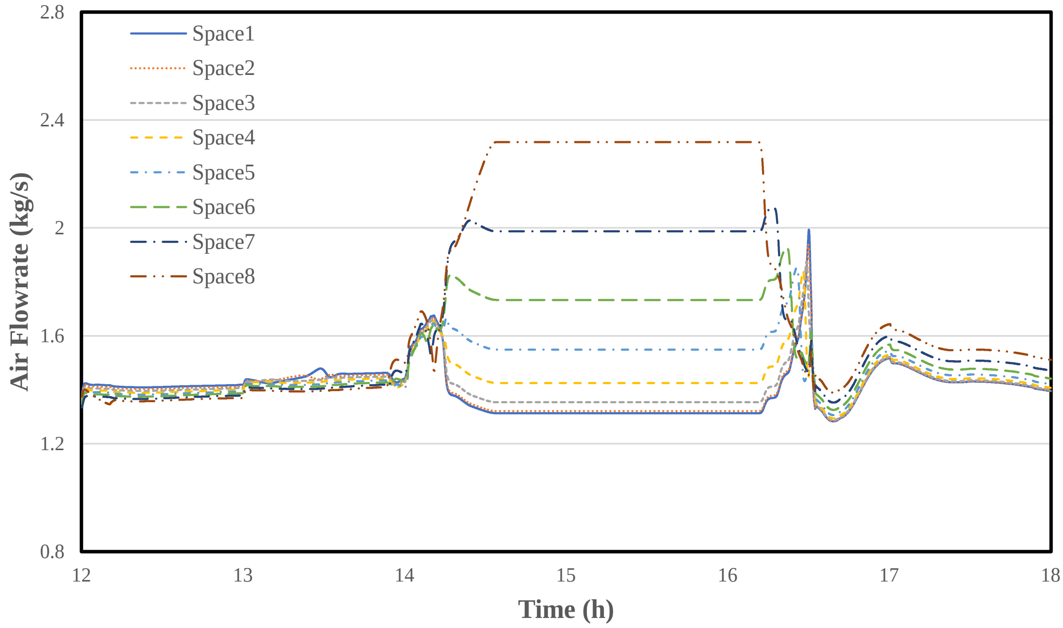

(a) Conventional control

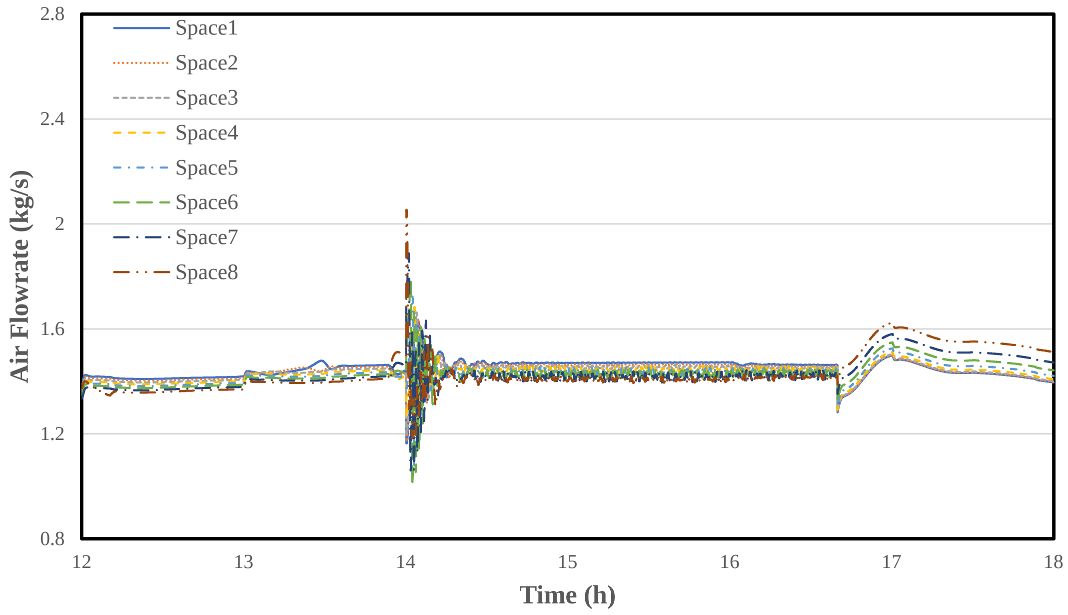

(b) Proposed control

Figure 7.9 Supply air flowrate profiles under the conventional control and proposed controls

7.3.2.3 Indoor air relative humidity

Figure 7.10 illustrates the relative humidity profiles of these spaces during this test, comparing the different control strategies. Figure 7.10 (a) depicts the relative humidity of each space increases significantly from the start of the demand response event at 14:00, with the maximum indoor air relative humidity reaching up to 76% for space 8 at the end of the event. Notably, the relative humidity of the spaces differs significantly. However, when the proposed control is used, the humidity rise among the eight spaces is more uniform during and immediately after the demand response period, as depicted in Figure 7.10 (b). Although neither the conventional nor proposed control strategies prioritize relative humidity, the proposed strategy performs better in maintaining lower relative humidity levels in the spaces after the shut down of the chillers. The average relative humidity of the spaces during the power limiting event under the proposed control is 67% , with the maximum relative humidity reduction reaching around 12% (i.e., for space 8). This is attributed to the supply fans control, where total supply air rates of individual AHUs remain the same as those at the start of the power limiting event, and supply air temperature of individual AHUs does not increase significantly due to the fan speed limiting control.

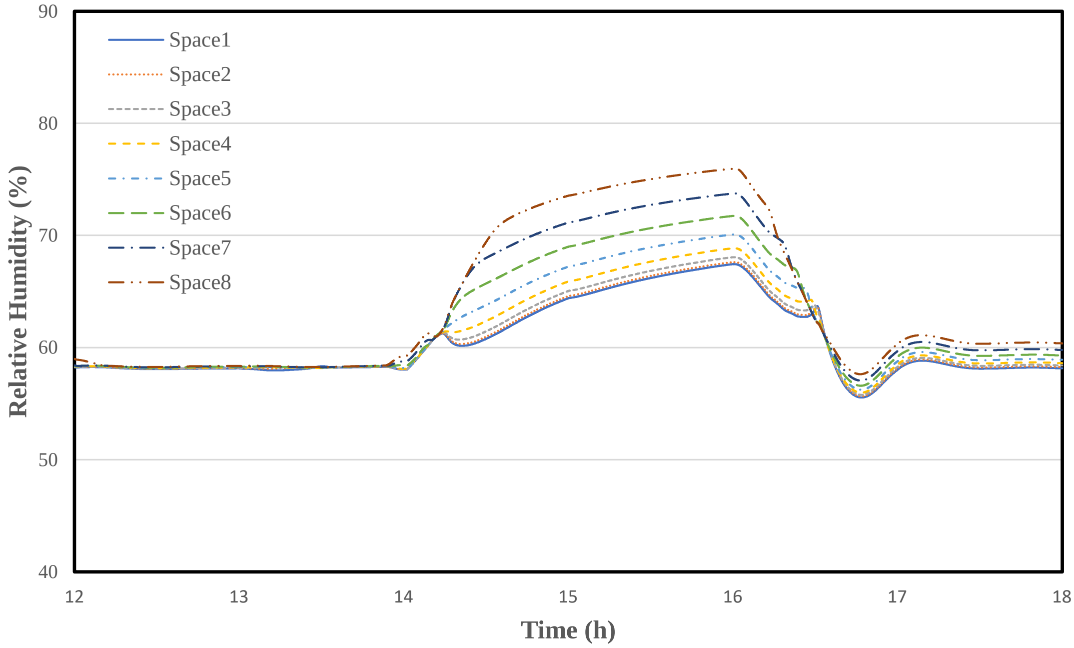

(a) Conventional control

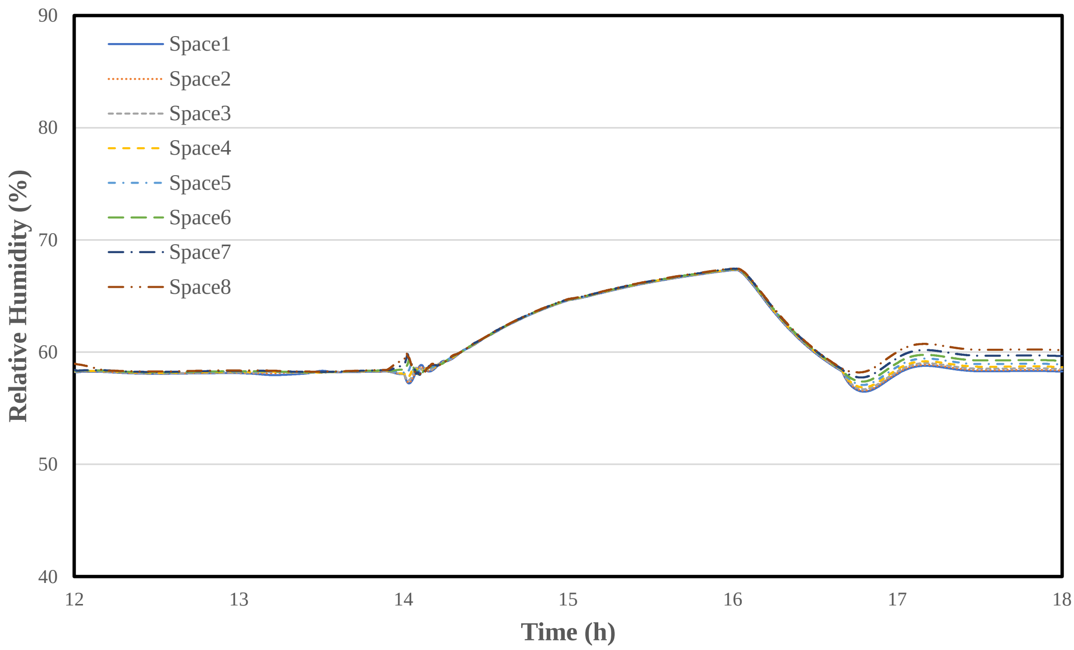

(b) Proposed control

Figure 7.10 Indoor relative humidity profiles under the conventional and proposed controls during the test

7.3.3 Power consumption

The main goal of fast demand response is to fulfill energy consumption reduction requests from power supply side. Figure 7.11 illustrates the power consumption of this central air-conditioning system, which includes chillers, primary chilled water pumps, secondary chilled water pumps, and AHU fans, under both conventional and proposed controls. The results indicate that the conventional control leads to additional energy consumption, as the secondary chilled water pumps and AHU fans will operate at their maximum speed. When shutting down two operating chillers under the conventional control, extra power consumption appears during the demand response event. Additionally, significant power rebound occurs after the demand response event. However, adopting the proposed control achieves an extra energy saving of 860 kW, which accounts for 14.2% of the energy consumption compared to using the conventional control before this demand response event at 14:00. The proposed control saves a total of 2,562 kWh of electricity during the demand response event, which accounts for 19.7% of the power consumption using the conventional control. Additionally, this proposed control strategy can significantly mitigate the power rebound effect, reducing it by 1,360 kW, accounting for 16.5% of the power consumption using conventional control after this demand response event.

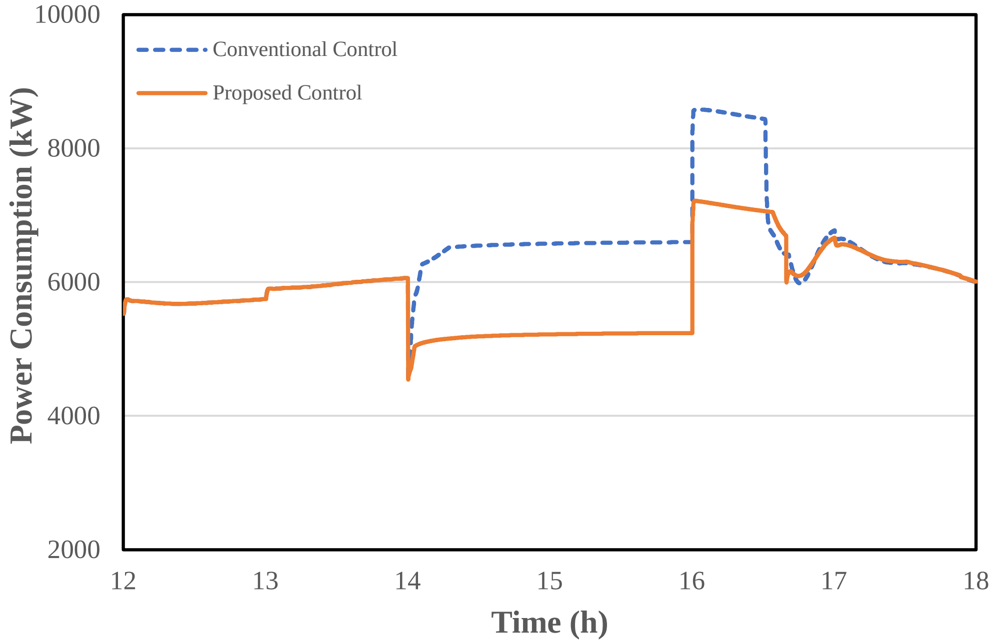

Figure 7.11 Power consumption using the conventional and proposed controls

7.4 Summary

The utilization of air-conditioning control for fast demand response is particularly valuable in addressing urgent power balance requirements. Limiting the number of operating chillers through direct load control has shown great promise as an effective means for power limiting. However, this approach can result in uneven thermal comfort sacrifices among different air-conditioned spaces, as conventional control fails to manage the limited cooling supply effectively. To address this problem, this study proposes a distributed cooperative control method. This strategy works through a multi-agent system that includes valve agents and damper agents, each performing on-site control based on collected information from its own and neighboring agents in a distributed architecture, allowing good scalability and reconfigurability. This approach is tested and validated on a virtual dynamic simulation platform. Major findings and conclusions are listed here:

- The proposed control method can effectively address uneven temperature rises of the building zones/spaces when performing direct load control, while also significantly alleviating the relative humidity rise.
- The disordered cooling distribution (including chilled water distribution and supply air distribution) can be effectively addressed in a self-organizing manner by the multi-agent system.
- In comparison to conventional control, the proposed strategy can better follow urgent power reduction requests from the power grid while significantly reducing the power rebound effect immediately following the power limiting event. Test results demonstrate the proposed control saves a total of 2,562 kWh of electricity and reduces power rebound by 1,360 kW during the demand response event.

CHAPTER 8 IMPLEMENTATION OF SUPPLY-BASED COOLING DISTRIBUTION CONTROL STRATEGIES

This chapter aims at implementing and validating the reconfigurable feedback control for supply-based cooling management under limited cooling supply over the entire building daily cycle, including the morning start period, demand limiting period and soft stop period. The implementation involves the detailed control strategy along with corresponding hardware placement, is illustrated in Section 8.1. Section 8.2 presents the hardware-in-the-loop test platform and the test arrangement. Test results and analysis are elaborated in Section 8.3. Section 8.4 summarizes the conclusions.

8.1 Implementation of supply-based feedback control

8.1.1 Outline of implementing supply-based feedback control

Figure 8.1 shows the outline of implementing supply-based feedback control. Optimal control settings for chiller plants are adopted for various objectives over the entire building life cycle. The control settings determine the operating state of each chiller at every moment for enhancing the energy efficiency and energy flexibility. There is extensive literature dedicated to researching optimal control settings for chiller plants. This study focuses on developing the subsequent steps of incorporating supply-based feedback control into the conventional demand-based control for proper cooling management under limited cooling supply (i.e., morning start period, demand limiting period and soft stop period). There are two feedback control loops for supply-based and demand-based controls, respectively. Control mode switching module determines when to switch between the supply-based control and demand-based control. The whole process is accomplished using the reconfigurable feedback control strategy, which is detailed in the subsequent sections.

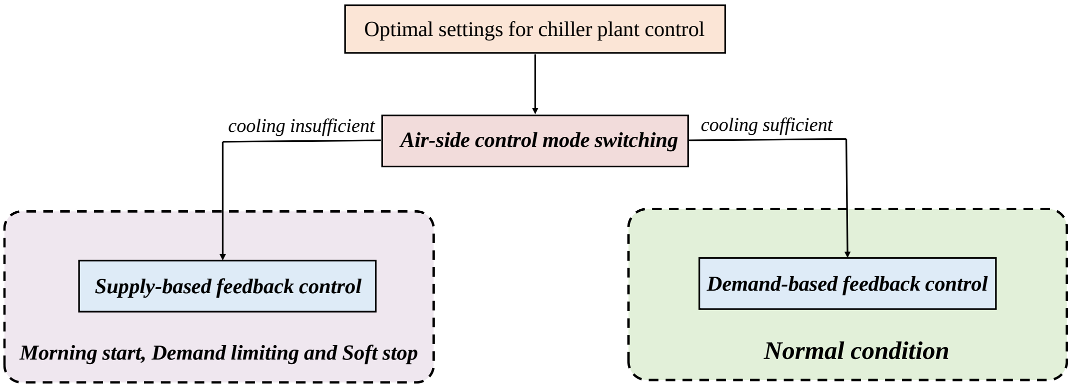

Figure 8.1 Outline of implementing supply-based feedback control

8.1.2 Utilization of reconfigurable feedback control strategy

The architecture of reconfigurable control strategy is presented in Figure 8.2. The basic idea is to reconfigure the local feedback control loops to match different objectives of demand-based control and supply-based control. It consists of a control loop reconfiguration scheme, a setpoint reset scheme, supply-based feedback control loops, and demand-based feedback control loops. The control loop reconfiguration scheme and the setpoint reset scheme are deployed in the supervisory control level, while the feedback control loops are implemented in local control level. The control loop reconfiguration scheme dictates the timing for control mode switching between demand-based and supply-based control. The setpoint reset scheme calculates setpoints for local controllers in two modes correspondingly.

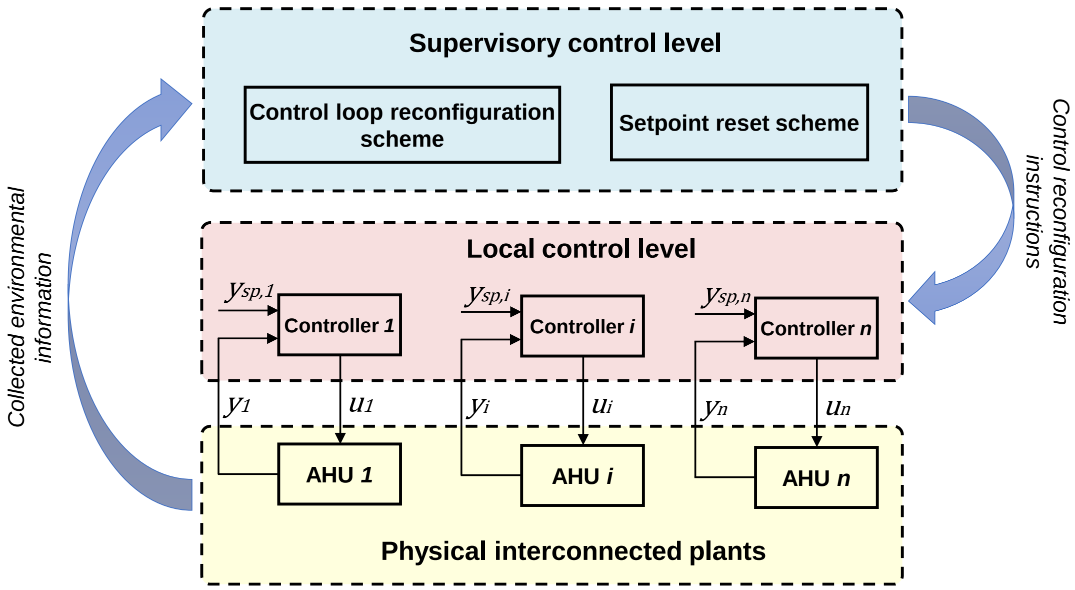

Figure 8.2 Architecture of the reconfigurable control strategy

Figure 8.3 shows the block diagram of the reconfigurable control. There are two built-in feedback control loops corresponding to two control modes in each local controller. The two control modes share the same feedback control algorithm as shown in Eq. (8.1) and Eq. (8.2) (i.e., the PID control algorithm). Note that the control strategy commonly employed in practical applications is the combination of a proportional term and an integral term as shown in Eq. (8.1), known as PI control.

$$u(t) = K\left[e(t) + \frac{1}{T_i}\int_0^t e(\tau)d\tau + T_d\frac{de(t)}{dt}\right] \tag{8.1}$$

$$e(t) = y_{sp}(t) - y(t) \tag{8.2}$$

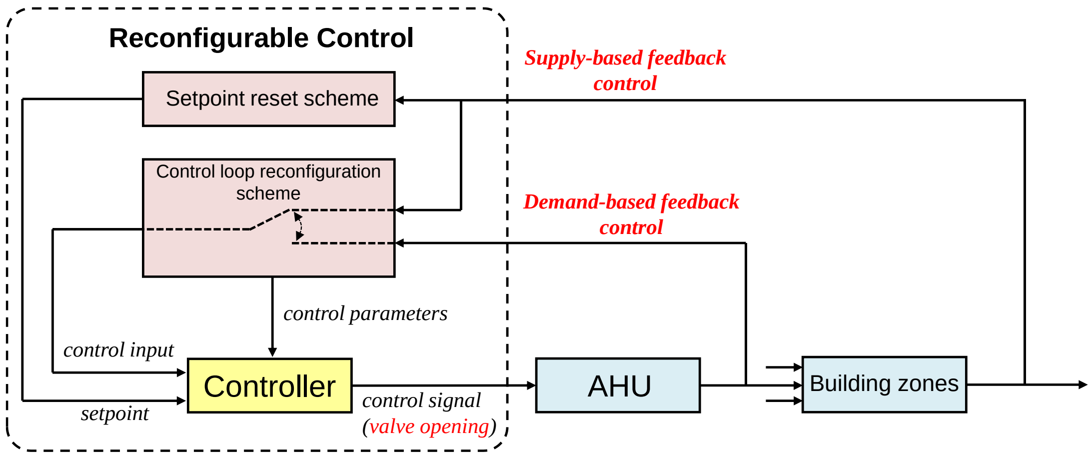

Figure 8.3 Block diagram for control reconfiguration

For demand-based control, the goal is to maintain the desired supply air temperature. The controlled variable (i.e., y_i) for *AHU i* is defined as the sensed supply air temperature in Eq. (8.3). The setpoint (i.e., $y_{sp,i}$) of the controlled variable is set as a fixed value (e.g., 14 °C) as shown in Eq. (8.4). The PI control algorithm is adopted to calculate the control output (i.e., valve opening) for each AHU. The local controllers keep operating in this control mode until a control loop reconfiguration signal is received from the supervisory control level.

$$y_i = T_{sup,i} \tag{8.3}$$

$$y_{sp,i} = const \tag{8.4}$$

The control mode is switched to the supply-based control when the cooling supply is limited, including the morning start period, the soft stop period and the demand limiting period. In these situations, the goal changes to maintaining even cooling distribution among different building zones. The controlled variable (i.e., y_i) for *AHU i* is set to the return air temperature as indicated in Eq. (8.5). The setpoint (i.e., $y_{sp,i}$) of the controlled variable is calculated through the setpoint reset scheme as indicated in

Eq. (8.6), in which n is the number of the air-conditioned building zones within the building.

$$y_i = T_{zone,i} \tag{8.5}$$

$$y_{sp} = \frac{\sum_{i=1}^{n} T_{zone,i}}{n} \tag{8.6}$$

8.1.3 Hardware architecture

Figure 8.4 depicts the typical hardware architecture of the building automation system. The architecture enables the management and control of various devices and subsystems within a building. Each network controller functions as a central hub for the subsystems, to manage and control the different devices within them. As the principal nexus for connectivity and communication, it enables efficient monitoring, control, and coordination of building automation functions, ensuring all system components operate in concert. Each local controller is responsible for monitoring and regulating operation of a specific subsystem (i.e., AHU in this study). It works in coordination with the network controller to exchange data and commands, ensuring a synchronized and cohesive operation across the entire building automation system. To control the valve opening of the AHU, each local controller collects data (i.e., supply air temperature) from local sensors, and calculates the control action needed to bring the controlled variable (i.e., supply air temperature) closer to the desired setpoint based on the built-in PID control algorithm.

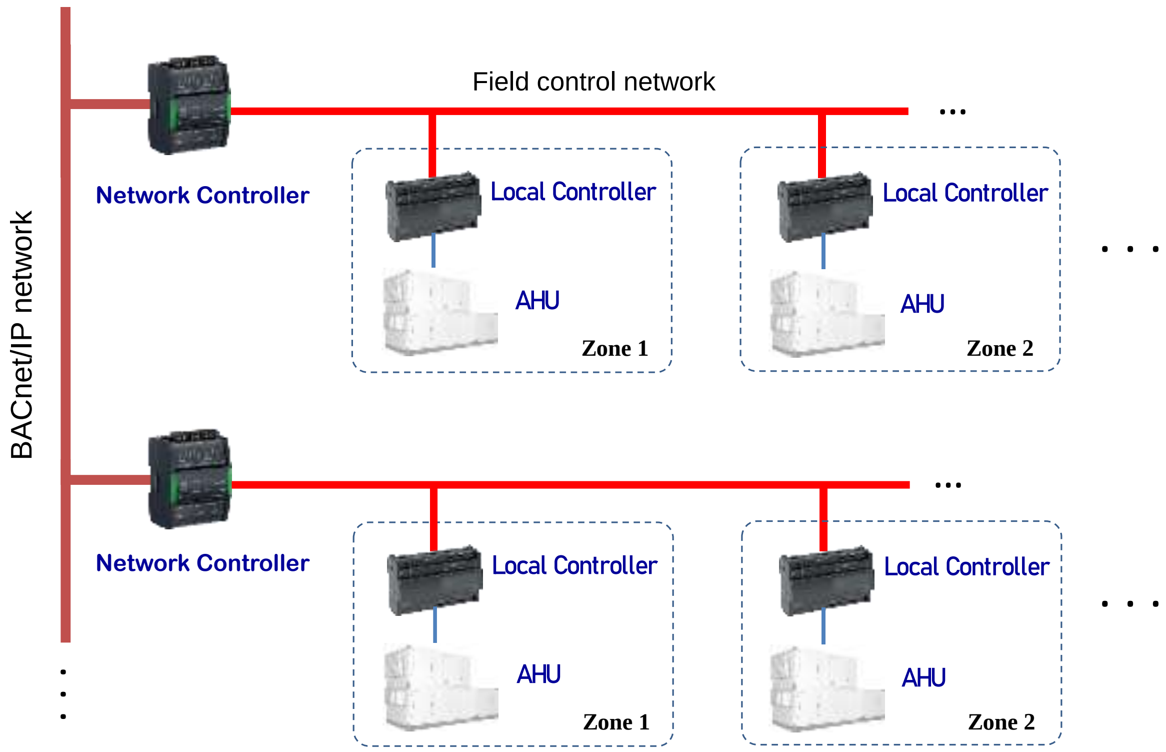

Figure 8.4 A typical hardware architecture of the building automation system

Conventional feedback control is deployed in this hardware architecture, where chilled water distribution of the air-conditioning system is determined by the demand in each air-conditioned zone. However, this control approach is effective only when the cooling supply is sufficient. In this study, reconfigurable feedback control is deployed to facilitate cooling management over the entire building daily cycle when cooling supply is limited. A new supervisory control module is introduced, which is essential to manage the transition between the control modes of conventional and supply-based control. Given the design and characteristics of this hardware architecture, this new module is suitable to be integrated into the network controller. The integration of this supervisory control module does not disrupt the existing architecture or control logic of the local controllers. The local controllers can continue to operate autonomously, collecting data from local sensors, performing local control actions based on their built-in control algorithms, and exchanging data and commands with the network controller as before. The network controller, integrated with the supervisory control module, acts as a higher-level coordinator and optimizer, providing additional decision-making capabilities to local feedback control loops for reconfigurable control.

8.1.4 Control logic flow chart

The control flow chart for implementing the reconfigurable control is illustrated in Figure 8.5. The functions are programmed into the network controller. It starts with an initial decision point, which aims at selecting the operating mode of the system. This decision point establishes the foundation for subsequent control actions. In this study, the supply-based control mode is adopted in three situations with insufficient cooling supply (i.e., morning start period, demand limiting period, and soft stop period). The decision for activating the supply-based control mode is determined based on a binary signal (i.e., 1 for yes, 0 for no). The settings of the activation signal in different situations are introduced as follows:

- *Morning start:* The activation signal is interlocked with the signal for switching on the chillers at the morning start period (i.e., when the chillers are activated before the start of the office hours in the morning for precooling, the activation signal is set to 1). When all the air-conditioned zones are cooled down to the comfort indoor air temperature setpoint (e.g., 24 °C), the activation signal is set to 0.
- *Demand limiting*: The activation signal is set to 1 when performing demand limiting through switching off chillers. After the demand response event, the activation signal maintains at 1 until all the building zones are cooled down back to the comfort indoor air temperature setpoint.

- *Soft stop*: The activation signal is interlocked with the signal for switching off part of the chillers before the end of the office hour (e.g., 18:00). The activation signal remains at 1 until the end of the office hour.

When the activation signal is 1, the control mode switches to supply-based control. The supply-based control loop signal is set to 1. The monitored variable is return air temperature indicated in Eq. (8.5). The setpoint reset scheme works by calculating the setpoint as shown in Eq. (8.6). The real-time indoor environment data are collected for determining whether to reset the activation signal back to 0 as illustrated above.

When the activation signal is 0, the control mode switches to the demand-based control. In this situation, the demand-based control loop signal is set to 1, while the supply-based control loop signal which is interlocked with the demand-based control loop signal is set to 0 at the same time. The monitored variable is supply air temperature, and the setpoint is a constant value as illustrated in Chapter 8.2.1.

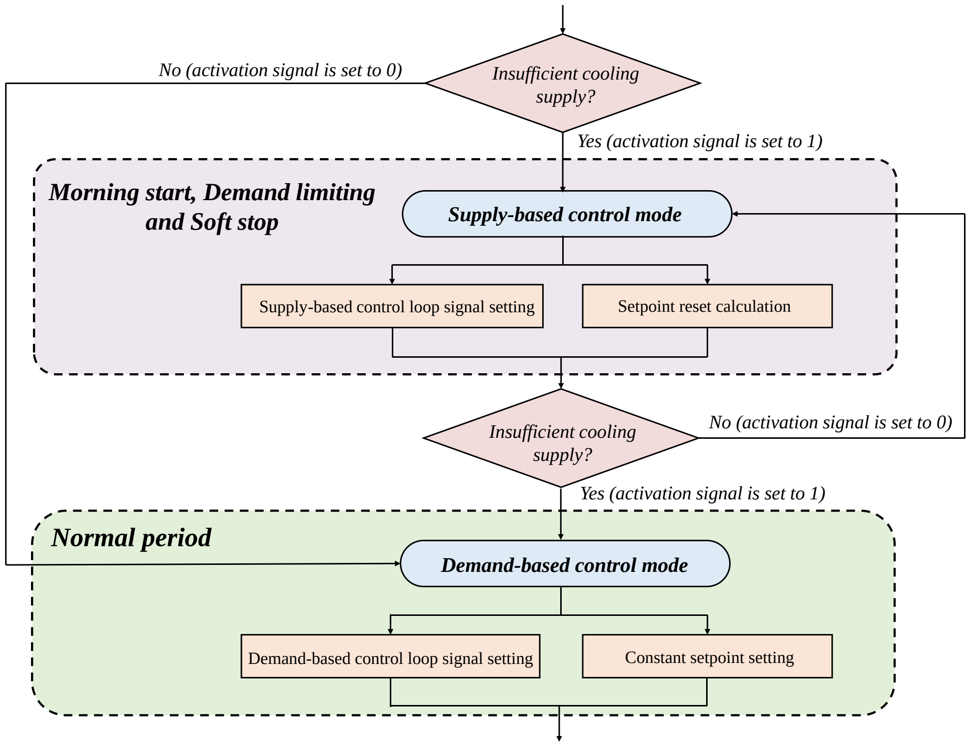

Figure 8.5 Control flow chart for implementing the reconfigurable control

8.2 Hardware-in-the-loop tests

8.2.1 Experimental test platform

Figure 8.6 shows a schematic for the implementation of reconfigurable control. Hardware-in-the loop tests are conducted to verify the feasibility and performance of the proposed reconfigurable control for supply-based cooling management. The air-conditioning system is constructed using TRNSYS, with reference to a commercial building located in Hong Kong West Kowloon Station. The network controller is simulated using MATLAB, which integrates the basic communication functionality based on the Modbus communication protocol, along with control schemes illustrated in Chapter 8.2. The Modbus communication protocol facilitates communication between various devices over different types of networks, making it suitable for monitoring and controlling industrial equipment such as sensors, actuators, and other field devices. The local controller adopted is the SIMATIC S7-1200 controller from Siemens. It is a versatile and compact programmable logic controller (PLC) designed for a wide range of automation applications, allowing for easy expansion with additional modules to meet specific application requirements. The actual controller is equipped with the basic PID control modules. It collects the environmental data (i.e., supply air temperature values and return air temperature values of individual AHUs for demand-based control mode and supply-based control mode respectively) from TRNSYS and receive advanced control instructions from MATLAB, and send control signals (i.e., AHU valve openings) to the simulated air-conditioning system. Hardware-in-the-loop testing is performed in real-time experiments, which allows for the evaluation and validation of the control implementation in a realistic and dynamic environment and enables the assessment of the reconfigurable control strategy's performance in a time-critical manner.

The air-conditioning system addressed in this study is also depicted in Figure 8.6. It consists of three identical chillers, three variable-frequency chilled water pumps, AHUs, and other associated components. The rated capacity of each chiller is 3,517 kW, and the rated flowrate for each pump is 152.3 L/s. Four representative air-conditioned zones are selected in this study, and each building zone has a floor area of 750 m^2. The building zones are cooled to the desired comfort temperature setpoint by passing chilled water through their corresponding AHU. As the virtual part of the test platform, the central air-conditioning system is simulated to represent the dynamic processes of heat transfer, hydraulic characteristics, and water flow balance etc. within the entire system.

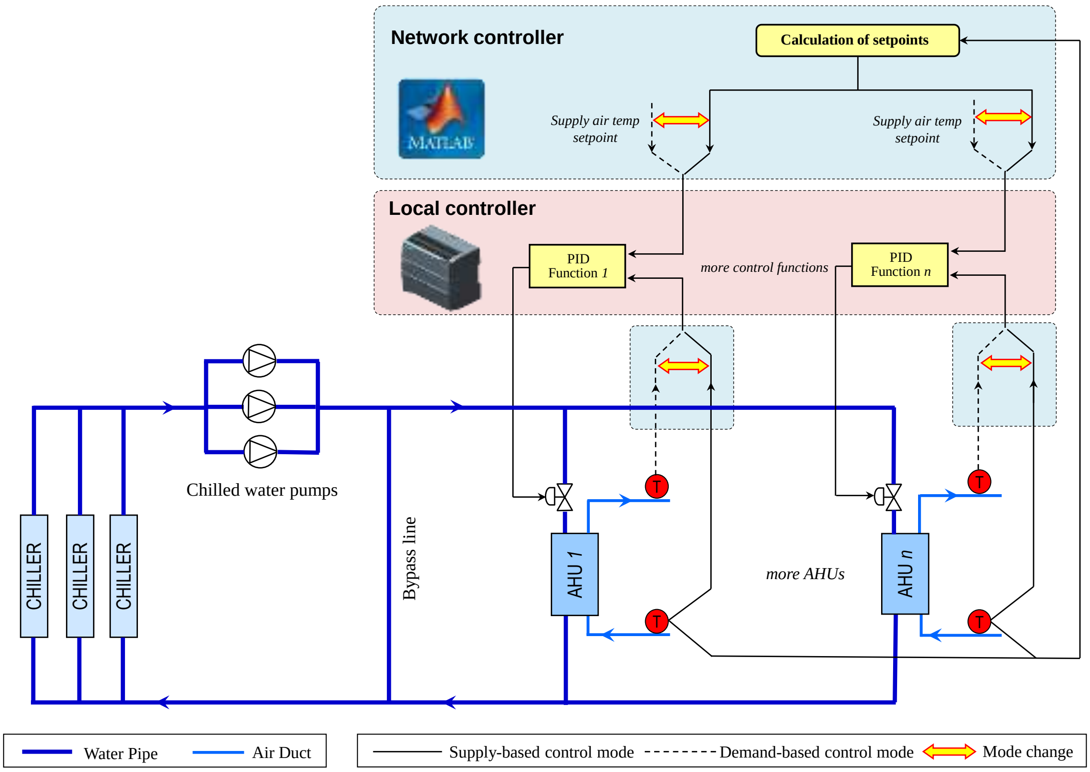

Figure 8.6 Schematic of the reconfigurable control implementation

8.2.2 Test arrangement

In order to validate the feasibility and effectiveness of the implementation of the reconfigurable control strategy, comparative tests are conducted using the proposed reconfigurable control and conventional control respectively. Three representative periods under limited cooling supply (i.e., morning start period, demand limiting period, and soft stop period) on a typical summer day (i.e., 23rd July) in Hong Kong are selected for validation tests. Detailed test arrangements for the corresponding three test periods in the same day are illustrated below. Note that only two chillers are operating under normal control on this day.

Morning start: Comparative tests using the reconfigurable control and conventional control are conducted to ensure that the building zones are cooled down to the comfort indoor air temperature setpoint (i.e., 24 °C) before office hours commence at 8:00.

Demand limiting: Comparative tests are conducted during a half-hour fast demand response event from 13:30 to 14:00. One operating chiller is switched off for demand limiting.

Soft stop: One operating chiller is switched off at 17:30 (i.e., before the end of the office hours at 18:00). Comparative tests are conducted using the reconfigurable control and conventional control.

8.3 Test results and analysis

8.3.1 Cooling distribution

The chilled water flowrates under conventional control and reconfigurable control during the morning start period are presented in Figure 8.7. It is observed that under the conventional control (as shown in Figure 8.7 (a)), the air conditioning system exhibits a disorder in the distribution of chilled water after switching on the chillers due to insufficient cooling supply. In this situation, each building zone competes for chilled water to facilitate cooling from the night setback. However, due to the difference in the hydraulic resistances within the piping network, the zone (e.g., zone 4) located closer to the chillers receives a higher allocation of chilled water. The uneven distribution of chilled water results in the need for the chillers to start operating well in advance, enough to ensure that all building zones are cooled to the desired temperature right before the office hours commence at 8:00. In contrast, the implementation of reconfigurable control provides a more energy-efficient solution for chilled water distribution during the morning start period. By dynamically adjusting the chilled water distribution as shown in Figure 8.7 (b) based on the control reconfiguration, which optimizes the cooling distribution process, it thereby enables energy-saving benefits by delaying the start of the chillers (e.g., by 0.2 hours in the test case).

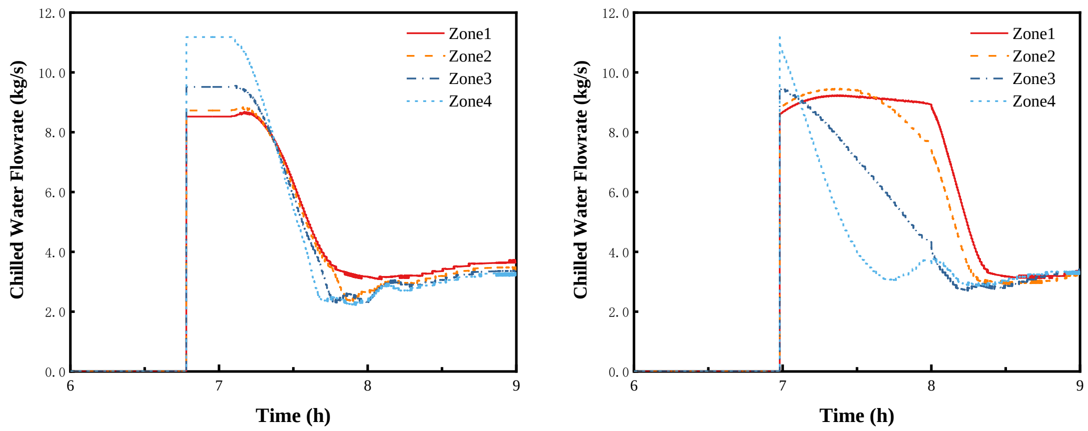

(a) Conventional control (b) Reconfigurable control

Figure 8.7 Comparation of chilled water flowrates under conventional control and reconfigurable control during morning start period

Figure 8.8 shows the comparison of chilled water flowrates under conventional and reconfigurable control when performing demand response. Under conventional control, the air-conditioning system experiences disruptions in chilled water distribution as shown in Figure 8.8 (a) when a partial shutdown of chillers is implemented for demand response. The phenomenon of chilled water competition arises at 13:30, which can result in significant discrepancies in comfort levels among different building zones. This occurs because the zones (e.g., zone 1) with high cooling loads are at a disadvantage during the chilled water competition process, while the zones (e.g., zone 4) with lower cooling loads have an advantage during the same period. Additionally, this phenomenon of chilled water competition also exacerbates the unnecessary power consumption of chilled water pumps. By implementing reconfigurable control, the allocation of the limited cooling capacity is properly managed as shown in Figure 8.8(b). It ensures that each zone receives an appropriate amount of chilled water even thermal comfort and avoids overburdening the pumps. The reconfigurable control strategy continues to work at 14:00 to cool down the zones, ensuring proper cooling distribution and reducing the rebound effect.

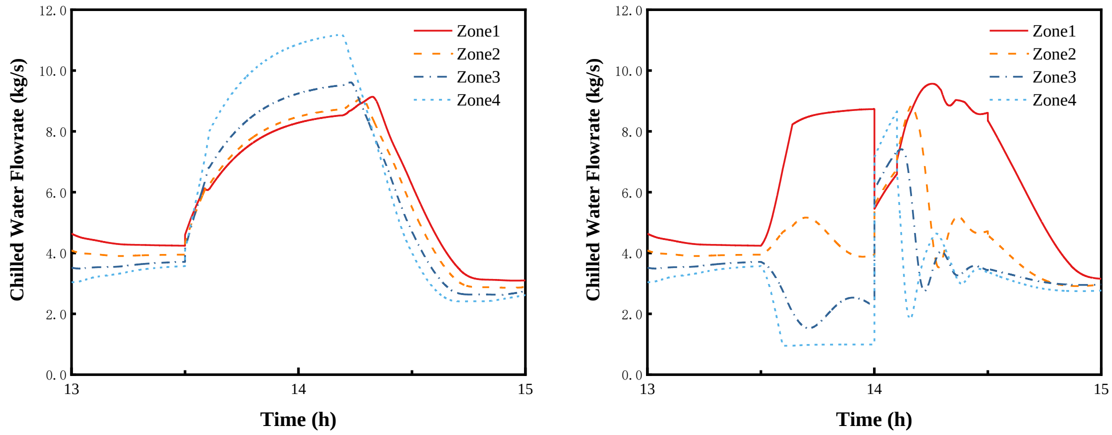

(a) Conventional control (b) Reconfigurable control

Figure 8.8 Comparation of chilled water flowrates under the conventional and reconfigurable control during demand limiting period

The chilled water flowrates under conventional and reconfigurable control during soft stop period are also compared as shown in Figure 8.9. A similar disorder in the cooling distribution is observed using conventional control, as shown in Figure 8.9 (a), when shutting down an operating chiller to conserve energy before the end of the office hour at 18:00. However, with the implementation of reconfigurable control, the distribution of limited cooling capacity is rationalized and effectively managed after the early shutdown of chillers.

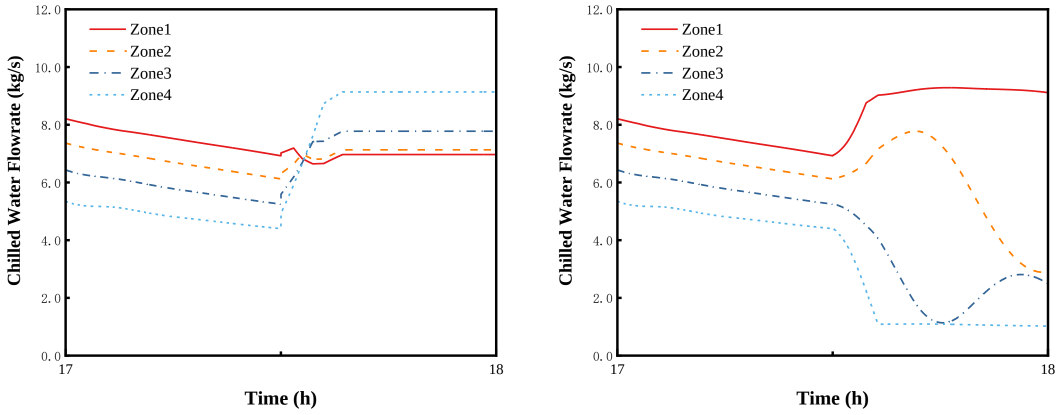

(a) Conventional control (b) Reconfigurable control

Figure 8.9 Comparation of chilled water flowrates under the conventional control and reconfigurable control during the soft stop period

8.3.2 Thermal environmental control performance

Figure 8.10 depicts the indoor air temperature variations during the morning start period. During the morning start period, conventional control approach fails to optimize chilled water distribution, resulting in disruptions and imbalances as illustrated before. As a consequence, different building zones experience varying timeframes to reach the comfort temperature setpoint for office hours as shown in Figure 8.10(a). Specifically, Zone 4 requires a precooling time of 0.72 hours, while Zone 1 requires a longer precooling time of 1.22 hours. However, with proper chilled water distribution under the reconfigurable control strategy, a more synchronized precooling process across different building zones is achieved as shown in Figure 8.10 (b). By allocating an appropriate amount of chilled water to each zone, the proposed control strategy ultimately allows for a delay of 0.2 hours in the activation time of the chillers.

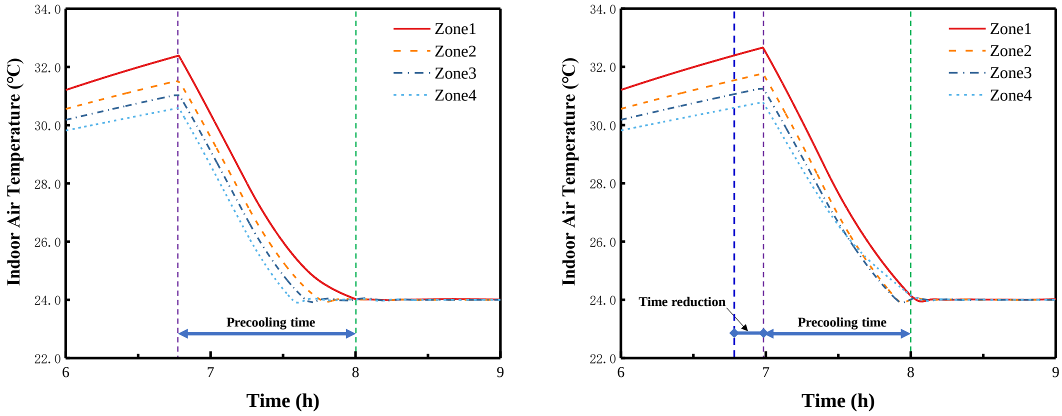

(a) Conventional control (b) Reconfigurable control

Figure 8.10 Temperature profiles under conventional and reconfigurable control at morning start period

Temperature profiles under two different controls during demand limiting period are shown in Figure 8.11. During the half-hour fast demand response period (13:30-14:00), the conventional control approach does not effectively optimize the cooling distribution, leading to uneven temperature increases among the building zones as shown in Figure 8.11 (a). The observed maximum temperature difference among the zones is approximately 1 K (i.e., between Zone 1 and Zone 4) during demand limiting period, which indicates an uneven cooling distribution. Test results demonstrate the effectiveness of the reconfigurable control approach at minimizing the temperature discrepancies as shown in Figure 8.11 (b). The maximum temperature difference across zones is controlled to be below 0.3 K.

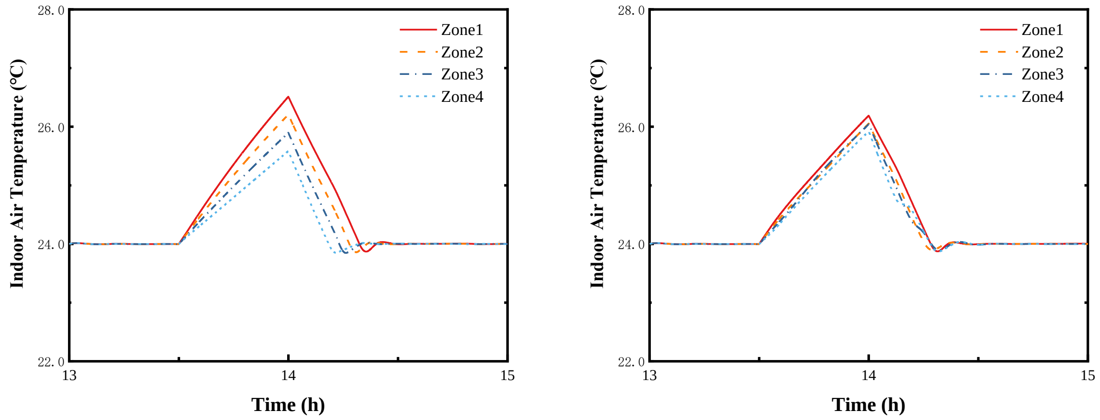

(a) Conventional control (b) Reconfigurable control

Figure 8.11 Temperature profiles under different controls during demand limiting period

The indoor air temperature under two different controls is also compared during soft stop period as shown in Figure 8.12. The conventional control results in uneven temperature increases across different building zones after shutting down one operating chiller before the end of office hours, as shown in Figure 8.12(a). Among them, Zone 1 experiences the highest temperature rise, reaching approximately 26.5 °C at 18:00, while Zone 4 has the lowest temperature rise (approximately 25.5 °C). When the reconfigurable control is adopted, the temperature increases in all building zones become consistent and uniform as depicted in Figure 8.12 (b). The average temperature across the four zones remains below 26 °C at 18:00, indicating the successful mitigation of uneven cooling distribution.

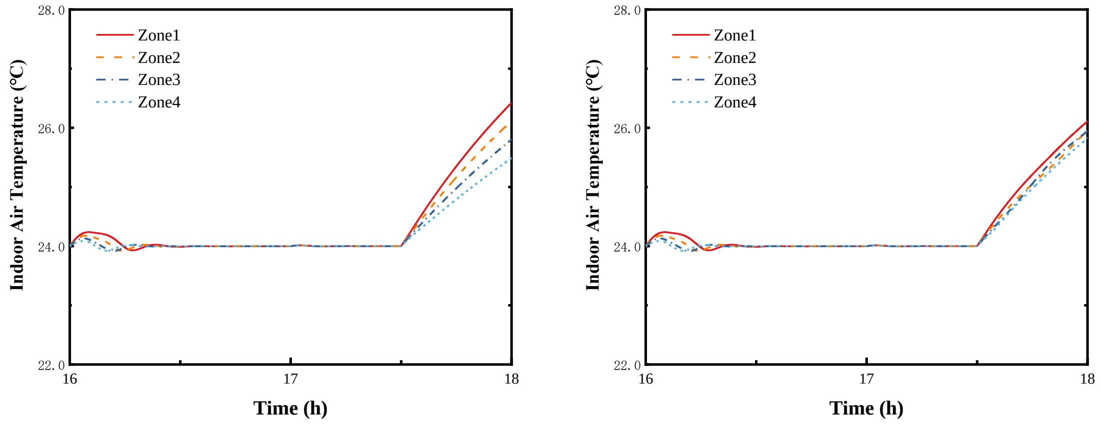

(a) Conventional control (b) Reconfigurable control

Figure 8.12 Temperature profiles under different controls during soft stop period

8.3.3 Energy performance

The power consumption under conventional and reconfigurable control is also investigated. Figure 8.13 presents the power consumption profiles during the morning start period. Under the conventional control, the chillers are activated 0.2 hours earlier than those under the reconfigurable control, resulting in higher energy consumption. This early activation of the chillers signifies an inefficient use of energy resources. By synchronizing the cooling process and dynamically adjusting the allocation of chilled water, the proposed reconfigurable control achieves significant energy savings during the morning start period. The results reveal that the energy saved by implementing the reconfigurable control strategy amounts to 172.85 kWh.

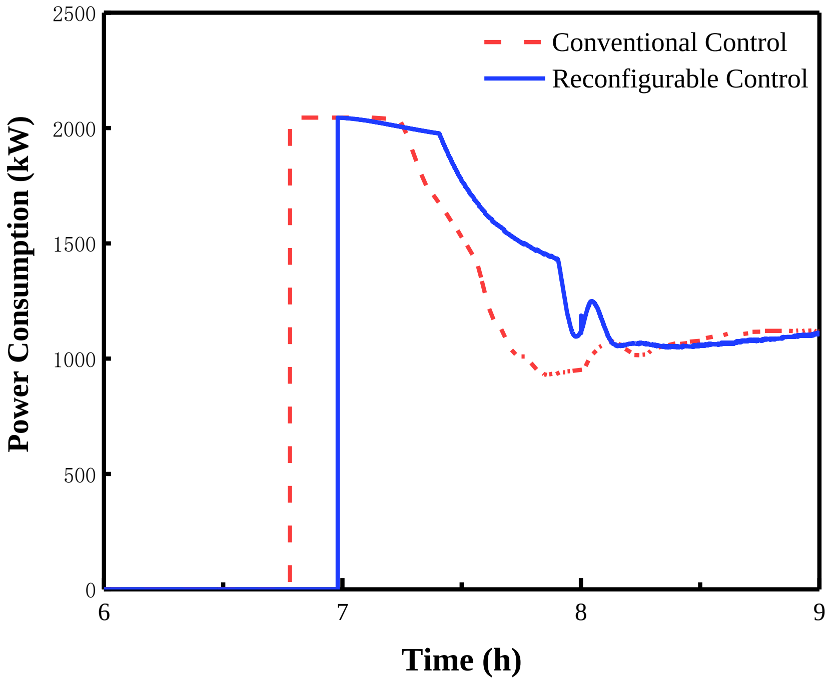

Figure 8.13 Comparation of power consumption under different controls during morning start period

Figure 8.14 shows the comparison of energy consumption under the conventional and reconfigurable control during the demand limiting period. The air-conditioning system experiences disruptions in chilled water distribution, leading to increased power consumption of chilled water pumps when performing demand limiting (i.e., 13:30 to 14:00). It undermines the effectiveness of demand limiting. In contrast, the reconfigurable control demonstrates improved performance in terms of demand limiting during the demand response period through dynamically adjusting the cooling distribution and thus reducing power consumption of chilled water pumps. The maximum power reduction in this period is 572.7 kW compared to that under conventional control. Furthermore, when demand response ends at 14:00, the conventional approach exhibits a larger rebound effect. The implementation of the reconfigurable control effectively mitigates this rebound effect by 11.2 %.

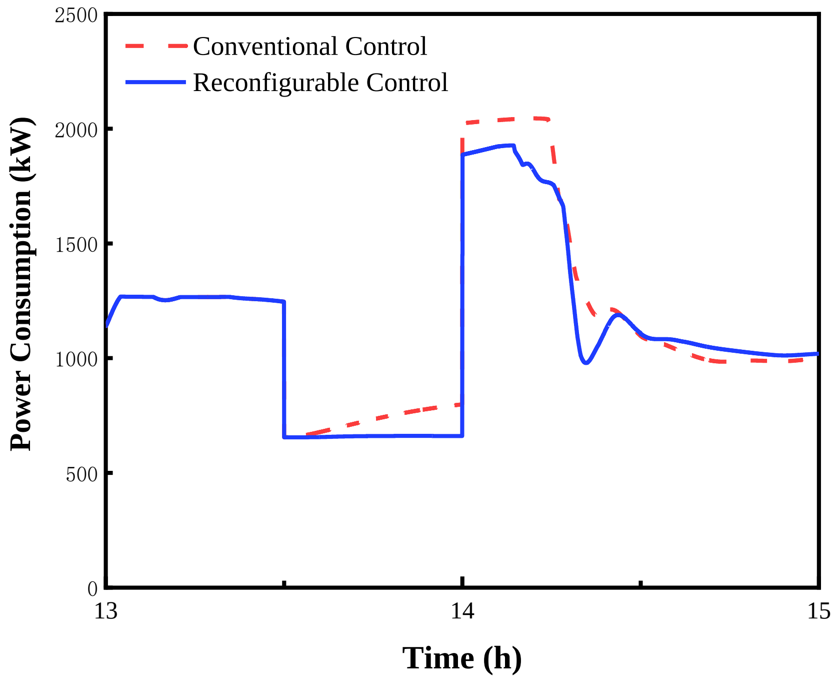

Figure 8.14 Power consumption under the conventional and reconfigurable control during the demand limiting period

The power consumption under conventional and reconfigurable control is also compared during the soft stop period as shown in Figure 8.15. When using conventional control, disruption of cooling distribution during the soft stop period results in increased power consumption of the pumps. It affects the overall energy efficiency of the air-conditioning system, offsetting some of the potential energy savings. Test results demonstrate the energy-saving benefits of reconfigurable control approach. By effectively managing the distribution of chilled water, the proposed the reconfigurable control unlocks an additional energy-saving potential of 51.4 kWh compared to the conventional control.

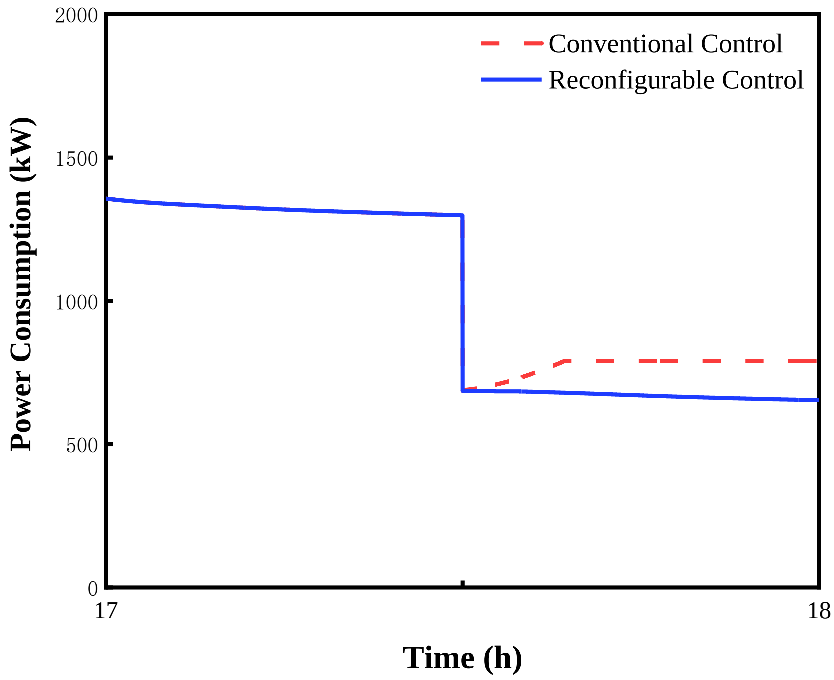

Figure 8.15 Power consumption under different controls during soft stop period

8.4 Summary

A reconfigurable feedback control strategy integrating both the supply-based and demand-based controls is developed to address the problems arising from disordered cooling distribution when cooling supply is insufficient using conventional feedback control. The implementation of reconfigurable feedback control is realized for the first time for energy-efficient and grid-interactive cooling management in the entire building daily cycle, including the morning start period, soft stop period and demand limiting period. Hardware-in-the-loop tests are conducted for validation. Based on the experiences of practical implementation of the control logics and results of the validation tests, the following major conclusions can be derived:

- Reconfigurable feedback control can address the problem of disordered cooling distribution arising from the conventional control strategy in situations with limited cooling supply (i.e., morning start period, demand limiting period and soft stop period).

- Compared with the conventional control, significant energy savings can be obtained during the morning start period (i.e., 9.1 %) and soft stop period (i.e., 13.3 %) under the reconfigurable control. Additionally, reconfigurable control can achieve a further reduction in power consumption by 30.8 % during the demand limiting period while mitigating the rebound by 11.2 % right after demand limiting period.
- The reconfigurable control strategy can be conveniently deployed in commonly used digital controllers at field level, facilitating seamless integration with the current building automation systems.

In the future work, field implementation of reconfigurable control strategy in four large buildings under construction will be performed in collaboration with industrial partners to further investigate the practical implementation issues of the supply-based cooling management for enhanced energy efficiency and flexibility and validate their benefits in practice.

CHAPTER 9 CONCLUSIONS AND FUTURE WORK

This chapter presents the concluding remarks and outlines the future directions for research based on the findings and contributions of this study. This chapter is divided into three sections, each addressing different aspects of the research conducted: Section 9.1 highlights the main contributions of this study. Section 9.2 presents the conclusions drawn from the analysis and interpretation of the research outcomes. Section 9.3 focuses on recommendations for future work based on the research conducted.

9.1 Main contributions of this study

The main contributions of this PhD study are summarized as follows:

i. The problems arising from disordered cooling distribution in conventional demand-based feedback control are identified. The concept of supply-based feedback control is introduced to deal with the problems.

ii. A comprehensive and robust reconfigurable control strategy is developed for the implementation of the smart control concepts in conventional building automation systems. The reconfigurable control strategy integrates supply-based feedback controls, for demand response and demand limiting events, and demand-based feedback controls, for normal situations with sufficient cooling supply.

iii. A reinforcement learning-enabled iterative learning control strategy of air-conditioning systems at the morning start period is developed to effectively shorten the precooling time and reduce energy consumption. The control strategy is model-free and does not require extra sensors nor additional experimental work for thermodynamic characteristic parameter identification.

iv. An event-driven demand response control strategy of air-conditioning systems is developed to properly distribute the limited cooling supply when facing urgent requests from smart grids. The control strategy is convenient for on-site implementation, and avoids unnecessary wear and tear of the terminal units during the control process.

v. A distributed cooperative control strategy of air-conditioning systems based on the multi-agent system is developed to perform building fast demand response. The control strategy allows good scalability and reconfigurability, which are cost-effective and efficient control strategies to be applied in large commercial buildings for demand limiting.

vi. The implementation of the reconfigurable control strategy is developed in the limited cooling supply situations, including the morning start period, demand limiting period and soft stop period. It incorporates the detailed control strategy architecture along with corresponding hardware placement.

9.2 Conclusions

On the reconfigurable feedback control deployable in conventional digital controllers

- The conventional building automation systems that adopt conventional feedback control face challenges in distributing cooling supply effectively during fast demand response periods when the cooling supply is insufficient after switching off some of the operating chillers. This results in disordered chilled water distribution, leading to imbalanced thermal comfort sacrifices among building zones. In addition, a severe deficit flow problem might arise, causing increased energy consumption of the secondary pumps.

- The proposed reconfigurable control strategy offers a solution for managing the distribution of cooling supply effectively to address the above issues. This strategy can be implemented on conventional building automation systems that adopt digital controllers commonly used today, such as DDC and PLC.
- Test results show satisfactory control stability in valve opening control and proper chilled water distribution. This enables uniform space temperature distribution and thermal comfort control among the building zones during both demand response and rebound periods. The temperature deviation among the zones is controlled within 0.2 K for the majority of the time. Furthermore, the proposed reconfigurable control achieves 11.6% and 27% of power demand reductions during demand response and rebound periods respectively, compared with those using conventional controls.

On the iterative learning control strategy for morning start period

- The proposed iterative learning control strategy can update the control outputs at each control interval (each day) to continuously track the goal of consistent precooling lead time for different building zones.
- The proposed iterative learning control strategy can reduce the maximum return time among multiple zones from night setback (tmax) and the cooling diversity indicator (cdi). The average reduction of the daily precooling time was 0.1 hour (10.9% reduction) and the accumulated reduction of the precooling time was 2.48 hours during the test period of four weeks.
- The proposed iterative learning control strategy can significantly achieve energy saving. The average overall daily energy saving of the chilled water plant was 400

kWh and the accumulated overall energy saving was 9615 kWh over the test period of four weeks.

On the event-driven control strategy for fast demand response

- The proposed event-driven control strategy can maintain the uniform indoor air temperature rises among different building zones during the demand response period. The limited cooling supply can be distributed properly and the same indoor air temperature profiles among the zones can finally achieved using the proposed event-driven control strategy.
- The power demand and energy consumption of the chiller plant can be further reduced significantly during the demand response period when using the proposed event-driven control strategy, e.g., power demand reduction by 170 kW (i.e., 5%) and the reduction of electricity consumption by 246 kWh (5%). Furthermore, the power rebound effect right after the demand response period can also be mitigated to some extent.
- Both the proposed event-driven control and the time-driven control can achieve the control objective during the demand response period. But the accumulated valve travel distance of AHUs for different building zones can be reduced by 54.6% in average under the event-driven control compared with the time-driven control.

On the multi-agent based distributed cooperative control strategy for enhanced scalability

- The proposed control method can effectively address uneven temperature rises of the building zones/spaces when performing direct load control, while also significantly alleviating the relative humidity rise.

- The disordered cooling distribution (including chilled water distribution and supply air distribution) can be effectively addressed in a self-organizing manner by the multi-agent system.
- In comparison to conventional control, the proposed strategy can better follow urgent power reduction requests from the power grid while significantly reducing the power rebound effect immediately following the power limiting event. Test results demonstrate that the proposed control saves a total of 2,562 kWh of electricity and reduced power rebound by 1,360 kW during the demand response event.

<u>On the implementation of supply-based cooling distribution control strategies</u>

- Reconfigurable feedback control can address the problem of disordered cooling distribution arising from the conventional control strategy in the limited cooling supply situations (i.e., morning start period, demand limiting period and soft stop period).
- Compared with the conventional control, significant energy savings can be obtained during the morning start period (i.e., 9.1%) and soft stop period (i.e., 13.3%) under the reconfigurable control. Besides, the reconfigurable control can achieve a further reduction in power consumption by 30.8% during the demand limiting period while mitigating the rebound by 11.2% right after demand limiting period.
- The reconfigurable control strategy can seamlessly integrate with the current building automation systems, achieving smooth transition between the demand-based control (i.e., normal control mode) and supply-based control.

9.3 Recommendations for future work

This PhD study has made great efforts in developing supply-based cooling distribution management strategies for air-conditioning systems for building-grid interaction and demand-limiting. Recommendations for future work are listed as follows.

- Although this PhD study has theoretically and practically developed smart cooling distribution management strategies, on-site tests are necessary for real implementation in commercial buildings. In the future, conducting field-implementation case studies in an actual building will be required to demonstrate the effectiveness of the control strategies.
- In this PhD study, the indoor air temperature is considered as the key indicator for evaluating the thermal comfort during the demand response events. However, the relative humidity should also be considered especially in humid subtropical areas. Future work should be conducted to quantify the impacts on both indoor air temperature and relative humidity in the demand limiting process.
- Actually, in addition to direct load control by shutting down part of the operating chillers, the air-conditioning systems can participate in demand response and provide energy flexibility services through various other control pathways. Future work should also be conducted to explore how to practically implement these control strategies.

REFERENCES

Åarzén, K.-E. (1999). A simple event-based PID controller. *IFAC Proceedings Volumes*, *32*(2), 8687–8692.

Álvarez, J. D., Redondo, J. L., Camponogara, E., Normey-Rico, J., Berenguel, M., & Ortigosa, P. M. (2013). Optimizing building comfort temperature regulation via model predictive control. *Energy and Buildings*, *57*, 361–372.

Astrom, K. J. (1995). *PID controllers: Theory, design, and tuning*.

Bae, Y., Bhattacharya, S., Cui, B., Lee, S., Li, Y., Zhang, L., Im, P., Adetola, V., Vrabie, D., Leach, M., & Kuruganti, T. (2021). Sensor impacts on building and HVAC controls: A critical review for building energy performance. *Advances in Applied Energy*, *4*, 100068.

Braun, J. E. (1990). *Reducing energy costs and peak electrical demand through optimal control of building thermal storage*. *pt 2*, 876–888. Scopus.

Braun, J., Montgomery, K., & Chaturvedi, N. (2001). Evaluating the Performance of Building Thermal Mass Control Strategies. *HVAC&R Research*, *7*(4), 403–428.

Bristow, D. A., Tharayil, M., & Alleyne, A. G. (2006). A survey of iterative learning control. *IEEE Control Systems Magazine*, *26*(3), 96–114.

Chen, Y., Norford, L. K., Samuelson, H. W., & Malkawi, A. (2018). Optimal control of HVAC and window systems for natural ventilation through reinforcement learning. *Energy and Buildings*, *169*, 195–205.

Dai, M., Lu, X., & Xu, P. (2021). Causes of low delta-T syndrome for chilled water systems in buildings. *Journal of Building Engineering*, *33*, 101499.

Doyle, J. C., Francis, B. A., & Tannenbaum, A. R. (2013). *Feedback Control Theory*. Courier Corporation.

Geng, G., & Geary, G. M. (1993). On performance and tuning of PID controllers in HVAC systems. *Proceedings of IEEE International Conference on Control and Applications*, 819–824 vol.2.

Global Energy and CO2 Status Report 2018 (p. 29). (2018). IEA.

Godsil, C., & Royle, G. F. (2001). *Algebraic Graph Theory*. Springer Science & Business Media.

Gunay, B., Shi, Z., Ashouri, A., & Newsham, G. (2019). Development of a clustering-based morning start time estimation algorithm for space heating and cooling. *Proceedings of the 6th ACM International Conference on Systems for Energy-Efficient Buildings, Cities, and Transportation*, 297–305.

Halhoul Merabet, G., Essaaidi, M., Ben Haddou, M., Qolomany, B., Qadir, J., Anan, M., Al-Fuqaha, A., Abid, M. R., & Benhaddou, D. (2021). Intelligent building control systems for thermal comfort and energy-efficiency: A systematic review of artificial intelligence-assisted techniques. *Renewable and Sustainable Energy Reviews*, *144*, 110969.

Heemels, W. P. M. H., Sandee, J. H., & Van Den Bosch, P. P. J. (2008). Analysis of event-driven controllers for linear systems. *International Journal of Control*, *81*(4), 571–590.

Henze, G. P., & Schoenmann, J. (2003). Evaluation of Reinforcement Learning Control for Thermal Energy Storage Systems. *HVAC&R Research*, *9*(3), 259–275.

Hong Kong Energy End-use Data. (2023).

Hong, T., Wang, Z., Luo, X., & Zhang, W. (2020). State-of-the-art on research and applications of machine learning in the building life cycle. *Energy and Buildings*, *212*, 109831.

Karimi, M., Mokhlis, H., Naidu, K., Uddin, S., & Bakar, A. H. A. (2016). Photovoltaic penetration issues and impacts in distribution network—A review. *Renewable & Sustainable Energy Reviews*, *53*, 594–605.

Li, B., Cai, W., & Liu, X.-K. (2022). A Novel Min-Consensus-Based Distributed Control Method for Multi-Zone Ventilation Systems. *IEEE Transactions on Industrial Electronics*, *69*(8), 8284–8295.

Li, W., Li, H., & Wang, S. (2021). An event-driven multi-agent based distributed optimal control strategy for HVAC systems in IoT-enabled smart buildings. *Automation in Construction*, *132*, 103919.

Liang, W., Quinte, R., Jia, X., & Sun, J.-Q. (2015). MPC control for improving energy efficiency of a building air handler for multi-zone VAVs. *Building and Environment*, *92*, 256–268.

Lu, X., Pang, Z., Fu, Y., & O'Neill, Z. (2022). Advances in research and applications of CO2-based demand-controlled ventilation in commercial buildings: A critical review of control strategies and performance evaluation. *Building and Environment*, *223*, 109455.

Olfati-Saber, R., Fax, J. A., & Murray, R. M. (2007). Consensus and Cooperation in Networked Multi-Agent Systems. *Proceedings of the IEEE, 95*(1), 215–233.

Qiu, S., Li, Z., Li, Z., Li, J., Long, S., & Li, X. (2020). Model-free control method based on reinforcement learning for building cooling water systems: Validation by measured data-based simulation. *Energy and Buildings*, *218*, 110055.

Ran, F., Gao, D., Zhang, X., & Chen, S. (2020). A virtual sensor based self-adjusting control for HVAC fast demand response in commercial buildings towards smart grid applications. *Applied Energy*, *269*, 115103.

Renewables 2019. Analysis and forecast to 2024. (2019). IEA.

Seem, J. E., House, J. M., & Alcala, C. F. (2016). *Model Selection for Predicting the Return Time from Night Setback*.

Shan, K., Wang, J., Hu, M., & Gao, D. (2019). A model-based control strategy to recover cooling energy from thermal mass in commercial buildings. *Energy*, *172*, 958–967.

Shan, K., Wang, S., Gao, D., & Xiao, F. (2016). Development and validation of an effective and robust chiller sequence control strategy using data-driven models. *Automation in Construction*, *65*, 78–85.

Shan, K., Wang, S., Yan, C., & Xiao, F. (2016). Building demand response and control methods for smart grids: A review. *Science and Technology for the Built Environment*, *22*(6), 692–704.

Siano, P. (2014). Demand response and smart grids—A survey. *Renewable and Sustainable Energy Reviews*, *30*, 461–478.

Su, B., & Wang, S. (2020). An agent-based distributed real-time optimal control strategy for building HVAC systems for applications in the context of future IoT-based smart sensor networks. *Applied Energy*, *274*, 115322.

Sutton, R. S., & Barto, A. G. (2018). *Reinforcement Learning, second edition: An Introduction*. MIT Press.

Tang, R., Wang, S., Gao, D.-C., & Shan, K. (2016). A power limiting control strategy based on adaptive utility function for fast demand response of buildings in smart grids. *Science and Technology for the Built Environment*, *22*(6), 810–819.

Tang, R., Wang, S., Shan, K., & Cheung, H. (2018). Optimal control strategy of central air-conditioning systems of buildings at morning start period for enhanced energy efficiency and peak demand limiting. *Energy*, *151*, 771–781.

Tang, R., Wang, S., & Yan, C. (2018). A direct load control strategy of centralized air-conditioning systems for building fast demand response to urgent requests of smart grids. *Automation in Construction*, *87*, 74–83.

Vrettos, E., Kara, E. C., MacDonald, J., Andersson, G., & Callaway, D. S. (2018a). Experimental Demonstration of Frequency Regulation by Commercial Buildings—Part I: Modeling and Hierarchical Control Design. *IEEE Transactions on Smart Grid*, *9*(4), 3213–3223.

Vrettos, E., Kara, E. C., MacDonald, J., Andersson, G., & Callaway, D. S. (2018b). Experimental Demonstration of Frequency Regulation by Commercial Buildings—Part II: Results and Performance Evaluation. *IEEE Transactions on Smart Grid*, *9*(4), 3224–3234.

Wang, J., Hou, J., Chen, J., Fu, Q., & Huang, G. (2021). Data mining approach for improving the optimal control of HVAC systems: An event-driven strategy. *Journal of Building Engineering*, *39*, 102246.

Wang, J., Huang, G., Sun, Y., & Liu, X. (2016). Event-driven optimization of complex HVAC systems. *Energy and Buildings*, *133*, 79–87.

Wang, S. (1998). Dynamic simulation of a building central chilling system and evaluation of EMCS on-line control strategies. *Building and Environment*, *33*(1), 1–20.

Wang, S. (2009). *Intelligent Buildings and Building Automation*. Routledge.

Wang, S., & Ma, Z. (2008). Supervisory and Optimal Control of Building HVAC Systems: A Review. *HVAC&R Research*, *14*(1), 3–32.

Wang, S., & Tang, R. (2017). Supply-based feedback control strategy of air-conditioning systems for direct load control of buildings responding to urgent requests of smart grids. *Applied Energy*, *201*, 419–432.

Wang, Z., & Hong, T. (2020). Reinforcement learning for building controls: The opportunities and challenges. *Applied Energy*, *269*, 115036.

Windham, A., & Treado, S. (2016). A review of multi-agent systems concepts and research related to building HVAC control. *Science and Technology for the Built Environment*, *22*(1), 50–66.

Xue, X., Wang, S., Yan, C., & Cui, B. (2015). A fast chiller power demand response control strategy for buildings connected to smart grid. *Applied Energy*, *137*, 77–87.

Zhang, Z., Chong, A., Pan, Y., Zhang, C., & Lam, K. P. (2019). Whole building energy model for HVAC optimal control: A practical framework based on deep reinforcement learning. *Energy and Buildings*, *199*, 472–490.

Zou, Z., Yu, X., & Ergan, S. (2020). Towards optimal control of air handling units using deep reinforcement learning and recurrent neural network. *Building and Environment*, *168*, 106535.